A toolset for 3D *in vitro* kidney tissue engineering

A dissertation submitted by

Erica Palma Kimmerling

In partial fulfillment of the requirements for the degree of

Doctor in Philosophy
In
Biomedical Engineering

February 2017

Advisor: David L. Kaplan, PhD

Research Committee:

David. L Kaplan

Lauren D. Black III

Barbara Ehrlich

Ronald Perrone

ABSTRACT

Tissue-engineered approaches are required to better understand the causes of renal failure and for the development of new treatment options. Upon renal failure, due to acute or chronic causes, renal replacement therapies such as dialysis or transplantation are necessary to restore function. Currently, 185,000 Americans have a functioning kidney transplant and 450,000 are on dialysis. However, recapitulating the functions of the human kidney *in vitro* remains challenging due to the anatomical complexity required to mimic renal physiology. Despite these challenges, advancements in microfluidic and 3D tissue culture techniques have demonstrated the importance of both microenvironment and mechanosensory stimulation in establishing physiologically relevant, *in vitro* models for disease studies and drug development. Accordingly, we have developed a 3D *in vitro* tissue toolset that can be utilized to achieve the necessary phenotypes for studying kidney development and disease. In order to understand the development of polycystic kidney disease we established static hydrogel cultures to characterize long-term development of cysts and changes in structural morphologies. Additionally, we developed a modular, three dimensional perfusion culture system to support the controlled fluidic stimulation of a planar cell layer seeded on a 3D porous, silk protein scaffold. Lastly, we established a simple, robust assay for the *in vitro* formation of renal epithelial tubules by a telomerase immortalized human proximal tubule cell line (RPTEC/tert1). This methodology yields polarized, luminal tubules that were responsive to TGFβ stimulation and co-culture with stromal cells. These *in vitro* model systems, which yield physiologically relevant phenotypes without complex differentiation protocols or culture methods, comprise a necessary toolset for future *in vitro* studies of disease pathogenesis and nephrotoxicity.

Acknowledgements

First and foremost, I would like to thank my advisor David Kaplan for welcoming me into his lab and giving me the freedom to pursue my interests. The experiences in your lab have not only made me a stronger bench scientist and engineer but a better collaborator, grant writer, mentor and organizer. I appreciate the opportunity to emerge from graduate school with a fuller perspective due to the range of roles you supported me in.

I would also like to thank my thesis committee members Lauren Black and Ron Perrone for always being available for support and feedback. To committee member Barbara Ehrlich, thank you for all of your support and enthusiasm as a collaborator. You and your lab members including, Ivana Kuo, Fernanda Lemos and Sophie Duong have provided feedback and insights into cell biology that significantly informed the direction of my work.

Thank you to my Re-building a Kidney collaborators, the labs of Leif Oxburgh, Thomas Carroll, and Ondine Cleaver, for introducing me to the world of developmental biology and its potential as a strategy for tissue engineering. It was a pleasure to work with you and I cannot wait to see where the project goes.

Thank you to the administrative staff, specifically Milva and Monica Ricci, Laura Suarez, and Carmen Preda for all of your hard work to keep things running behind the scenes. The work I did would not be possible without you. To Milva Ricci, thank you for always looking out for me, I appreciate all of your support over the years.

Thank you to my colleagues in the Kaplan lab group, current and former, I have enjoyed our shared experiences and learning from every one of you. Specifically to the people who I have worked alongside over the years on the kidney projects. To Tessa DesRochers for teaching me the fundamentals of cell culture and tissue engineering when I was first starting

out in the lab. To Jeannine Coburn for always pushing me to be the best scientist I could be. To Shreyas Jadhav and Sophie Szymkowiak, your enthusiasm and optimism have made it a pleasure to work with you. To Jonathan Grasman your support and friendship towards the end have been invaluable and I am grateful that we had the chance to work together. To other internal collaborators including but not limited to Lorenzo Tozzi, Yu-Ting Dingle, Ying Chen, Whitney Stoppel, Jelena Rnjak, and Chiara Ghezzi I have enjoyed working alongside you and your insights and assistance have significantly advanced my scientific training and the development of these projects. To my former undergrads, Jaclyn Foisy and Cory Sago, my experience training you taught me so much about myself as a mentor and has excited me about the future.

Thank you to my office-mates and friends, Rosalyn Beauregard, Dana Cairns, and Karolina Chwalek, you are all brilliant and inspiring, I will never forget the time we spent together and will always be grateful for our time working alongside one another. Our discussions grounded my work and gave me the motivation to keep going. To Karolina, you are a tireless advocate and I appreciate all of your efforts to keep me focused on my end goals. To Dana, the expansiveness of your talents never ceases to amaze and inspire me, your ability to bring people together is a force to be reckoned with. To Ros, I knew from that first summer that we were kindred spirits and your friendship came at a time when I needed it the most, your ability to give everything one hundred percent has pushed me to be a better person.

Thank you to my family. To my parents, you have given me all of the love and support I have ever needed to succeed. To my father, you are my source of insight and wisdom, the steady hand that has guided me the whole way. To my mother, you are my best friend and your strength and perseverance have inspired me to make the most out of every experience. To my brother, your intelligence always pushed me to work harder and I can always count

on you as a source of love and support. To my extended family, my aunts, uncles and all of my cousins, you are always there for me and I will forever seek to make you proud. To Kathleen, who is like a sister to me, even though graduate school has put physical distance between us, I know you will always have my back. To the Kimmerling family, thank you for being my second family and supporting Rob and I along this journey. To Kaylee and Ben, you remind me of the important things in life and I strive to be the best role model I can be for you. To the grandparents I have lost along this very long way, your sacrifices have gotten me to where I am now and I will always carry you with me as a reminder of where I come from and who I am.

Of all the people that have gotten me to this point, a special thanks is reserved for my husband Rob. Ever since I met you, at age 12, your natural brilliance motivated me to perform at the limits of my abilities. As my husband, you continue to bring out the best in me and inspire me on a daily basis. I would not be able to forge my own path and pursue my passions without your constant support and unwavering belief in my potential. I am happiest when I am with you and excited to be taking another step forward with my best friend.

Table of Contents

LIST OF TABLES

List of Figures

Chapter 1. INTRODUCTION

1.1. KIDNEY TISSUE ENGINEERING

Through a process of filtration, secretion and absorption the kidney regulates the excretion of waste and retention of solutes such as electrolytes and amino acids. In processing the blood the kidney also functions to maintain acid-base homeostasis, plasma osmolality and blood pressure. These functional roles of the kidney are the basis for the recent interest in developing *in vitro* kidney models that can be applied to drug development, disease studies and nephrotoxicity testing.

Recapitulating the functions of the human kidney *in vitro* remains challenging due to the anatomical complexity required to mimic renal physiology. The kidney is composed of numerous region-specific epithelial cell types, interstitial cells, and a complex microvasculature (1). Although cell type and matrix composition are the primary considerations for achieving a specific function, the incorporation of mechanical stimulation also needs to be considered due to the influence of fluid flow in maintaining epithelial cell phenotype. Based on the downstream application of the system, three dimensional (3D) tissue culture and kidney-on-a-chip systems are typically designed to mimic only a narrow set of functions. Accordingly, these simplified approaches preclude important, multicomponent functions such as the renin-angiotension-aldosterone system, which regulates blood pressure and has been shown to drive the progression of

chronic kidney disease (2). In this introductory chapter we will explore the anatomy and physiology of the kidney, the design considerations, common methods for assessing phenotype and function, and the benefits and limitations of state-of-the-art *in vitro* kidney model systems.

1.1.1. Clinical Motivations

There is a significant clinical need for the development of in vitro kidney tissue models. Tissue-engineered approaches are required to better understand the causes of renal failure and for the development of new treatment options. Upon renal failure, due to acute or chronic causes, renal replacement therapies such as dialysis or transplantation are required to restore function. Currently, 185,000 Americans have a functioning kidney transplant and 450,000 are on dialysis (3). Dialysis is able to replace the essential filtration functions of the kidney but long-term dialysis can lead to quality of life issues due to malnutrition and depression. Additionally, patients in chronic renal failure undergoing dialysis are still at risk for anemia as a result of a decreased production of erythropoietin, which stimulates the production of red blood cells. While kidney transplants are able to completely restore function, this treatment option is limited by donor supply, with the majority of people on the organ transplant waiting list requiring a kidney. Tissue engineered models can be utilized to study the causes of renal disease and assess the efficacy of preventative and restorative treatments which would ultimately reduce the need for renal replacement therapies. In addition to drug development and disease modeling, these approaches have considerable utility in assessing drug-induced nephrotoxicity during pharmaceutical development. The kidneys are inherently exposed to a high proportion of pharmaceuticals that enter the body, considering that a quarter of the total cardiac output passes through the kidneys. Renal toxicity is a significant

contributor to late-stage failure of drugs undergoing clinical trials and this failure adds to the high cost of drug development. These occurrences can potentially be attributed to the limitations of two-dimensional cell culture and animal models to accurately predict human toxicity outcomes. Additionally, it is unknown whether drugs that cause toxicity in animals are representative of the human response (4). As such, tissue-engineered systems that better predict the human response to treatment would be capable of reducing drug development costs and improving patient outcomes.

1.2. KIDNEY ANATOMY AND PHYSIOLOGY

The human kidney can be distilled down to three primary structural components: the nephron, the microvasculature, and the collecting system, as shown in Figure 1.1. These components are located beneath the renal capsule, a tough, fibrous protective layer, within the outer and inner layers known as the cortex and medulla respectively. Each of the one million nephrons in the human kidney consists of a renal corpuscle and a tubular portion. The precise localization of components is vital to renal function with filtration occurring in the cortical layer and reabsorption within the medulla.

A basic understanding of renal anatomy is necessary in order to assess the strengths and limitations of *in vitro* systems designed to mimic renal functions. Simplified models typically attempt to mimic nephron function, so more emphasis is placed on this structural component. However, the role of the endothelium, interstitium, and lymphatic system should be investigated before designing a kidney tissue model for a specific application.

1.2.1. Renal Corpuscle

A renal corpuscle consisting of a glomerulus and a Bowman capsule is at the start of each nephron. The renal artery that supplies blood to each kidney branches to eventually form the interlobular arteries. These arteries are the source of the afferent arterioles at the leading end of the glomerulus (see Figure 1.1). Blood is filtered as it passes through the capillary tuft of the glomerulus and exits through the efferent arterioles. The Bowman capsule, consisting of a parietal epithelial layer, collects the filtrate before entering the lumen of the tubular portion of the nephron. Glomerular filtration is regulated by the glomerular basement membrane (GBM) in addition to glomerular endothelial cells, specialized epithelial cells known as podocytes, and specialized smooth muscle cells known as mesangial cells which interact with each other, as shown in Figure 1.2.

Mesangial cells and their anchoring mesangial matrix, known as the mesangium, are the support structure of the glomerular capillaries. In this role, these contractile cells are able to regulate the fluid flow and filtration through the capillaries. These cells are also known to generate their own matrix and regulate matrix turnover and as such are implicated in diseases, including diabetic nephropathy, where glomerulosclerosis occurs (5). Mesangial cells also play a significant role in glomerular paracrine signaling as exemplified by the secretion of transforming growth factor beta-1 (TGF-β1) and vascular endothelial growth factor (VEGF), in response to changes in capillary tension (6) .

Glomerular endothelial cells, which form the capillary tuft, are surrounded by the mesangium on one side and the GBM on the other. These highly fenestrated endothelial cells, with pore sizes ranging 60 to 80 nanometers and a negatively charged glycocalyx, are the initial component of the three-layer glomerular filtration barrier (7). The GBM is

a thick (approximately 350 nanometers), specialized extracellular matrix consisting of specific isoforms of type IV collagen (α3, α4, and α5), laminin 11 (α5, β2 and γ1) nidogen, and heparan sulfate proteoglycan (primarily agrin) (8). The negative charge of the heparan sulfate proteoglycans and the endothelial glycocalyx are the basis of the charge-based selectivity of the filtration barrier. The final component of the filtration barrier is the highly differentiated cell-type known as podocytes, which also carry a negative surface charge due to sialoglycoproteins. These cells are fixed to the GBM via interdigitating extensions known as foot processes with transmembrane proteins specific to the GBM. Podocytes are particularly susceptible to paracrine signaling with surface receptors including, but not limited to, transient receptor potential cation channels and the angiotension II type 1 receptor known to influence cytoskeletal organization (9). Ultimately, the glomerular filtration barrier allows for uncharged macromolecules smaller than 1.8 nanometers to progress through uninhibited, and essentially prohibits molecules larger than 4 nanometers. In between these sizes, fractional clearances are dependent on size and charge. While there are currently few tissue-engineered glomerular models, the incorporation of this component will be critical to mimicking basic renal functions in future in vitro systems.

1.2.2. Tubule and Collecting Ducts

The remaining portion of the nephron, the renal tubule system, consists of distinct segments: the proximal tubule, thick and thin segments of the descending loop of Henle, the thin and thick segments of the ascending loop of Henle, and the distal tubule, as shown in Figure 1.3. The connecting tubule links the nephron with the collecting duct system. Transport through the renal epithelium of the renal tubules is accomplished by

both paracellular and transcellular transport. Particular epithelial phenotypes and transport mechanisms are specific to the different tubular segments.

Reabsorption of water and solutes begins in the proximal tubule. The luminal surface of the proximal tubule consists of a brush border for increasing surface area and leaky tight junctions. The basolateral sodium potassium adenosine triphosphatase (Na+K+ ATPase) pumps work in conjunction with the luminal sodium hydrogen (Na+H+) ion exchanger for the reabsorption of ions. In addition to ion transport, aquaporin 1 (AQP1) channels and lysosomes are used for transporting water and proteins respectively.

Generally, the loop of Henle is water permeable in the descending loop and water impermeable in the ascending loop. In addition to being water impermeable, the epithelium of the thick ascending loop contains luminal sodium potassium chloride (Na+K+2Cl−) cotransporters and robust tight junctions. This differential permeability establishes an osmotic gradient within the renal medulla that drives the countercurrent system known for establishing urine concentration before excretion.

The distal convoluted tubule segment is differentiated from the loop of Henle by its specific luminal sodium chloride (Na+Cl−) transporter, known for its sensitivity to thiazide diuretics, basolateral interdigitations, and apical microvilli. Both the collecting tubules and the collecting duct system consist of principle and intercalated cells with the number of intercalated cells decreasing as the collecting duct system progresses. Principle cells possess luminal aquaporin 2 (AQP2) channels sensitive to vasopressin, also known as arginine vasopressin or antidiuretic hormone, which induces water permeability within these segments. Intercalated cells are responsible for active secretion and reabsorption of protons.

The segment distinct sodium transporters discussed in this section exemplify the unique epithelial phenotypes within the renal tubule and collecting duct system but are not an inclusive list of the all the phenotypic differences. The specialization of renal epithelia is an important consideration when designing tissue engineered models, specifically with respect to cell choice and functional outcomes. Accordingly, most systems are limited to a specific set of applications based on the cell phenotypes utilized in the kidney tissue model.

1.3. CELL SOURCES

1.3.1. Animal Cell Sources

Although the differences between animal and human cell biology are not completely understood, the availability and ease of culture of animal cell lines supports their use in tissue engineered models. More importantly, some animal cell lines, such as Madin-Darby canine kidney (MDCK) epithelial cells, have been in use for over 50 years, and as such have been characterized in a plethora of biological contexts and for a range of phenotypes. Another common animal cell line originating from pig kidney, known as LLC-PK$_1$ has a proximal tubule- like phenotype and divides rapidly in culture (10). The MDCK cell line was originally derived from the kidney of a healthy female adult cocker spaniel with the specific kidney segment of origin remaining unknown. MDCK cultures display characteristics such as tight junction formation and epithelial polarization and transport but are considered to be a heterogeneous cell population (11). MDCK subpopulations and clones have been shown to have distinct phenotypes with characteristics indicative of different segments such as the collecting duct (1). Accordingly, MDCK cells can be used to model specific renal functions but the heterogeneity of the specific culture must be adequately understood. While the use of animal cell lines will not provide a direct

understanding of human renal cell behavior, the ease of culture and the extent of prior characterization support their use in targeted model systems.

1.3.2. Human Cell Sources

When working with human cells there is often a trade-off between ease of culture and well-characterized cell behavior, as with cell lines, and improved phenotypic characteristics, as seen in primary cells. Immortalized cell lines have a well characterized phenotype, can be continuously passaged, and eliminate the patient-to-patient variability affiliated with primary cell culture. Conversely, considering primary cells can be isolated from normal biopsies, systems which seek to observe patient-specific responses to perturbations would need to work with primary cell sources. While primary human cells are known for improved phenotypic characteristics, these cells are limited to only a few passages before dedifferentiation occurs. Human kidney-2 (HK-2) cells are one of the more common immortalized normal adult kidney cell lines. This cell line was established from proximal tubule cell culture using the human papilloma virus (HPV 15) E6/E7 genes (12). These cells maintain some characteristics of the proximal tubule phenotype such as a parathyroid hormone–stimulated adenylate cyclase response and irresponsiveness to antidiuretic hormone. RPTEC/TERT1 (renal proximal tubule epithelial cells/ telomerase) is an alternative human cell line that possesses a similar phenotype and functional responses to HK-2 cells (13). The immortalization of RPTEC/TERT1 cells is the result of ectopic expression of the catalytic subunit of telemorase as opposed to the use of oncogenes. Most available human renal cells are a mixed cortical epithelial cell population or cells that have been verified to possess proximal tubule-like phenotypes. As a result of the available cell sources, humanbased tissue models are significantly limited in the amount of phenotypes that can be studied. To address this problem most current

approaches focus on a specific mechanism or function required to model a particular aspect of a disease or toxic response. However, when establishing these tissue models it is important to recognize that cell phenotypes have been shown to change in response to microenvironmental cues such as a 3D matrix or fluid induced shear stresses. Therefore, targeted cell phenotypes should be reassessed in the context of an optimized microenvironment over the course of system development.

1.3.3. Stem Cells

Using insights from renal development there have been recent advancements in the ability to differentiate human stem cells along renal lineages. For instance, embryonic stem cells have previously been differentiated through the posterior primitive streak to an intermediate mesodermal phenotype (14). Similarly, uretic bud and metanephric mesenchyme committed renal progenitor cells have been formed from human-induced pluripotent stem cells (15, 16). The differentiation of renal progenitors from stem cells has the potential to significantly influence the development of future tissue-engineered models. Induced stem cell sources offer the opportunity for personalized tissue models for treatment response. While significant research is still required before these cells can be consistently differentiated into specialized renal cell types, these cells may be used one day to accurately recapitulate kidney cell function.

1.4. GLOMERULAR TISSUE MODELS

A significant scientific and clinical need exists for the development of new methods for understanding of the development of glomerular diseases and the effect of drugs on the glomerular filtration barrier. The nature of patient studies limits the ability to study early mechanisms involved in drug response and disease development. Currently, the

primary method for assessing kidney function and the extent of chronic kidney disease is a metric known as glomerular filtration rate. Glomerular filtration rate is indirectly determined using algorithms which associate the level of serum creatinine in a patient's urine to their sex, race, and age (17). In vitro tissue models would provide direct insight into human cell behavior that cannot be obtained from clinical metrics. Despite the need for these models, limited progress has been made in their development due to limited sources of the highly differentiated glomerular cell phenotypes. While primary glomerular endothelial and mesangial cells can be obtained commercially, these specialized cells do not readily propagate in culture and easily lose their phenotype. To circumvent this issue, intact glomeruli have been used to investigate drug-induced nephrotoxicity of known glomerular toxicants such as gentamicin and cisplatin (18). Intact glomerular tufts can be isolated from human tissue through a process of mechanical and enzymatic tissue degradation and size dependent sieving. In this approach the cross-sectional area of the isolated glomeruli was used as a metric of toxicity and confirmed in vivo drug response. While this method circumvents issues associated with glomerular cell culture, working with whole glomeruli requires repeated isolation of primary tissue for each experiment. The use of conditional immortalization has been employed over the last ten years to establish glomerular cell lines. Transfection of cells with the SV40-T gene causes cells to proliferate at 33°C and differentiate at 37°C (19). Conditionally immortalized glomerular endothelial cells capable of expressing fenestrations and podocytes expressing in vivo podocyte markers have been established (20, 21). This cell source has the benefit of both continual propagation and a differentiated phenotype, but there is still a limited understanding of their ability to mimic glomerular function. A functional glomerular tissue model is not only dependent on the cell sources but the structural organization and the

incorporation of a matrix mimicking the glomerular basement membrane. While the basement membrane isolated from Engelbreth-HolmSwarm sarcoma is commonly used in 3D tissue–engineered models, this matrix does not contain the specific isoforms of collagen and laminin of the glomerular basement membrane. One model used electrospun collagen 1 and polycaprolactone on a nickel mesh support to co-culture conditionally immortalized glomerular endothelial and podocytes cells (22). Although this approach does not use a physiologically relevant mimic of the glomerular basement membrane, it does provide a method for studying glomerular cell paracrine signaling. This glomerular tissue model exemplifies how downstream applications need to be considered when developing new systems.

1.5. MICROFLUIDIC APPROACHES

Microfluidic systems are intrinsically desirable for renal cell culture, considering the channel sizes are typically within one order of magnitude of renal tubule diameters which can range from 20 to 200 microns depending on the segment. The scale of these systems enables mechanical stimulation with physiologically relevant fluid induced shear stresses which are typically estimated to be between 0.2 and 20 dyn/cm2. Renal microfluidic systems are typically of either a single or dual layer construction with the latter design supporting basolateral stimulation in addition to apical/luminal flow. Most renal microfluidic systems are designed as potential drug induced nephrotoxicity models

1.5.1. Animal Cell Systems

MDCK cells were a commonly used cell type in early renal microfluidic systems. A number of studies have cultured MDCK cells for 96 hours on a fibronectin coated polydimethylsiloxane (PDMS) device (23-25). The upregulation of drug metabolism

enzymes on the microfluidic device compared to static culture emphasizes the benefit of a dynamic environment (24). This study also highlights the ability to still perform standard transcriptomic and proteomic analysis after perfusion culture and the need to perform additional cell characterization to understand the effect of mechanical stimulation on phenotype. The functionality of the approach was demonstrated using a two-chamber device for liver cell culture upstream of the MDCK cell chamber (26). MDCK cells in this device experienced an increased toxicity to ifosfamide treatment compared to MDCK cells alone. This response is suggested to be a result of the toxicity of the liver metabolized byproduct of ifosfamide, chloroacetylaldehyde, which caused the same toxicity response when cells were treated directly. These microfluidic systems demonstrate the benefits of dynamic stimulation and the ability to do physiologically relevant co-cultures. While Snouber et al. were able to recapitulate a specific example of drug-induced nephrotoxicity, further optimization is necessary to develop a model suitable for nephrotoxicity screening applications considering the phenotypical heterogeneity of MDCK cell populations. The use of a homogenous cell source enables specific research questions to be tackled in the context of mechanical stimulation.

A multilayer renal microfluidic device capable of mimicking the luminal and interstitial spaces has been established, as depicted in Figure 1.4 (27). This approach enables cell stimulation through osmotic gradients, localized hormone treatment, and shear stress. Rat inner medullary collecting duct (IMCD) cells incorporated into the device demonstrated a more physiologically relevant phenotype, such as a columnar phenotype and AQP2 basolateral localization, after 5 hours of fluid-induced shear stress (27). The applicability of this two-layer system was further tested by using the interstitial compartment to stimulate with arginine vasopressin and establish an osmotic gradient;

both conditions are known to influence AQP2 localization in collecting duct cells (28). The observed translocation of AQP2 in this system upon perturbation demonstrates the benefit of choosing cell types and a culture environment specific to the desired outcome.

1.5.2. Human Cell Models

In human cell microfluidic models there has been a recent push to develop more advanced designs to mimic the physiological microenvironment and to explore the applications of established designs.

A dual perfusion system meant to mimic both tubular flow and extracapillary flow was recently developed (29). In this approach, serpentine microchannels were etched into a glass substrate and the channels were sealed around a polycarbonate membrane. While cell phenotype within this device was not extensively studied, the approach supported long-term cell viability of RPTEC cells under dynamic conditions for 10 days. Additionally, techniques such as hot embossing are now being used to topographically pattern the culture surface of renal microfluidic devices in order to mimic the complex structural organization of tubular basement membrane. HK-2 and RPTEC cells cultured on porous, 1-micron ridges of polycarbonate substrates demonstrated tight junction staining and alignment in the direction of the topography (30). Microfluidic devices have also been designed specifically to measure functional outcomes. Human cortical epithelial cells and MDCK cells were cultured in a bilayer microfluidic system that was able to measure transepithelial electrical resistance (TEER) (31). This quantitative measurement of tight junction formation is both an indicator of cell phenotype and cell health and as such is a useful metric for disease models and nephrotoxicity.

While additional fabrication techniques are being used to develop mimetic microenvironments, established systems are being tested for their utility for conducting translatable research. For example, in 2013, a human kidney proximal tubule-on-achip model was described for use in nephrotoxicity studies (32). This study used a similar multilayer device to the previous studies with IMCD but instead incorporated human RPTEC cells on a collagen IV–coated membrane. Under dynamic conditions these cells had upregulated expression of the Na+K+ ATPase transporter and AQP2. Additionally, these cells had higher albumin uptake, glucose transporter, and alkaline phosphatase activity compared to static conditions. Dosing in cisplatin, a known proximal tubule toxin, caused cellular injury as would be expected. This toxicity was shown to be through physiologically mimetic mechanisms when the cisplatin transporter, organic cation transporter OCT1, was inhibited and toxicity was prevented.

1.5.3. Microfluidic Models Summary

Microfluidic systems optimized for renal cell culture have great potential as future tools for modeling drug-induced nephrotoxicity and drug screening applications. These approaches inherently mimic physiological forces, and complex microenvironments can be fabricated using common techniques. The current progress with these microfluidic systems reiterates the need for application-targeted designs such as the use of osmotic gradients and hormone stimulation to induce a phenotypic response in collecting duct cells, as Jang et al. demonstrated (2011).

While proper consideration of cellular phenotype and environment stimulation can yield the best outcomes with microfluidic systems, there are also intrinsic limitations to this approach. Most of these established microfluidic culture systems are unable to

recapitulate a 3D tissue environment due to the use of solid membrane supports for cell culture. Without a bulk matrix environment these systems are unable to model changes in the interstitium associated with diseases states and diseases with structural phenotypic outcomes such as polycystic kidney disease. Moreover, most of the established systems have only been conducted as short-term culture, less than 4 days, with only one system maintaining culture for over a week, as seen in Table 1.1. Approaches capable of sustaining viability over long-term culture will be necessary for investigating chronic diseases and assessing nephrotoxicity. It is important to keep in mind that while significant progress has been made in optimizing kidney cell culture in microfluidic environments, these systems are not to the point of capturing kidney function as a whole, and new devices should be characterized with respect to the specific renal functions they are designed to recapitulate.

1.6. THREE DIMENSIONAL MODELS

Although 3D tissue–engineered kidney models lack the fluid-induced stimulation offered by microfluidic approaches, these methods allow for a more accurate recapitulation of structural morphologies. To enable more physiologically relevant outcomes, these systems are typically fabricated using biopolymer-based hydrogels such as type 1 collagen and basement membrane isolates consisting of proteins including laminin and type IV collagen. These hydrogels have the benefit of being susceptible to cellular remodeling, a response particularly relevant to disease phenotypes. In addition to dissociated cell culture, 3D environments have been used to maintain organoid culture ex vivo. The utility of these approaches has been demonstrated for study areas including, but not limited to, polycystic kidney disease and drug-induced nephrotoxicity (33).

1.6.1. Polycystic Kidney Disease Models

Polycystic kidney disease is a disorder characterized by the formation of fluid filled cysts within the kidney, the most common form of which is autosomal dominant polycystic kidney disease (ADPKD). While animal models and patient studies have been the primary means of studying disease pathogenesis and treatment efficacy, the development of in vitro disease models has offered a complementary method of characterizing the structural phenotype associated with this disease. The models have thus far been used to investigate disease development in the context of fluid secretion, extracellular matrix interactions, and cell growth kinetics.

One of the most common approaches for modeling PKD involves culturing MDCK cells in type 1 collagen hydrogels. This method is known to yield physiologically relevant cystic structures with a layer of polarized epithelial cells surrounding a fluid filled cavity. While these cells automatically form cystic structures in 3D, they can be stimulated—through hormonal stimulation with hepatocyte growth factor—to undergo tubulogenesis (34). The localization of polycystin-1, a key protein implicated in this disease, to the cell membrane of luminal structures in a manner similar to the in vivo phenotype highlights the benefits of structural organization for PKD studies. 3D cell culture techniques can also be used to address the inherent heterogeneity of MDCK cell populations discussed earlier. Studies have been conducted on MDCK cysts formed from cells subcloned from a single cyst (35). The cystic phenotype and the highly investigated epithelial characteristics of MDCK support the use of this model to investigate mechanisms behind cyst growth.

3D PKD models have also been adapted for mechanistic, high-throughput, and long-term applications. Characterizing potential disease mechanisms in a 3D environment

enables a direct understanding of how a cell process affects structure formation and organization. In recent work, the easily-transfected LLC-PK1 cell line was used to study how the genetic loss of intracellular calcium release channels altered cyst structure development in a 3D tissue model (36). Observations of the cystic structures in this model enabled researchers to associate cyst growth with a loss of the primary cilia, a functional cellular component. A tubule-to-cyst conversion model was developed using immortalized mouse collecting duct cells in a 20 microliter type 1 collagen-Matrigel drop culture (37). The nature of this approach is amenable to high-throughput screening applications for identifying therapeutics capable of stalling early cyst development. At the same time, a method was established for extended in vitro culture that would enable long-term studies of targeted therapeutics. To prevent the degradation of a collagen-Matrigel hydrogel over time, matrix and cellular components were infused into a porous silk protein scaffold (38). The inclusion of a silk scaffold support also allowed for the use of a perfusion bioreactor system that maintained culture for 8 weeks. Over the course of long-term culture, polycystin 1–deficient immortalized mouse collecting duct cells developed cystic phenotypes in conjunction with abnormal extracellular matrix deposition and cell cycle progression (39). These tissue-engineered approaches highlight the ability to design 3D PKD models for specific disease progression and drug screening applications. However, a significant weakness of the approaches discussed thus far is the use of animal cell types.

Tissue models using diseased human ADPKD cell sources are well established and allow for drug screening on 3D cystic structures formed with the same underlying genetic mechanisms that cause cyst formation in patients (40, 41). ADPKD epithelial cells isolated from extracted cysts are cultured in type 1 collagen and stimulated with forskolin to

induce cyst formation. These physiologically relevant cysts have been tested with treatments suspected of halting cyst progression such as Sorafenib (42). While these 3D models are useful for assessing compounds meant to slow cyst progression, they are not applicable to studies looking to elucidate early disease pathogenesis before cyst formation.

1.6.2. Drug induced Nephrotoxicity

3D tissue culture systems specifically designed for testing drug-induced nephrotoxicity are limited. For this purpose, an organoid culture system where isolated mouse proximal tubules were cultured in a modified hyaluronic acid-based hydrogel has been developed (43). Culture of proximal tubules within this gel allowed for phenotypic stability for up to 6 weeks as demonstrated by maintained AQP1 and megalin expression along with glucose regulation similar to in vivo proximal tubules. Treatment of this culture with the nephrotoxic compounds such as cisplatin resulted in the production of a clinical biomarker of kidney injury, Kim-1. This type approach, which uses primary structures from animal cell sources, could potentially be used to better understand the causes of nephrotoxicity in animal models.

Similar to the organoid approach to drug-induced nephrotoxicity, immortalized human proximal tubule–like cells have been stably cultured for 8 weeks (44). In this model, cells suspended in a type 1 collagen-Matrigel mix formed tubule-like structures without additional stimulation. These structures were positive for organic ion transporters and cytokeratin in addition to displaying sodium dependent glucose uptake. Cells within this system displayed a greater sensitivity to gentamicin and doxorubicin when compared to standard cell culture techniques. The ability to observe drug effects

over the course of long-term culture is beneficial for studies of chronic tissue response to treatment.

1.7. THREE DIMENSIONAL MICROFLUIDIC APPROACHES

3D microfluidic systems incorporate the strengths of both traditional microfluidic and static 3D culture. As previously discussed, these approaches inherently mimic physiological forces with the additional benefit of utilizing complex microenvironments amenable to co-culture and modification. Recent technical advancements in microfabrication and 3D printing have enabled the development of 3D microfluidic systems.

One of these approaches includes the utilization of hollow fibers for human proximal tubule epithelial cell culture. Culture within these hollow fibers demonstrated tight junction formation, visualized via zonula occludens-1 (ZO-1) and organic cation transporter 2 expression which corresponded with barrier function and active transport (45). The strengths and weaknesses of this approach can be attributed to the material utilized for 3D culture. Unlike other approaches, this methodology uses a purchasable MicroPES type TF10 hollow fiber capillary membrane which does not require the use of complex fabrication techniques or expensive equipment. However, this synthetic material is not bioactive and cannot remodeled and has a fixed inner diameter of 300 microns with a wall thickness of 100 microns which is larger than *in vivo* tubules. These characteristics ultimately limit the benefit of utilizing a 3D culture environment.

Alternative 3D microfluidic approaches have adapted traditional soft lithography and photolithography techniques to fabricate PDMS molds for patterned hydrogel formation. Mu et al. used this approach to form channels within a composite collagen type 1 and

sodium alginate hydrogel (46). Channel formation required systematic layering and crosslinking via temperature and calcium chloride exposure. This technique can be used to form perfusable channels from 30-400 microns in diameter which are capable of supporting parallel MDCK and HUVEC culture for 3 days in culture. While the approach demonstrated by Mu et al. enables complex pattern formation and co-culture, the use of traditional lithographic techniques does not yield the formation of reproducible circular channels that are necessary for understanding the effects of flow on renal cell culture.

3D channels have also been formed through the use of fugitive inks as part of 3D bioprinting protocols. Homan et al. formed convoluted constructs within a gelatin and fibrin ECM with a similar elastic modulus to that of the healthy kidney cortex (47). This approach was able to yield channels ranging from 150 to 700 microns however perfusion experiments were conducted in channels larger than 400 microns. Cultures of TERT immortalized human proximal tubule epithelial cells remained viable for up to 2 months and demonstrated a polarized epithelium with functional albumin uptake and Cyclosporine A toxicity. Perfusion culture was conducted at shears stress ranging from 0.1 to 0.5 dyn/cm^2. This technique presents a promising approach to complex 3D perfusion culture which incorporates the strengths of both 3D and microfluidic environments. Moreover, future work will seek to demonstrate tubule culture a physiologically relevant sizes with multiple cell types.

In addition to the custom 3D microfluidic approaches that have been utilized for renal tissue culture, there is also commercially available platform from Nortis Inc. In these devices 125 micron microfibers are used to form a linear channel in a type 1 collagen gel (48). Proximal tubule cells in this system also demonstrated physiologically mimetic cell

polarity, basolateral solute transport and apical solute uptake (49). As a commercially available platform this system does require complex fabrication protocols however system modification is limited with respect to altering channel configurations or channel number.

The novel approaches to 3D kidney culture offer a promising opportunity to recapitulate the complex kidney microenvironment. These approaches allow for tubule formation, ECM signaling, co-culture and fluid induced shear stresses (50). Nevertheless, at their current stage these approaches are relatively laborious compared to other culture methods and are not readily amenable to standardized, high-throughput culture. Additionally, as with other methods these systems remain limited with respect to their ability to model kidney function as a whole.

1.8. ORGANOID CULTURE

Recently, there have been significant developments in the ability to differentiate human pluripotent stem cells into kidney organoid structures. As opposed to traditional 3D culture techniques organoid cultures are typically formed from stem cell aggregates or pellets grown on top of a filter at an air-liquid interface or on an ECM surface. Accordingly, organoids are 3D structures which self-organize and differentiate into multiple cell types and structures found *in vivo*. This novel approach to kidney tissue engineering has already demonstrated significant promise with respect to nephrotoxicity testing and disease modeling.

In the Takasato protocol published in 2015, pluripotent stem cells are induced to an intermediate mesoderm stage before aggregation via centrifugation (50,000 cells per aggregate) and culturing on a transwell filter for at least 18 days before experimentation

(51). An alternative approach to kidney organoid culture relies on the systematic differentiation of human pluripotent stem cells into multipotent nephron progenitor cells prior to pelleting cells in the bottom of round bottom, ultra-low attachment plates (52). Both protocols require stimulation with small molecules such as CHIR99021, a WNT agonist, and growth factors such as FGF9 (fibroblast growth factor-9). At day 18 the Takasato produced organoids were found to contain multiple renal lineages including interstial and endothelial cells in addition to rudimentary nephron organization (53). These 4 compartment structures showed positive staining for glomerular, proximal tubule, distal tubule and collecting duct markers. Within the organoids, dual positive tubules (LTL, lotus tetragonolobus lectin and ECAD, e-cadherin) were considered to be a more mature proximal tubule phenotype compared to LTL positive and ECAD negative structures. As a demonstration of future utility for nephrotoxicity testing the organoids were treated with the nephrotoxin cisplatin (53). In these experiments, the mature proximal tubules exhibited a higher rate of apoptosis in response to cisplatin compared to the immature phenotype. Although these experiments provide evidence to support the use of organoids for nephrotoxicity testing, further validation with known nephrotoxins and a better understanding of the differential response with respect to the "maturity" of the structures is required. It was concluded the transcriptional profile of these organoids more closely resembles the profile during the first trimester of kidney development (53). As such, at this stage these organoids are a useful tool for studying human kidney development *in vitro* but the known lack of the diverse, mature cell populations found in the adult kidney limit their utility as adult nephrotoxicity models.

Additionally, organoids have been formed via sandwiching pluripotent stem cells between thin layers of collagen type 1, matrigel or both (54). In these cultures, CHIR99021

stimulation differentiated epithelial spheroids into tubular organoids. These organoids demonstrated luminal accumulation of fluorescent cargo and upregulation of Kim-1 in response to cisplatin or gentamicin treatment. CRISPR/Cas9 editing was also used to introduce truncating mutations of *PKD1* or *PKD2* in order to mimic PKD development in organoid culture. In these studies, 6% of organoids formed noticeable cysts after 35 days in culture. These results support the ability to conduct long term disease studies on organoid culture. However, the cellular mechanism for the cystogenesis within this system is not yet known.

Organoid culture is a promising new approach to *in vitro* kidney tissue engineering due to the use of human derived stem cells and the differentiation of organized, multicellular structures. Unlike traditional 3D and microfluidic models, organoids allow for the interactions between interstitial, endothelial and epithelial cell types to be studied. Additionally, this culture method is capable of yielding multiple different epithelial phenotypes such as collecting duct and proximal tubule. However, these cell types are considered to be immature thereby requiring further optimization of tubule differentiation in organoid cultures before a mimetic structure is achieved. Moreover, further studies with respect to patient specific organoid formation are required before this approach can be utilized as a tool for personalized medicine.

1.9. SUMMARY

3D tissue models have the benefit of recapitulating structural phenotypes over prolonged culture periods. The inclusion of an extracellular matrix environment has been shown to support long-term functional viability, a valuable parameter for certain kidney disease and drug response studies. Moreover, a 3D culture environment in vitro is

necessary to study disease development for diseases such as ADPKD where a shift in structural phenotype in vivo is part of the pathogenesis.

Despite their demonstrated utility, current 3D tissue models fall significantly short of mimicking the in vivo kidney environment, and as such disease models and toxicity studies will continue to provide an incomplete picture. 3D models are readily adaptable to co-culture experiments, and the inclusion of multiple cell types would enable the exploration of more complex biological mechanisms. A culture method which established a confluent monolayer of human proximal tubule cells atop a type 1 collagen gel seeded with dermal fibroblasts was able to show epithelial-based regulation of fibroblast phenotype in response to injury (55). Additionally, in line with recent evidence suggesting macrophages play a role in PKD progression, macrophage inclusion with cystic ADPKD cells yielded a higher total number of microcysts (56).

1.10. LOOKING FORWARD

Current in vitro kidney tissue systems provide a physiologically relevant environment capable of supporting specific kidney cell phenotypes and functions. Microfluidic platforms for renal cell culture enable mechanical stimulation via fluid induced shear stresses. Moreover, 3D tissue models have supported structure formation within long-term cultures. In order to advance these systems for drug development and disease modeling applications, future systems will either need to be tailored for higher throughput or more complex culture environments. Renal microfluidic systems have the potential to be adapted for high-throughput applications for screening drug toxicity or efficacy due to the simplicity of the design. For mechanistic studies, systems which incorporate both fluidic stimulation and a 3D culture environment are desirable.

Furthermore, co-culture of renal epithelial cells with endothelial and interstitial cells will be necessary to mimic in vivo paracrine signaling between cell types. A significant challenge to establishing complete renal function in vitro is the limited availability of segment specific cell types. Future advancements in stem cell differentiation through renal lineages will be important to developing systems capable of recapitulating a broader range of kidney cell phenotypes and functions.

1.11. TABLES AND FIGURES

Table 1.1: Kidney cell 2D microfluidic culture systems

Cell Type	Matrix coating	Culture duration	Functional outcomes	(Author, Year)
MDCK	fibronectin	96 hrs (24 hrs static, 72 hrs dynamic)	glucose consumption, ammonia production	(Baudoin et al. 2007, 1245-1253)
	fibronectin	96 hours (24 hrs static, 72 hrs dynamic)	transcriptomic and proteomic analyses; ifosamide treatment; liver co-culture	(Snouber et al. 2012b, 474-484; Snouber et al. 2012a, 27-34; Choucha-Snouber et al. 2013, 597-608; Jang et al. 2013)
	collagen IV	>7 days	TEER	(Ferrell et al. 2010, 707-716)
IMCD	none	4 days (5 hrs dynamic)	Arginine vasopressin stimulation, osmotic gradient	(Jang and Suh 2010, 36-42; Jang et al. 2011, 134-141)
RPTEC	collagen IV	6 days (3 days dynamic)	Albumin uptake, cisplatin toxicity	(Jang et al. 2013)
	Matrigel	10 days dynamic	Cell viability	(Gao et al. 2011, 907)
	collagen IV	N/A	Cell alignment	(Frohlich, Zhang, and Charest 2012, 75-83)
HK-2	Cultrex	72 hrs dynamic	Epithelial-to-mesenchymal transition	(Zhou et al. 2014, 1390-1401)
	collagen IV	N/A	Cell alignment	(Frohlich, Zhang, and Charest 2012, 75-83)

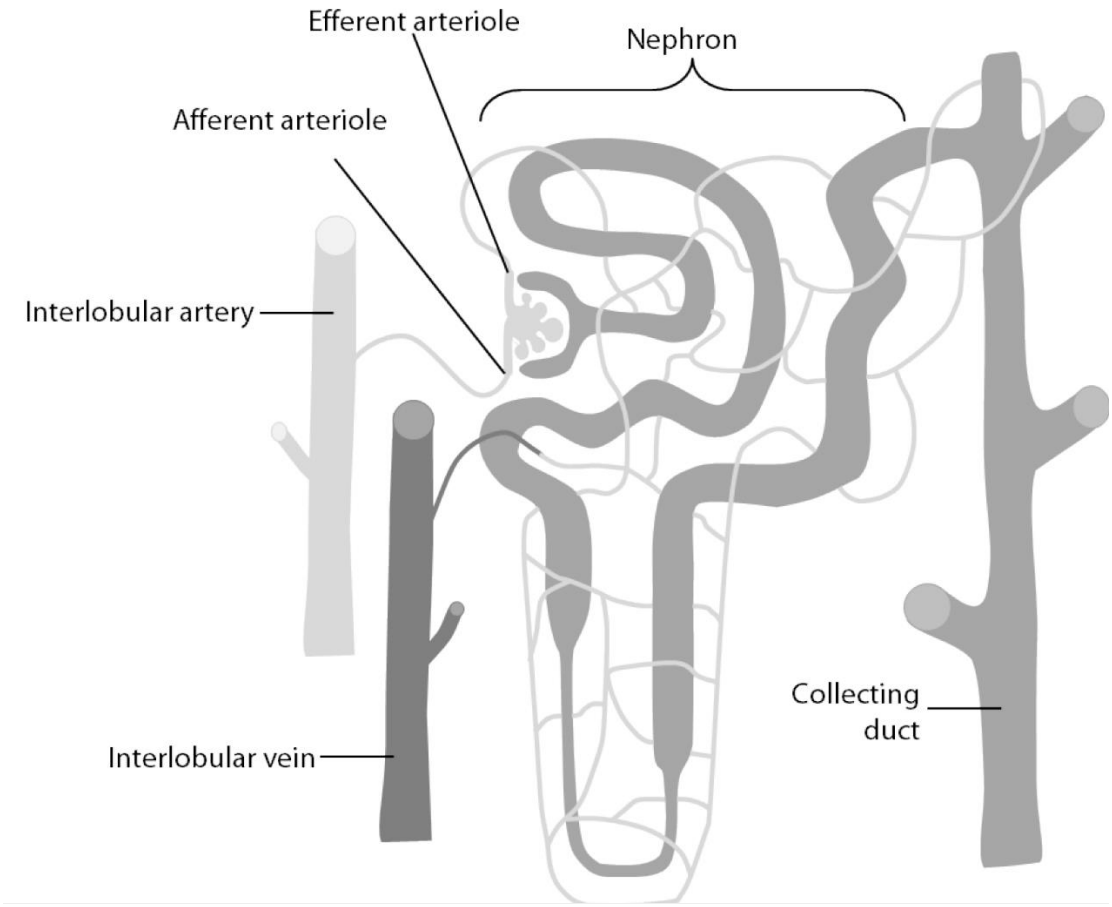

Figure 1.1 Structural components of the kidney

Figure 1.2 Cross-section of the glomerular lobule

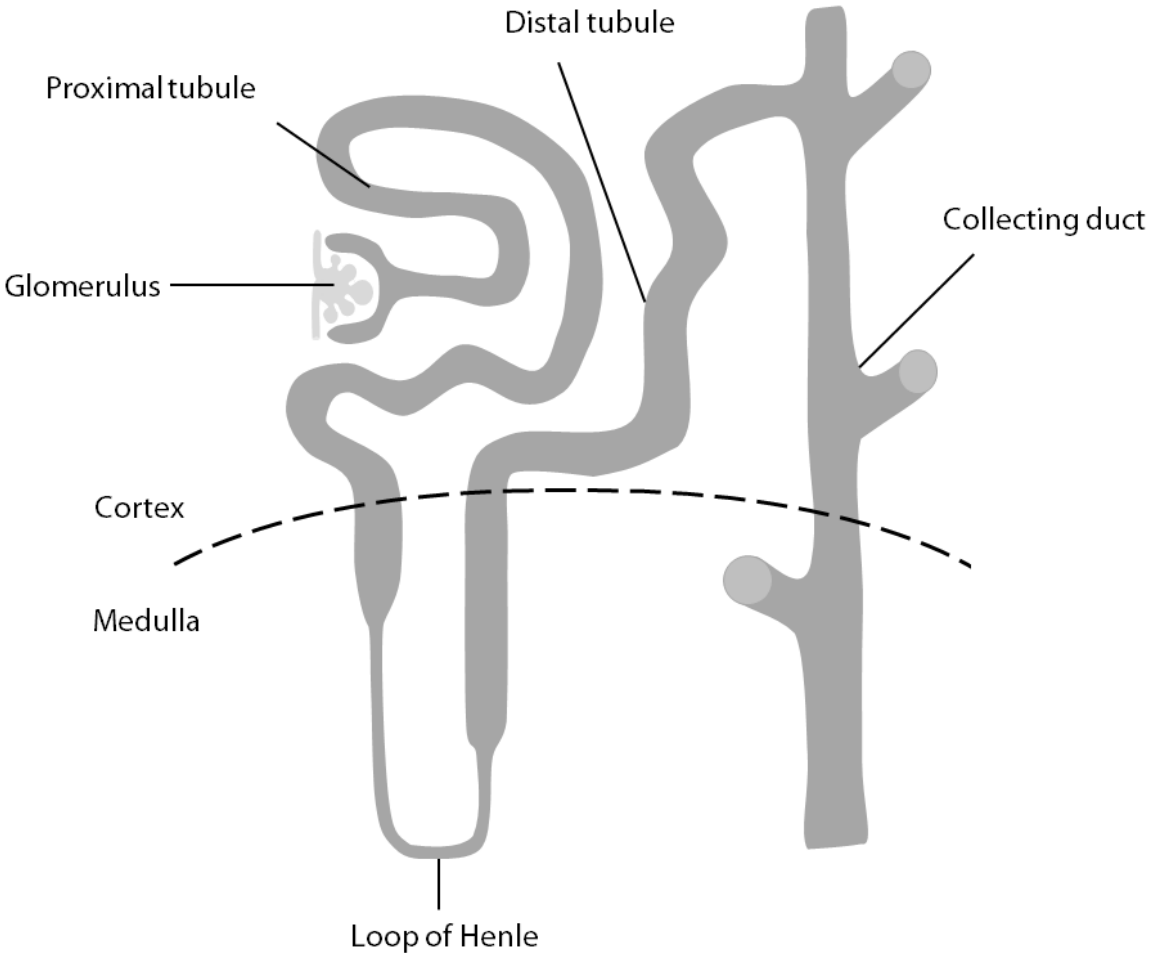

Figure 1.3 Components of the nephron

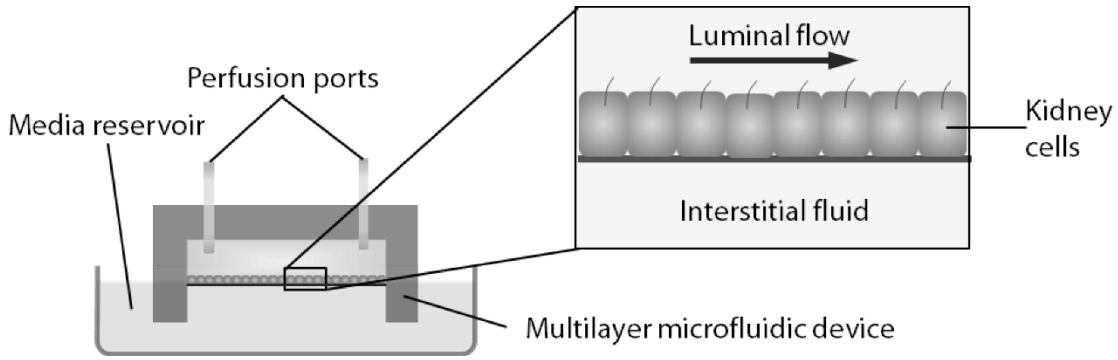

Figure 1.4 Multi-layer microfluidic device for renal cell culture

Chapter 2. 3D KIDNEY TISSUE CULTURE FOR POLYCYSTIC KIDNEY DISEASE MODELING

This chapter contains text and figures from Kuo, Desrochers, Palma et al. published in *PNAS* (36)). All figures sampled in this text resulted directly from my contributions to this paper. Accordingly, I established and maintained all of the long-term, 3D LLC-PK1 cultures used in the final publication. I also conducted the tissue post-processing, histological preparation, whole mount and fluorescent imaging in the figures below (Figures 2.1 and 2.2). Furthermore, I contributed to the writing and editing of the published manuscript.

Abstract

Three dimensional tissue engineered kidney models have provided a better understanding of renal morphogenesis and disease development. These approaches are specifically amenable to studies of polycystic kidney disease considering the pathophysiology includes changes in cellular polarization and structural morphology. Unlike standard two dimensional cell culture, the use of a 3D microenvironment allows for differentiated morphogenesis that mimics *in vivo* phenotypes. Accordingly, we used long term 3D culture of LLC-PK1 cells in a type 1 collagen – Matrigel extracellular matrix to monitor changes in cyst size and morphology over time. This approach revealed a relationship between calcium channel loss and cyst progression. To build on this success we explored the development of an inducible knockdown model for monitoring tubule to cyst transition in immortalized human cortical epithelial cells. Although tubule dilation in this system occurred in response to *PKD1* loss, the lack of a polarized, luminal structure limited the applicability of this model. To achieve the necessary *in vitro* phenotypes we optimized the culture of a second immortalized human cortical epithelial cell line and

pursued alternative culture approaches including the incorporation of a silk protein scaffold and hanging drop culture for high density cell aggregation. Insights from these optimization studies informed the development of the luminal tubule assay discussed in Chapter 4.

2.1. INTRODUCTION

ADPKD is a monogenic disorder that causes the development of bilateral focal cysts which ultimately result in renal failure and the need for renal replacement therapy such as dialysis or transplantation. Considering the disease affects over 600,000 people in the United States patients with ADPKD account for approximately 4% of all renal replacement therapy (57). Although the disease is associated with a mutation of either *PKD1* or *PKD2* the disease phenotype has a high level of variability with respect to onset of cyst formation and disease severity (58). Due to an incomplete understanding of the disease pathogenesis there are targeted specific treatments for ADPKD and current *in vitro* tissue models are limited in their capacity for elucidating the mechanisms behind cyst development (59).

Due to limitations in the ability to acquire data from patient analysis and animal models, in vitro studies are a critical tool for investigating the pathophysiology of ADPKD (57). Patient studies are useful in later stage testing of potential treatments and population based analysis but cannot be used for hypothesis based analysis of the mechanisms initiating cyst formation. Alternatively, animal studies can be applied for this purpose but there are few models which sufficiently represent the human ADPKD disease phenotype and are genetically orthologous (60). Although in recent years some animal models have been used to identify potentially promising target therapies differing

biological processes between animals and humans, such as gene expression and metabolism, still limit the ability of these models to mimic human disease and treatment response (61).

In vitro kidney models of ADPKD have been established using porous silk sponges as a means of providing the mechanical integrity necessary for supporting long term kidney cell culture within hydrogels such as Matrigel and collagen type 1 (38, 39). Porous silk sponges were fabricated by adding 850-1000 μm sodium chloride to 7% w/v aqueous silk solution. For kidney tissue culture, normal or *PKD1*$^{null/null}$ mouse embryonic kidney cells co-cultured with fibroblasts were combined with a 1:1 ratio of Matrigel:Collagen type 1 were infused into the pores of the scaffold. With this approach, the disease cell types were shown to have formed a greater number of diseased structures, cysts, to healthy tube-like structures. Healthy and disease cultures were also compared in terms of structural polarity by studying the localization of markers such as E-cadherin and N-cadherin. The use of the silk biomaterial also allowed for a custom perfusion chamber which as a result of improved mass transfer increased the culture duration to 6 weeks. As such, the ability to maintain healthy and diseased kidney structures in an optimized ECM hydrogel environment within a silk scaffold has been demonstrated but the need for human models remains.

In this chapter we will further explore the utility of 3D ECM cultures as a tool for elucidating the mechanisms of disease development. Comparative long term culture of LLC-PK1 cells were used to understand the effect of calcium channel loss on cyst progression. Additionally, we characterize an inducible knockdown of *PKD1* in immortalized renal cortical epithelial cells. Insights into the relationship between

structural morphology and cell response led to the development of additional approaches to 3D culture in order to yield physiologically relevant phenotypes.

2.2. METHODS

2.2.1. Cell culture

LLC-PK1 cells were cultured at 37°C in a humidified 5% CO_2 incubator in DMEM (Life Technologies, Grand Island, NY) with 10% fetal bovine serum and 5% penicillin-streptomycin (Life Technologies) Transient transfection of cells targeting InsP3R1, InsP3R3 or a scrambled sequence was conducted by the Ehrlich Lab according to the protocols detailed by Kuo et al. (36).

Immortalized renal cortical epithelial cells (RPTEC/TERT1, ATCC, Masasses, VA, USA) were cultured at 37°C in a humidified 5% CO_2 incubator according to the ATCC media preparation and detailed in Table 2.1 (62). NKi-2 immortalized epithelial cells (provided by our collaborator Jing Zhou) were cultured using the 2% kidney media composition.

2.2.2. 3D culture

A 1:1 mixture of growth factor reduced Matrigel-collagen (final collagen concentration 1.0 mg/ml, Corning Bioscience, Corning, New York) was used for all LLC-PK1 3D culture experiments according to the protocol developed by DesRochers et al (44). Briefly, the ECM mix containing 100,000 cells per well were cultured in 12-well transwells (Corning, Corning New York) and incubated at 37°C for 30 minutes to induce gelation before the addition of a hormone supplemented media. The media used for the 3D LLC-PK1 culture is the same as the 2% kidney media in Table 2.1. The media was replaced 3 times a week.

A modified version of this protocol was also used for the culture of NKi-2 or RPTEC/tert1 cells. These experiments were conducted using 200,000 cells and Matrigel-1.0mg/ml collagen unless otherwise specified. PKD1 knockdown inducible NKi-2 cells were created using a Tet-On/Off lentiviral vector and ShRNA was designed to target the UTR of *PKD1*. Transduced cells were selected for using puromycin.

2.2.3. 3D silk scaffold fabrication and culture

Silk fibroin (hereafter referred to as silk protein) solution extracted from *Bombyx mori* silk worm cocoons was prepared as previously described (63). To fabricate salt-leached scaffolds, 2ml aqueous silk solution (6% w/v, 30 minute extraction time) was mixed with 4g NaCl (300-500 µm particle size selected by sieving) in Teflon containers. Scaffolds were left to dry completely, approximately 48 hours, before soaking the containers in DI water for 2 days (38). For lyophilized scaffolds, aqueous silk (6% w/v, 30 minute extraction time) was added into standard 12-well cell culture plates at a volume of 2 mL per well and frozen from 4°C to -45°C and lyophilized (-0.25°C/min) and held for 480 min, followed by ramping to -20°C at 0.2°C/min. Drying was conducted at -20°C and 100 mT vacuum for 33 hr (VirTis Genesis 25L Super XL Freeze-Dryer, SP Scientific, Stone Ridge, NY) (64). Samples were lyophilized for 48 hours and autoclaved at 121°C for 20 minutes at 15 psi to induce beta-sheet formation. All scaffolds were biopsy punched to 6mm in diameter by 2mm thick and a 2mm plug was removed from the center to enable better nutrient penetration.

Sterilized silk scaffolds were vacuum dried and infused with a 1:1 mixture of growth factor reduced Matrigel-collagen (final collagen concentration 1.0 mg/ml, Corning Bioscience, Corning, New York) and RPTEC/tert1 cells at a density of $1x10^6$ cells per scaffold. Scaffolds were repeatedly squished and pipetted to ensure ECM penetration

before incubation at 37°C for 30 minutes to induce gelation. Media was replaced 3 times a week.

2.2.4. RPTEC/tert1 hanging drop culture

RPTEC/tert1 cells were seeded at a density of 80,000 cells per 10µl droplet on the surface of a non-tissue culture treated polystyrene dish. The bottom of the 10cm dish was filled with sterile DI water before flipping the lid and incubating for 48 hours. Aggregates from the hanging drops were gently pipetted off the lid of the petri dish into unsolidified 1:1 mixture of growth factor reduced Matrigel-collagen in transwells before incubation at 37°C for 30 minutes to induce gelation. Media was replaced 3 times a week.

2.2.5. Histology

To examine cyst size and structure, tissues were removed from culture at 2, 4, 6, and 8 wk post seeding and cut in half(36). One-half of the tissue was placed in 2 M sucrose overnight at 4 °C and then embedded in optimal cutting temperature (OCT) and stored at −20 °C for cryosectioning. The other half of the tissue was placed in 10% neutral buffered formalin for at least 48 h at 4 °C before whole-tissue staining with carmine and H&E. For H&E staining, 8-µm sections of paraffin-embedded, formalin-fixed tissue were used. For whole-mount preparations, tissues were washed and incubated overnight at room temperature in carmine solution.

All statistical analysis was conducted by the Ehrlich lab using the following protocol. Statistical analyses and regression were performed using Graph-Pad Prism software (Version 6). Groups were compared using one-way or two-way ANOVA, where appropriate, followed by Bonferonni's post hoc tests. All data are expressed as means ± SEM, unless stated. Differences were considered significant when $P < 0.05$

2.2.6. Immunohisto- and immunocyto- chemistry

TUNEL staining was conducted one eight-micrometer paraffin-embedded sections were deparaffinized and rehydrated, and DNA fragmentation was assessed fluorometrically following the manufacturer's instructions (Promega)(36).

For actin staining, samples were washed with PBS and probed with AlexaFluor488-phalloidin (1:40, Molecular Probes, Eugene, OR, USA) and DAPI (1:1000, Molecular Probes) for 1 hr at room temperature in 0.1% Triton and 1% bovine serum albumin (BSA). Samples with silk were counterstained using AdipoRed (1:1000, Walkersville, MD, USA). All actin imaging was conducted using a Keyence BZ-X700 inverted microscope (Osaka, Japan).

2.2.7. Scanning electron microscopy

Silk scaffolds were dehydrated in graded ethanol and dried overnight at room temperature. Samples were gold sputter coated before observation using a Zeiss EVO MA10 Scanning Electron Microscope (SEM) (Oberkochen, Germany).

2.3. RESULTS AND DISCUSSION

2.3.1. Using 3D culture to examine the effect of calcium channel loss on cyst formation

Mutations in *PKD1* or *PKD2*, which encode for polycystin 1 and 2 (PC1 and PC2 respectively), are the genetic commonality in patients with ADPKD that experience progressive cyst formation throughout adulthood. PC1 is a transmembrane protein that is thought to interact at the coiled-coil domain of the C-terminal domain of PC2 (65). PC2 is a calcium channel present on both the plasma membrane and endoplasmic reticulum (ER) in kidney epithelial cells and is thought to regulation cell proliferation, migration and

cell-to-cell interaction. As such, aberrant calcium signaling is thought to play role in cyst development in ADPKD patients (66). PC2 localized to the ER is also known to interact with the other calcium channels such as 1,4,5-triphosphate receptors ($InsP_3R$) to regulate intracellular calcium levels (67). To better understand the role of calcium signaling on cyst formation we conducted a series of comparative long term, 3D culture experiments on LLC-PK1 cells with a knockdown of PC2, $InsP_3R1$ and $InsP_3R3$ (receptor types 1 and 3 respectively) (36).

LLC-PK1 cultures were systematically analyzed at time points of 2, 4, 6 and 8 weeks. LLC-PK1 cells were utilized for these experiments due to the known role of PC2-dependent calcium signaling in this cell line. To visualize cyst size in 3D culture, a carmine stain was used in conjunction with whole mount brightfield imaging. While a cystic phenotype was observed within all cultures, including the scrambled control, cells with the $InsP_3R1$ knockdown were shown to form larger cysts compared to all other conditions starting at the 2 week time point (Figure 2.1). At later time points, the cysts found in all knockdown cultures were found to be significantly larger than the scrambled control which did increase in size over the course of the 8 week experiment (Figure 2.1b). Consistent with the results at week 2, at all time points the $InsP_3R1$ knockdown resulted in the most significant cyst growth over time.

In conjunction with size quantification, histological assessment was utilized to understand morphological changes over time and to analyze the mechanism of cyst formation. Cysts observed using H&E staining were consistent with the whole mount imaging results which clearly show significantly larger cyst size in $InsP_3R1$ culture (Figure 2.2a). Cystic structures were observed to consist of a ring of nuclei with an acidophilic

positive center. When visualized with deoxynucleotidyl transferase-mediated dUTP nick end labeling (TUNEL) the center of the larger $InsP_3R1$ and PC2 cysts was found to be the result cell death (Figure 2.2b). From week 2 to week 6 the increase in cyst size is associated with an increase in TUNEL-positive staining. Additionally staining with caspase-3 was used to verify that the cell death was the result of apoptosis-mediated cell death (data not shown) (36).

These experiments support the necessity for conducting long term, 3D cultures when studying ADPKD considering the most significant changes in phenotype were observed at the 6 and 8 week time point. While the knockdown of both PC2 and isoforms of $InsP_3R$ resulted in an increase in cyst size of LLC-PK1 cells it was evident that the loss of $InsP_3R1$ produced the most dramatic change in phenotype. This results suggest a more prevalent role of ER regulated calcium signaling in cyst development. Furthermore, this result is an agreement with the concept that multiple mechanisms are responsible for cyst development such as cyclic-AMP (cAMP) (68).

2.3.2. Modeling PKD using 3D culture of human cortical epithelial cells

We sought to establish a humanized model of ADPKD development in static 3D culture considering the utility LLC-PK1 for elucidating disease mechanisms. For this transition we utilized the NKi-2 immortalized cortical epithelial cell line previously characterized in our laboratory for nephrotoxicity experiments. NKi-2 cells were shown to form elongated, tubule-like structures that were maintained in 8 weeks of culture without structural breakdown making this culture method well-suited for long-term ADPKD studies (44). For disease studies, these cells were transduced with a pLKO-Tet-on lentiviral vector with shRNA targeted to the UTR of *PKD1*. Unlike cystic culture, tubular

structures allow for the transition from a tubule to cystic phenotype to be explored. Accordingly, the goal of this model was to induce cystic phenotypes after knockdown of *PKD1* in tubular structures.

Based on previously established protocols in our lab, we established static 3D cultures of renal epithelial cells for 2 weeks before induction of the knockdown. Carmine whole mount staining and H&E staining of tissue sections at 5 weeks confirm branching structure formation similar to previous reports of NKi-2 culture (Figure 2.4a) (44). After 3 weeks of doxycycline treatment at 100 ng/ml we observed a heterogeneous tissue response. Dilation of the tubular structures occurred at the edges of the gel whereas structures in center possessed a normal phenotype (Figure 2.4b). Accordingly, polycystin-1 plays a role in maintaining tubular diameter and morphogenesis *in vivo* and this loss of function leads to subsequent tubule dilation and cyst formation (69, 70). To exacerbate this phenotype, cultures were treated with the cAMP agonist forskolin which has been shown to induce cyst expansion *in vitro* through increased proliferation and fluid secretion (41, 42). Stimulation with forskolin did not produce notable changes in the histology of the knockdown tissues although tubule dilations were observed in some of the normal cultures treated with forskolin (data not shown).

The region specific localization of tubule dilation led to additional efforts to further optimize the cellular microenvironment to produce cyst formation. Specifically, the buildup of interstitial collagen I is associated with progression of PKD *in vivo* (71). Accordingly, an array of increased collagen I concentrations were assessed, including 1, 1.2, 1.5 and 1.8 mg/ml. As with prior experiments, collagen 1 was mixed 50:50 with Matrigel. In untreated culture, collagen concentrations of 1.5 mg/ml produced the most

consistent branching phenotype (Figure 2.4e). After 3 weeks of doxycycline induced culture, tubule dilation was found to increase as collagen concentrations were increased (Figure 2.4f). Moreover, this phenotype was not confined to the gel edges. While these treatments and matrix optimization resulted in dilated phenotypes, cyst formation was still not achieved in these static cultures.

Despite efforts to optimize the *in vitro* response of NKi-2 to knockdown we were unable to establish a model of tubule to cyst conversion. We hypothesize that this outcome was inhibited by the lack of an observable polarized phenotype. LLC-PK1, MDCK and ADPKD cystic cultures, which have been successfully used for disease studies, all display physiologically relevant planar cell polarity. Furthermore, loss of planar cell polarity has been implicated in disease development (70). Images of whole mount staining and sectioned tissue constructs did not reveal a differentiated cuboidal phenotypes observed in patient physiology.

2.3.3. Comparative culture between hTERT immortalized renal proximal tubule cell lines

In order to gain a better understanding of *in vitro* morphogenesis we compared NKi-2 structure formation to a commercially available hTERT immortalized renal proximal tubule cell line (RPTEC/tert1). RPTEC/tert1 cells have been extensively characterized with respect to barrier formation, hormone response and transporter expression (13, 72, 73). After 14 days in Matrigel-collagen 3D culture, NKi-2 cells displayed their established branching morphology (Figure 2.4a.i). As had been previously hypothesized, f-actin staining of the NKi-2 structures showed cytoplasmic localization indicative of a non-polarized phenotype. In differentiated epithelium f-actin accumulates along the cell membrane and the brush border (Figure 2.4a.ii). RPTEC/tert1 cultured using the same

methodology form a heterogeneous mix of multicellular aggregates or single cells (Figure 2.4b). Some structures, as indicated by the white arrows, resemble pre-cystic structures that occur early in the cyst formation process of MDCK cells (74). However, MDCK cells form cystic structures with open lumens within the first 24 hours, indicating that RPTEC/tert1 are not within an optimal microenvironment for differentiation. Although both cell lines are hTERT immortalized renal cortical epithelial cells they underwent significantly different morphogenesis in 3D culture. The only variable, other than the cell line, between the cultures for these media composition considering both cell types were cultured in their optimized media formulation.

The 2% kidney formulation, used by NKi-2 cells, and ATCC formulation, used by the RPTEC/tert1, included added hEGF, ITS, hydrocortisone and T3 (2% kidney concentration is significantly higher) (Table 2.1). However, the 2% kidney media uses a 2% concentration of FBS whereas the composition for RPTEC/tert1 is fully defined. Accordingly, the ATCC media also contains ascorbic acid, prostaglandin E1 and G418 as a selective pressure. Ascorbic acid has been shown to stimulate growth and oxidative metabolism in primary RPTEC culture in addition to increased activity of Na^+/K-ATPase and Na^+ dependent glucose transport (75). The kidney naturally produces hormones such as prostaglandins and prostaglandin E1 has been shown to be necessary for MDCK survival in serum-free media (76). The transition to a defined media has a significant benefits for disease modeling and regenerative tissue applications. In addition to known batch-to-batch variability, FBS provides additional cell stimuli which can confound mechanistic studies (77, 78). When NKi-2 cells were cultured in either 2% kidney or ATCC media a loss of tubular morphology was observed using bright field microscopy (Figure 2.4e-d). At the same time, culturing RPTEC/tert1 in the 2% kidney composition resulted in similar

extensions. Considering these branching structures are not polarized epithelial tubules we hypothesize that proteins within the FBS such as TGFβ1 (transforming growth factor β1) are potentially causing some cells to express a more mesenchymal phenotype. Further experiment should be conducted to fully understand the role of media composition on cell morphology.

2.3.4. Alternative 3D approaches

The inability to form a polarized tubule phenotype suitable for ADPKD studies using the established 3D culture approach led to the exploration of alternative culture approaches. Prior to the hydrogel-only used for the LLC-PK1 experiments, the collagen-Matrigel formulation was optimized for structure formation by mouse embryonic kidney cells in porous silk protein scaffolds (38, 39). Accordingly, we infused RPTEC/tert1 in Matrigel and collagen hydrogels into the pores of a salt-leached silk sponge in attempt to recapitulate these results. Silk scaffolds are known to adsorb DAPI staining so to distinguish nuclei staining from the silk surface the scaffolds were also stained with adipoRed which results in a purple co-stain (Figure 2.5). After 2 weeks in culture, RPTEC/tert1 in collagen gel infused salt leached sponges formed multicellular structures with no clear polarization (Figure 2.5a) while scaffolds infused with Matrigel yielded multicellular spheroids with no attachment on the silk surface (Figure 2.5b). To further understand the structure formation within Matrigel infused scaffolds we compared cell morphology between salt leached and lyophilized scaffolds. Salt leached scaffolds viewed using scanning electron microscopy show a large interconnect pore structure compared to 20-100μm honeycomb shaped pores in the lyophilized scaffolds (Figure 2.5c,d). Cells cultured within Matrigel infused into the silk pores yielded both multicellular tube-like and cystic structures (d). We hypothesize that RPTEC/tert1 cells form a polarized

phenotype in silk scaffolds compared to 3D transwell culture due to the increased cell density and the structural support provided by the silk scaffold.

To better understand the effect of cell density on RPTEC/tert1 morphogenesis we aggregated cells in hanging drop culture before embedding in an ECM hydrogel. After 48 hours, loose aggregates formed loose networks that could be transferred and adhered to 3D Matrigel-collagen 1 gel (Figure 2.6a-d). Staining of these structures for f-actin show the localization of f-actin towards the center of some of the elongated segments (Figure 2.6 e-f). In combination, these results support the potential of RPTEC/tert1 cells to form polarized structures *in vitro*. Moreover, structures can form independent of ECM when cells are cultured using high-density culture techniques.

2.4. CONCLUSION

Static 3D hydrogel cultures which display physiologically relevant phenotypes can be used to elucidate the mechanisms of ADPKD development. Long-term LLC-PK1 culture was successfully used to further elucidate the role of calcium signaling on cyst progression. The development of a static model which transitions from a tubule to cystic phenotype would allow for a greater understanding of disease pathophysiology. However, the transition to human cell models further reiterated the necessity for phenotypes which recapitulate *in vivo* morphology and functionality. Although tubule dilation was observed in response to *PKD1* knockdown induction, the lack of a patent lumen and cell polarization limited the relevancy of further analysis. Accordingly, these studies reiterated how systematic assessment of culture parameters can be used to optimize culture outcomes. Ultimately, we demonstrated the ability of RPTEC/tert1 to self-organize independent of ECM when cultured a high cell density. These insights led to

the development of the self-organizing renal epithelial tubule assay characterized in chapter 4.

2.5. TABLES AND FIGURES

Table 2.1 Human cortical kidney cell media comparison

Component	2% Kidney	ATCC
T3	107nM	5pM
hEGF	20 ng/ml	10 ng/ml
Ascorbic Acid	0	3.5 ug/ml
Insulin	10 ug/ml*	5 ug/ml
Transferrin	5 ug/ml*	5 ug/ml
Sodium Selenite	6.7 ng/ml*	8.65 ng/ml
Hydrocortisone	100 ng/ml	25 ng/ml
Pen/Strep	1%	1%
G418	0	100 ug/ml
Prostaglandin E1	0	25 ng/ml
FBS	2%	0
Base Media	DMEM/F12 (Gibco) , no HEPES, glutamax (2.5 mM L-Alanyl-L-Glutamine)	DMEM/F12 (ATCC), 2.5 mM L-glutamine, 15 MM HEPES

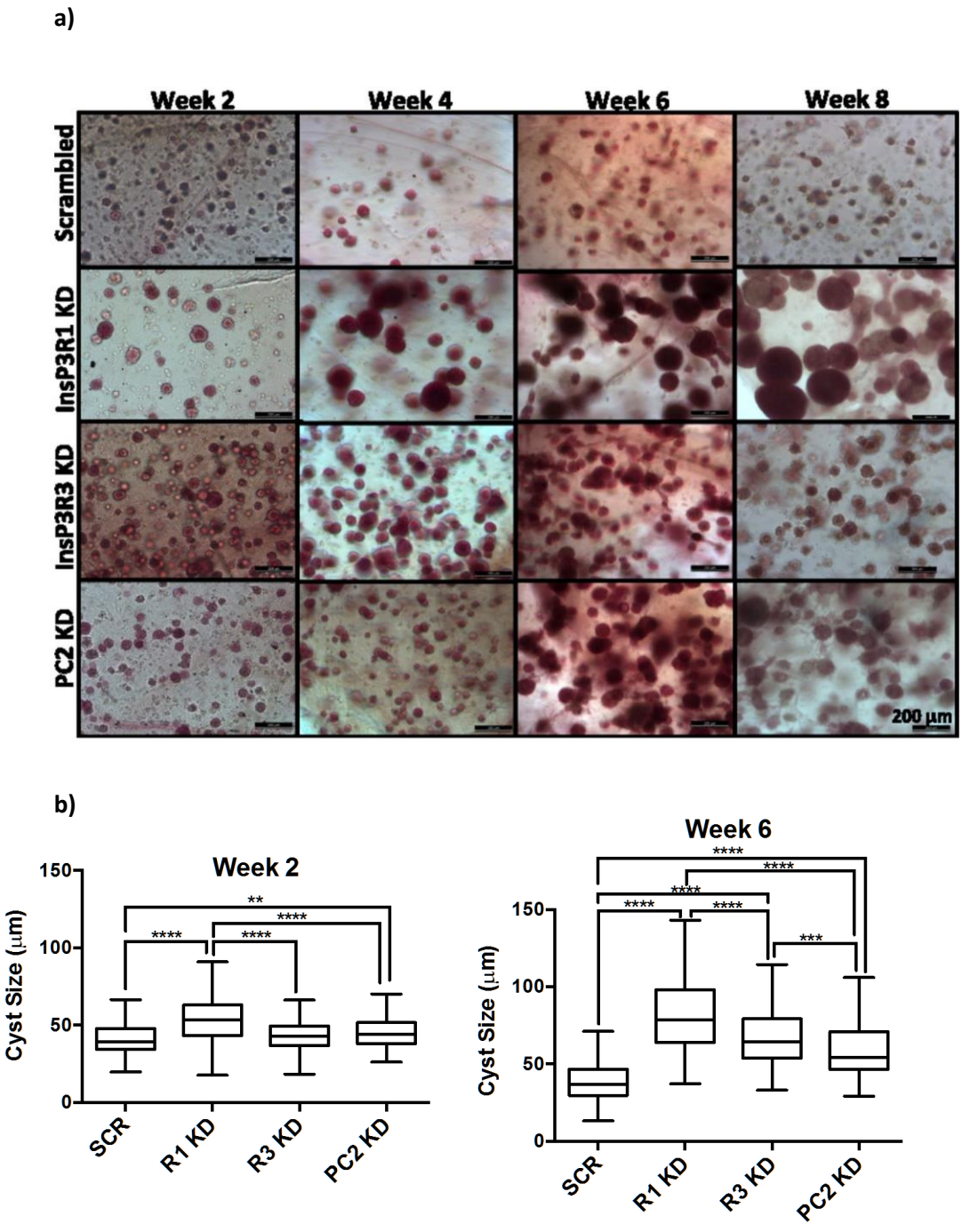

Figure 2.1. Effect of shRNA knockdown of InsP3R and PC2 on cyst development

(a)Carmine whole-mount staining of cyst development over an 8 week period (scale bar - 200µm). (b)Quantification of cyst size at weeks 2 and 8. Analysis was based upon 95-203 individual cysts from four separately cultured tissues. ****P<0.0001, ***P<0.001, **P<0.01. (Modified from Kuo, Desrochers, Palma et.al(36))

a)

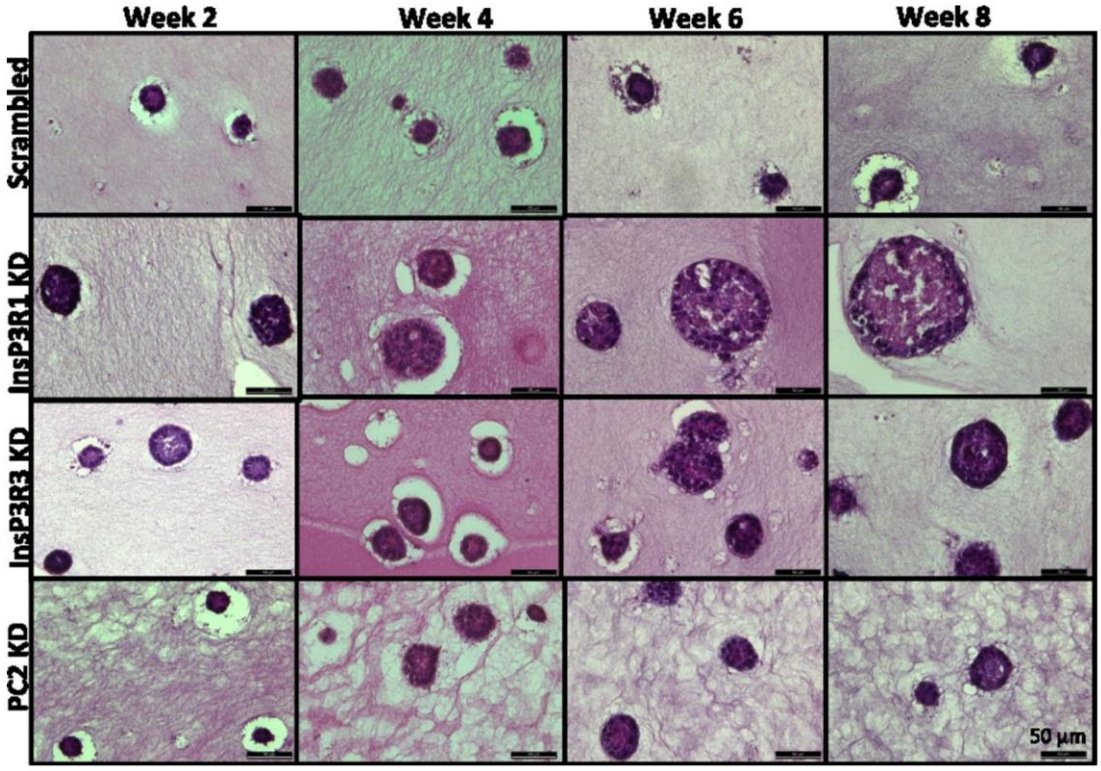

b)

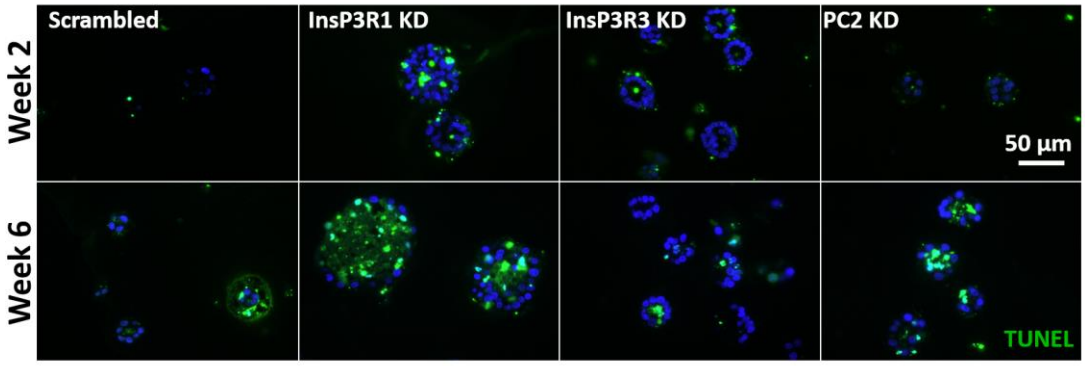

Figure 2.2 H&E and TUNEL staining of cysts

Representative images of (a) H&E staining used to assess the morphology of cysts in 3D tissues and (b) TUNEL staining (green) within the center of the cyst is indicative of apoptotic cell death. Nuclei (DAPI) are in blue). (Scale bar 50 µm in all images). (Modified from Kuo, Desrochers, Palma et.al(36))

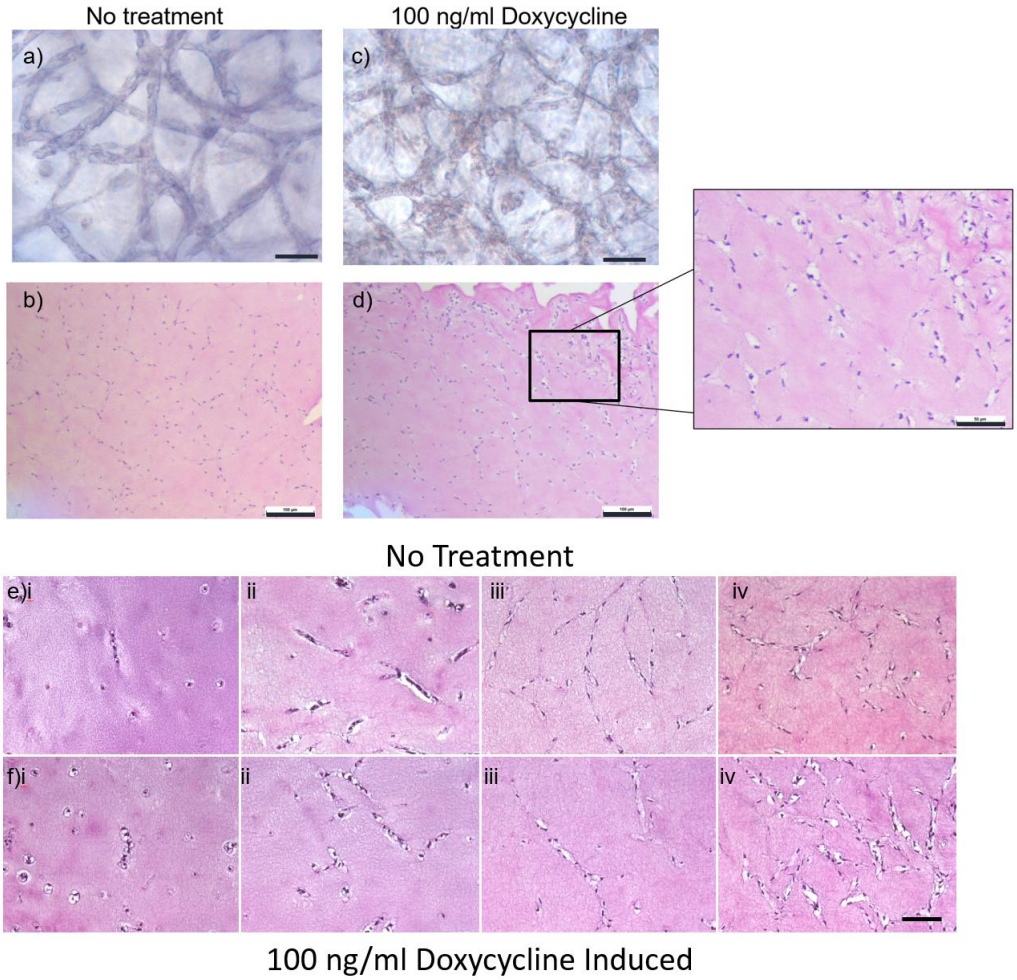

Figure 2.3 Histological analysis of NKi-2 culture in response to PKD1 knockdown induction

Renal cortical epithelial cells (NKi-2) after 5 weeks of culture. All cultures were established for 2 weeks prior to perturbing with 100ng/ml doxycycline for 3 weeks. Control controls (a,b,e) and treatment cultures (c,d,f) were analyzed using whole mount carmine staining (a&c) or H&E on tissue sections (c,d,e,f). The effect of collagen composition on tubule dilation was explored using culture of 1.0 mg/ml (i), 1.2 mg/ml (ii), 1.5 mg/ml (iii) and 1.8 mg ml (iv0/ (Scale bars –50 µm (a, c, & inlay), 100 µm (c,d,e,f))

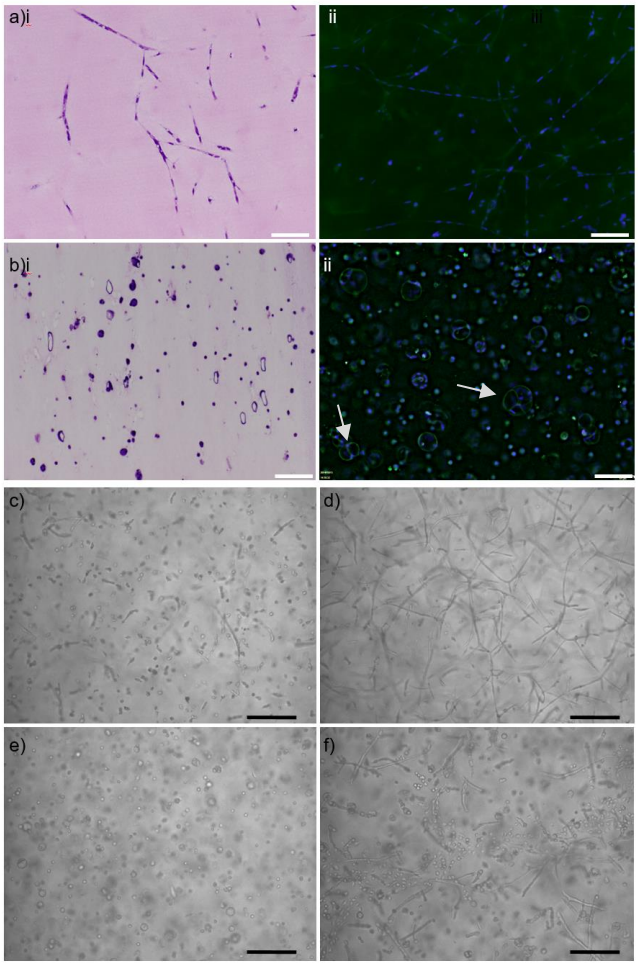

Figure 2.4 Comparative culture of NKi-2 and RPTEC cells and their respective media formulations

Immortalized renal epithelial cell lines NKi-2 (a) and RPTEC/tert1 (b) at day 14 of culture in Matrigel-collagen type 1 visualized using H&E staining of tissue sections (i) and fluorescent microscopy of f-actin (green) and nuclei (blue) in their respective media conditions (Table 2.1 – NKi-2 2% kidney formulation, RPTEC/tert1 – ATCC formulation) (Scale bars - 100µm). Comparative media experiments were performed to elucidate the role of media composition on morphology. Brightfield imaging at day 7 of NKi-2 cells in ATCC media (c) and 2% kidney media (d) and RPTEC/tert1 cells in ATCC media (d) and 2% kidney media (e) (Scale bars - 100µm).

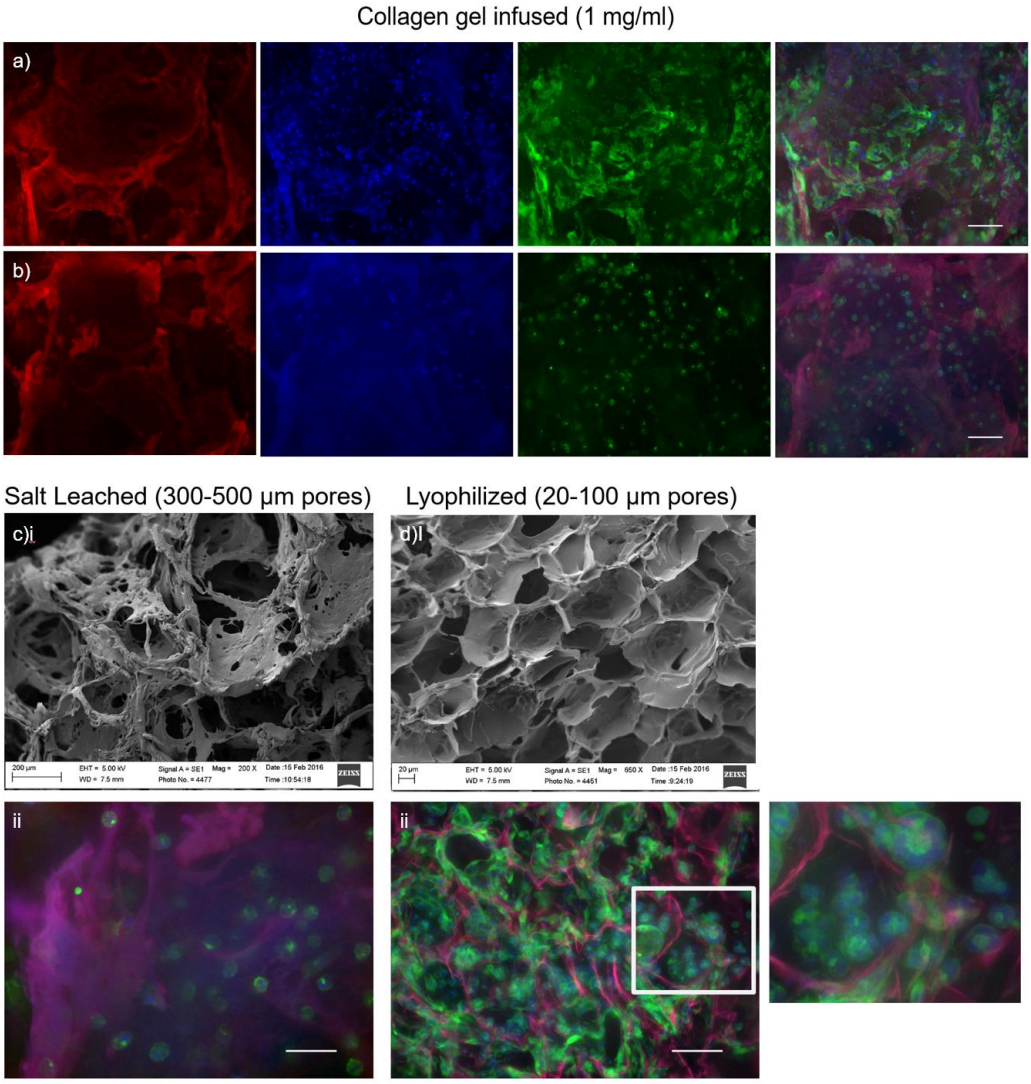

Figure 2.5 RPTEC/tert1 culture within porous silk scaffolds

Fluorescent and scanning electron microscopy of RPTEC/tert1 morphology after 2 weeks in porous silk protein scaffolds. RPTEC/tert1 were re-suspended in either a) collagen type 1 or b) Matrigel before infusion into salt leached sponges. Scanning electron microscopy of c) salt-leached and d) lyophilized silk sponges. Fluorescent microscopy of RPTEC/tert1 in Matrigel seeded within the different sponges. (Red-adipoRed (silk), Blue-DAPI, Green-phalloidin, Scale bars - 200µm (a,b) 100µm (c,d))

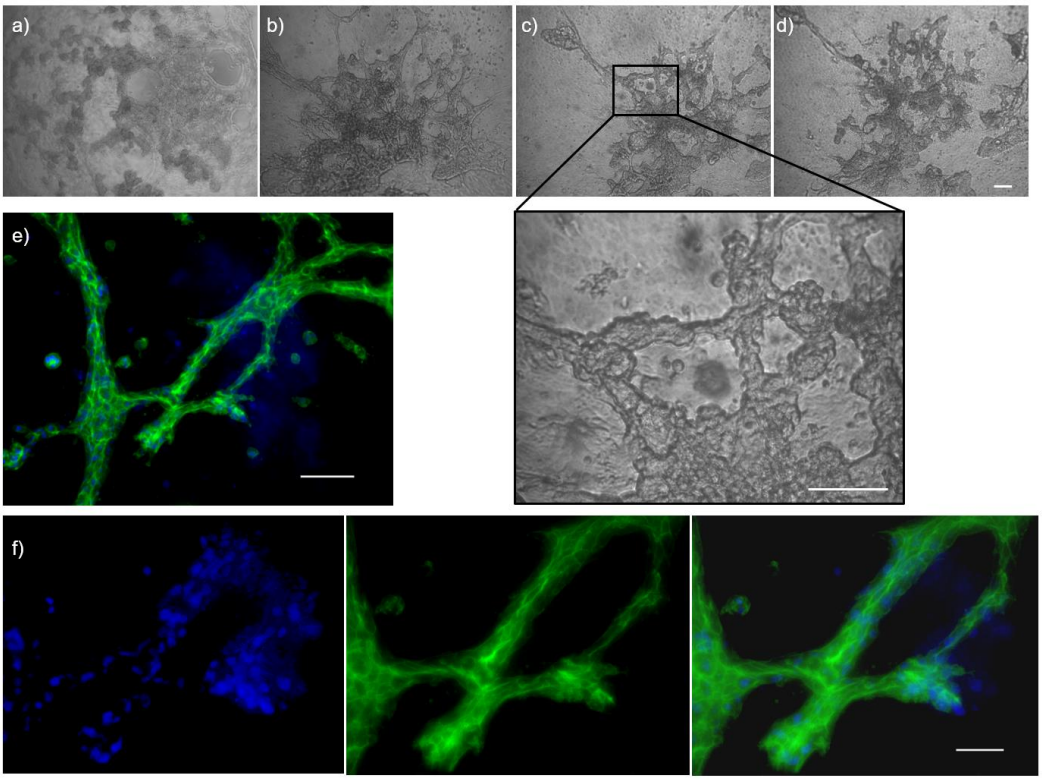

Figure 2.6 RPTEC/tert1 hanging drop aggregates embedded within 3D culture

RPTEC/tert1 cells were suspended in 10µl droplets, at a concentration of 80,000 cells per droplet, for 48 hours prior to embedding within Matrigel-collagen type 1 hydrogels. Bright field images of aggregates at a) 48 hours, b) 2, c) 5, and d) 12 days post-embedding (Scale bars – 100µm). Full focus z-stack fluorescent microscopy of day 12 structures (e&f) (blue-DAPI, green-phalloidin, Scale bars – 100/50µm)

Chapter 3. Perfusion Systems for 3D Kidney tissue Culture Applications

Abstract

Advancements in microfluidic and 3D tissue culture techniques have demonstrated the importance of both microenvironment and mechanosensory stimulation in establishing physiologically relevant, *in vitro* models for disease studies and drug development. We present a modular, three dimensional perfusion culture system that supports the controlled fluidic stimulation of a planar cell layer seeded on a 3D porous, silk protein scaffold. The use of the silk scaffold as a support material for perfusion culture enables optimized extracellular matrix incorporation, co-culture and cell seeding independent of the fluidic device before exposing the luminal cell layer to shear stress. Flow within the device is maintained using pressure-supported peristaltic flow that provides the benefit of media buffering and low media consumption despite the higher volumetric flow rates required to achieve the same shear stresses used in microfluidic culture platforms. Additionally, the device and fluidic setup allow for access to the basal and luminal surfaces during perfusion, thereby enabling dual side perturbations and easy access to the biomaterial scaffold for downstream measurements. In this approach the culture surface of the 3D silk scaffold is independent of the perfusion system, thus allowing the cell microenvironment to be optimized without effecting flow within the system. The utility of this bioreactor system was successfully demonstrated using kidney epithelial cells as a model cell type that have been shown to phenotypically respond to shear stress. This system provides for the fluidic control and cell stimulation achieved using standard microfluidic approaches but combined with physiologically relevant microenvironments of 3D culture.

3.1. INTRODUCTION

Tissue engineering approaches to increase the physiological relevancy of *in vitro* model systems are valuable tools for studying tissue and organ function, disease pathophysiology and drug efficacy and toxicity. Advancements in three dimensional (3D) tissue culture and microfluidic organ-on-a-chip technologies have demonstrated the importance of microenvironmental cues on cell phenotype and function. In 3D culture, the surrounding extracellular matrix (ECM) has been shown to be critical for recapitulating the insoluble and mechanical signaling experienced *in vivo* which can affect cell proliferation, polarity and differentiation (79-81). Similarly, the mechanical stimulation of luminal cell types with fluid induced shear stresses, offered by microfluidic culture systems, has been shown to alter cellular reorganization, barrier formation and protein expression (82-85). Due to the benefits of 3D and microfluidic culture techniques, there has been an increased effort to advance a combined 3D microfluidic approach.

Early organ-on-a-chip devices that rely on porous or solid substrates coated with a thin layer of ECM have demonstrated tissue-specific barrier functions and cell polarization in response to mechanical stimulation (86-88). However, the use of a solid synthetic substrate limits the direct cell-cell contact and ECM modifications that are observed in in vivo tissue development and disease progression (89-91). Recently, more complex organ-on-a-chip devices have emerged whereby channels are formed within ECM hydrogels and coated with luminal cell types. For instance, the chemotactic stimulation of neovessels formed via branching angiogenesis from the lumen of an endothelial lined collagen tube was reported (92). Similarly, a kidney proximal tubule luminal device was used to assess

the efficacy of a nephrotoxicity biomarker following exposure to a known nephrotoxin (93). Despite the success of these systems, their versatility is limited due to the constraints of current microfluidic luminal devices. Specifically, these devices rely on high concentration collagen gels and low shear stresses to maintain luminal integrity, meanwhile *in vivo* higher levels of type I collagen are typically associated with fibrotic phenotypes (94). Moreover, for luminal cells, such as kidney epithelial cells, the surrounding basement membrane is typically composed of type IV collagen and laminin (94, 95). The dependency on only ECM hydrogels as the sole supporting surface for these studies inherently limits the ability to modify the system to meet biological demands without re-designing the system. These factors are particularly relevant as the field moves toward patient derived stem cells, considering that the differentiation of immature cell types can be influenced by the microenvironment composition and mechanical properties (96).

The goal of this work was to develop a perfusion culture system that provides both luminal and interstitial cell culture surfaces that are independent of the perfusion system in order to increase the overall utility and modularity. In the system we utilized porous silk protein scaffold supports as they are structurally robust, biocompatible, and do not inherently contain any cell signaling motifs. Therein, they can be utilized for application driven microenvironments such as stem cell-based tissue development and disease modeling. This novel system incorporates the fluidic control and cellular stimulation achieved with standard microfluidic approaches with the physiologically relevant microenvironments of 3D culture.

3.2. METHODS

3.2.1. Device Assembly

Negative molds for the top reservoir and channel layers of the polydimethylsiloxane (PDMS) bioreactors were designed using AutoCAD and 3D printed using a Stratasys® Connex™ 500 3Dprinter. Printed molds were cleaned thoroughly as per manufacturer's instructions including soaking in a 1% sodium hydroxide for 3 hours followed by repeat washes in DI water. Rapidly prototyped negative molds were dried completely in a 60°C oven and silanized. PDMS pre-polymer, silicone elastomer and the curing agent (Sylgard 184 Silicone elastomer kit, Dow Corning, Midland, MI, USA), were mixed at a 10:1 ratio and degassed via centrifugation before casting over the negative molds (Figure 3.1). The PDMS positive masters were cured overnight in a 60°C oven before casting with polyurethane plastic (Smooth Cast 310, Smooth-On Inc., PA, USA) as has been described in detail (97). PDMS replicas were formed following the same process as the positive masters and cured in 60°C oven for 4 hours. Inlet and outlet holes were punched out using a 2mm biopsy punch (Integra Miltex, York, PA, USA). The PDMS channel layer was bonded to a clean glass slide after treating both with plasma, followed by plasma treatment to bond the PDMS reservoir layer. Then 18-gauge blunt tip needles (VWR, Radnor, PA, USA) with the leur lock connection removed were bent at 90° and inserted into the inlet and outlet holes to complete device assembly (83).

3.2.2. Fluidic Assembly

For all perfusion studies, fluidic system components (bioreactor, inlet and outlet tubing, media vial) were fully assembled and autoclaved at 121°C for 20 minutes. For each assembly, holes for the pressure input and inlet and outlet silicone pump tubing

(Masterflex BioPharm, Cole-Parmer, Vernon Hills, IL, USA) were punched in the top of the PTFE septa of a glass vial (Wheaton, Millville, NJ, USA)). Inlet tubing Regulated pressure (5% CO_2 in air) was supplied to each bioreactor through a multiway stopcock manifold (Cole-Parmer) run through a 0.2 μm hydrophobic filter (EMD Millipore, Billerica, MA, USA) to silicone tubing (Saint-Gobain Tygon, Fisher Scientific, Pittsburgh, PA). To eliminate the influence of hydrostatic pressure on the system the media in the scaffold compartment was kept at the same height as the media in the vial. COMSOL Multiphysics was used to model fluid flow within the device using the setup parameters of the system.

3.2.3. Scaffold Fabrication

Silk fibroin (hereafter referred to as silk protein) solution extracted from *Bombyx mori* silk worm cocoons was prepared as previously described (63). Aqueous silk solution (6% w/v, 30 minute extraction time) was added into standard 12-well cell culture plates at a volume of 2 mL per well and frozen from 4°C to -45°C and lyophilized (-0.25°C/min) and held for 480 min, followed by ramping to -20°C at 0.2°C/min. Drying was conducted at -20°C and 100 mT vacuum for 33 hr (VirTis Genesis 25L Super XL Freeze-Dryer, SP Scientific, Stone Ridge, NY) (64). Samples were lyophilized for 48 hours and autoclaved at 121°C for 20 minutes at 15 psi to induce beta-sheet formation. Scaffolds were hydrated, cut to 10x12x2 mm and autoclave sterilized.

3.2.4. Cell Culture

Immortalized renal cortical epithelial cells (RPTEC/tert1, ATCC, Masasses, VA, USA) were cultured at 37°C in a humidified 5% CO_2 incubator in DMEM:F12 (Life Technologies, Grand Island, NY), 5pM triiodo-L-tyronine (Sigma-Aldrich, St. Louis, MO, USA), 10 ng/ml recombinant human epidermal growth factor (Life Technologies), 1 % ITS (Life

Technologies), 25 ng/ml prostaglandin E_1 (Millipore). 25 ng/ml hydrocortisone (Sigma-Aldrich), 0.1 mg/ml G418 (Life Technologies), and penicillin-streptomycin (Life Technologies, Grant Island, NY) (13). Sterilized silk scaffolds were vacuum dried and infused with a 1:1 mixture of growth factor reduced Matrigel-collagen (final collagen concentration 1.5 mg/ml, Corning Bioscience, Corning, New York) by repeatedly pipetting and squeezing; the excess was removed to ensure a smooth, flat surface before scaffolds were incubated at 37°C for 30 minutes to induce gelation (38). In a 12-well plate the top surface of the scaffold were seeded at 0.5 x 10^6 cells/scaffold and cultured for at least 9 days before conducting static and flow experiments. For flow experiments, scaffolds were exposed to a shear stress 0.2 dyne/cm^2 for 4 days. All experiments were completed at least in triplicate. For seeding within the scaffold bulk, scaffolds were soaked in media for at least one hour before vacuum drying. Human foreskin fibroblasts were then seeded in the pores of the scaffold. 1 x 10^6 cells/scaffold were and incubated overnight before infusing the scaffolds with ECM. Foreskin fibroblasts were cultured in 10% fetal bovine serum and 1% penicillin-streptomycin in DMEM.

3.2.5. Immunocytochemistry

Scaffolds were washed with PBS and formalin fixed for 12 minutes. For actin staining, samples were washed with PBS and probed with AlexaFluor488-phalloidin (1:40, Molecular Probes, Eugene, OR, USA) and DAPI (1:1000, Molecular Probes) for 1 hr at room temperature in 0.1% Triton and 1% bovine serum albumin (BSA). For ciliary staining, 2 mm sections were biopsy punched from the scaffold, permeabilized for 20 minutes in 0.1% Triton, blocked and probed with acetylated tubulin (1:50, Sigma-Aldrich) overnight at 4°C. Samples were then incubated with anti-mouse secondary (molecular probes) for 1 hr at room temperature. Silk was counterstained using AdipoRed (1:1000, Walkersville,

MD, USA). All imaging was conducted using a Keyence BZ-X700 inverted microscope (Osaka, Japan).

3.2.6. Scanning electron microscopy

Silk scaffolds were dehydrated in graded ethanol and dried overnight at room temperature. Samples were gold sputter coated before observation using a Zeiss EVO MA10 Scanning Electron Microscope (SEM) (Oberkochen, Germany).

3.3. RESULTS AND DISCUSSION

3.3.1. Perfusion System Design

A modular 3D perfusion system was designed capable of supporting a porous silk protein scaffold for culturing luminal cells under sustained flow. The device consisted of two polydimethylsiloxane (PDMS) layers, a channel 44 x 6 x 2 mm and a 10 x 12 mm compartment, bonded to a glass slide (Figure 3.2a). The design allowed the bottom of a silk scaffold inserted into the top reservoir to be placed in direct contact with the flow field. The scaffold compartment width was offset by 2mm on each side of the channel in order to incorporate scaffold support ledges without disrupting the flow (Figure 3.2b). The perfusion device enabled both luminal and interstitial cell access (Figure 3.2). Luminal cells cultured on the bottom of the scaffold were exposed to flow while the cells within the interstitial compartment were stimulated through the media reservoir. If desired, interstitial media components and perturbations can be introduced through this chamber independent of the perfusion compartment. This approach enables dual conditions without having two fluidic setups.

In contrast to current state-of-the-art perfusion approaches, this system is based on supporting a modifiable, 3D culture interface. Flat-bottomed, lyophilized silk sponges

were utilized in the system with a pore size on the bottom surface of approximately 20 microns (Figure 3.2b). Silk protein scaffolds were utilized as the support material due to the well-documented ability for long-term culture of numerous of cell and tissue types including bone, skin, kidney, brain, intestine, and adipose (38, 98-100). The use of a silk scaffolds inherently increases the versatility of the system due to the availability of established methods for functionalizing the material surface based for tissue-specific culture requirements, along with control of pore size, pore orientation and mechanical properties (64, 101-103).

In the SEM images, the silk scaffold was shown to have a continuous mesh-like porosity. Consequently, a hydrogel was able to be infused and trapped within the pores in order to provide a culture surface. The silk scaffold provides the structural integrity independent of the composition and mechanical properties of the cell-matrix interface. As such, cells can be cultured on a surface with the desired stiffness, protein composition or organization necessary for achieving a particular phenotypic or functional outcome. This approach provides unique modularity that is unachievable in conventional perfusion setups, including microfluidic and channeled hydrogels, considering in these systems the culture surface needs to be optimized for structural integrity as opposed to cellular response. Accordingly, this system enabled perfusion studies without the loss of the physiologically relevant microenvironments that are necessary for studying tissue and disease development.

Within the device, the silk scaffold functioned as the top surface of the perfusion channel. Standard PDMS microfluidic devices can be designed with an aspect ratio as low as 1:20 (height:width) before occlusion of the channel due to sagging becomes an issue

(104). The present devices, however, were designed at a conservative 1:3. aspect ratio to accommodate a greater range of scaffold mechanical properties (97). Therefore, the system can be modified to accommodate larger or smaller scaffold dimensions following these design specifications.

3.3.2. Device Fabrication and Optimization

Soft lithography techniques were not necessary for the device due to the feature sizes, therefore the original master molds were produced using a Stratasys® Connex 500™ 3D printer. These molds were transitioned to biocompatible plastic masters though a modified version of standard protocols that accounts for the porosity of 3D printed materials (Figure 3.1) (97). Rapid prototyping of the molds was used to increase the precision and reproducibility of the devices, however this approach can also be applied to machined molds if desired.

The scale of the system and the need for open access to the top reservoir necessitated the development of a custom fluidic setup (Figure 3.3a). While the system parameters allow for laminar flow within the device (Figure 3.3b), higher volumetric flow rates are required to achieve the same shear stresses shown to result in phenotypic changes in comparable organ-on-a-chip microfluidic devices (32). Therefore, a peristaltic pump was used to enable recirculation of the media (Figure 3.3). Subsequently, the system only required enough media to fill the dead volume within the tubing (5 ml on average). The final fluidic setup also included a pressure source, consisting of 5% CO_2, connected to the media reservoir as a means of priming the inlet tubing. The use of an external pressure source allows for media buffering independent of the bioreactor or tubing permeability. The device was placed within a 10cm petri dish in order to maintain sterility.

To establish the biological utility of the system, human kidney epithelial cells were chosen as a model luminal cell type for proof of principle studies. These cells have an established phenotypic response to flow induced shear stresses as low as 0.2 dyn/cm^2.(32) COMSOL modeling was used to confirm that cells on the bottom of the silk scaffold would be exposed to uniform shear stress at the desired intensity (Figure 3.3c). For other cell types such as vascular endothelial cells, which are naturally exposed to higher shear stress, 2-20 dyn/cm^2, the system can be scaled down as necessary with the same 1:3 aspect ratio in order to use similar flow rates and achieve the higher shear stress (105). Although media consumption is not a limiting parameter within the system, the maximum volumetric flow rate was constrained by the peristaltic pump and tubing limitations.

3.3.3. Cell incorporation and perfusion

As described, the silk scaffold can be cultured independent of the device. To establish a confluent layer of luminal cells, the scaffolds were first infused with ECM proteins before direct cell seeding on the surface of the scaffold that was ultimately exposed to flow (Figure 3.4a). If desired, interstitial cells can be incorporated prior to, or at the time of, ECM incorporation. To demonstrate this capability we cultured human foreskin fibroblasts in the scaffold bulk for 24 hours prior to infusing the scaffolds with a Matrigel-collagen solution (Figure 3.4b). F-actin staining shows fibroblast elongation along and in-between the pores of the scaffold. As with standard 3D cell culture techniques, parameters such as cell density and ECM composition can be altered to accommodate the specific needs of the tissue system.

For the luminal cell type we utilized immortalized human renal cortical epithelial cells cultured on the Matrigel-collagen hydrogel infused silk scaffold. This ECM composition has supported physiologically relevant 3D structure formation in healthy and diseased kidney epithelial cultures.(36, 38) Renal epithelial cells on the scaffold surface exhibited the differentiated cuboidal phenotype of tubular epithelial cells with f-actin localized to the cell membrane (Figure 3.4d-e). The ability to establish this confluent monolayer using standard cell culture techniques supported the relevance of this system. After exposing the scaffolds to a shear stress of 0.2 dyn/cm^2 for 4 days, immunofluorescence microscopy analysis was used to assess primary cilia expression. Renal primary cilia are thought to be mechanosensors that regulate epithelial phenotype and cell signaling pathways (106). In kidney-on-a-chip devices, exposure to shear stress is typically shown to increase primary cilia expression (32). However, the RPTEC/tert1 cells utilized for this study are known to consistently express primary cilia in standard 2D culture and changes in cilia have been shown to occur as part of renal injury and repair processes *in vivo* (13, 107). In comparative culture of RPTEC/tert1 cells on the scaffold under static and perfused conditions, cilia expression was found to be consistent (Figure 3.5). This consistency demonstrates the benefit of using an optimized culture surface for static controls, whereby flow is not required to achieve a differentiated epithelial phenotype. Furthermore, the ability to maintain ciliary expression, a flow-sensitive physiologically relevant phenotype, demonstrates the utility of this new approach for fluidic perturbation studies seeing as the device itself does not yield an injured cell response.

The fluidic assembly and tissue culture capabilities presented here constitute a convergence of functionalities currently unavailable within 3D perfusion systems. For

instance, this platform offers the ability to fully optimize the cellular microenvironment and co-culture conditions prior to exposing the tissue construct to physiologically relevant shear stresses. This modular approach will enable novel multiplexed studies of physical and biological perturbations. Specifically, this system is uniquely suited for pursuing questions with respect to luminal cell phenotype (i.e. response to shear, polarization, differentiation) and overall barrier integrity (i.e. tight junction formation, cell damage) in healthy and diseased microenvironments (i.e. matrix stiffness, ECM composition, basal side cytokine stimulation). These questions are particularly important for better understanding disease progression in cancerous and fibrotic tissues.

3.4. CONCLUSIONS

The modular platform presented here represents a robust, scale-able approach to 3D perfusion culture. The simplicity of the design and the use of readily available materials maintains a low barrier to use. The use of a porous silk scaffolds as a support material allows for spatially controlled co-culturing of multiple cell types, scaffold functionalization and the use of physiologically relevant ECM compositions. Importantly, tissue constructs can be optimized without affecting the ability to perform perfusion studies. Moreover, the pressure-supported peristaltic flow setup provides features without compromising the ability to expose the cells on the luminal surface to controlled shear stresses while maintaining low media consumption. Overall, this combination of features constitutes a useful range of capabilities within a 3D perfusion system conducive to supporting studies of tissue development and disease progression.

3.5. TABLES AND FIGURES

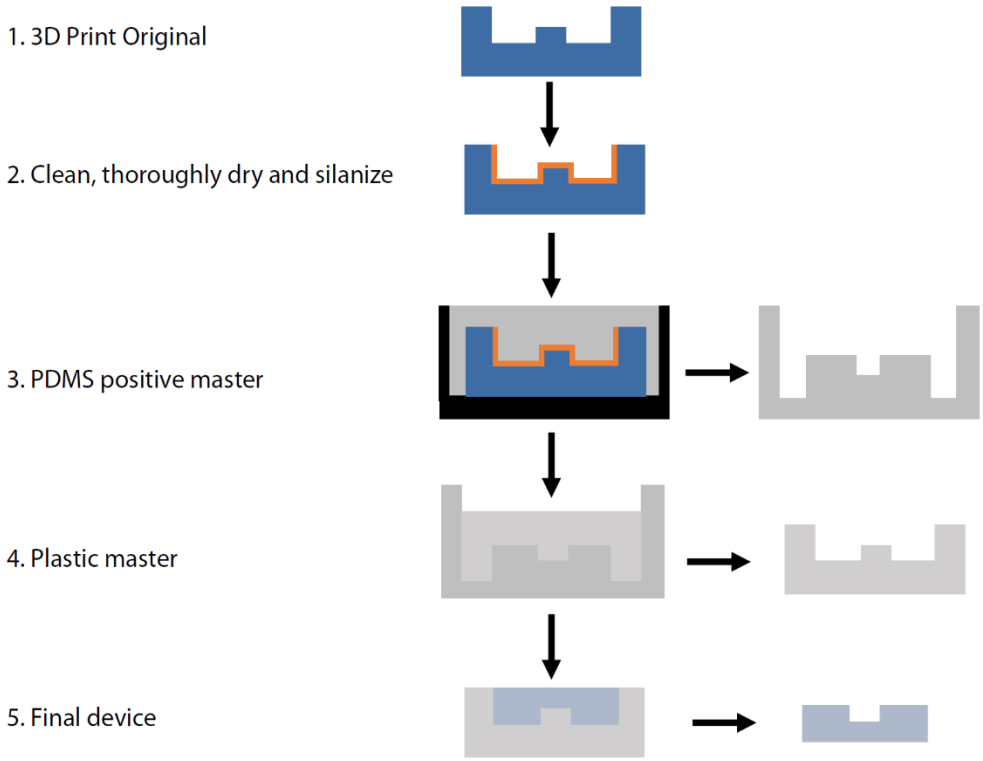

Figure 3.1 Bioreactor fabrication procedure

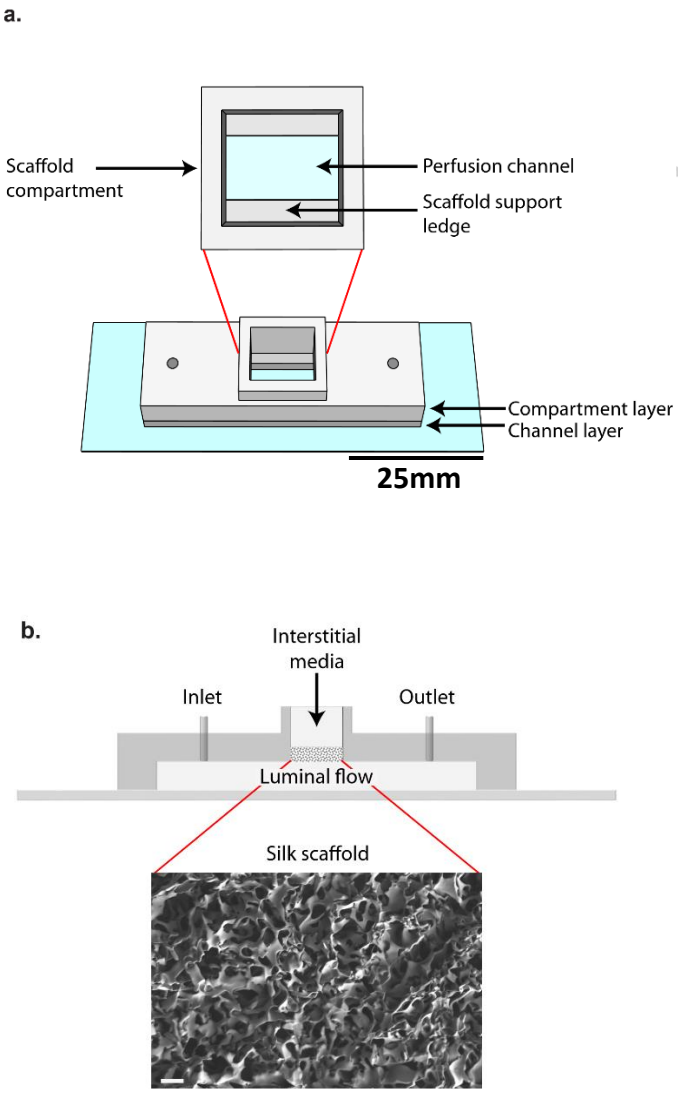

Figure 3.2 3D perfusion bioreactor design

(a) AutoCad model of the assembled polydimethylsiloxane (PDMS) channel and compartment layers bonded with plasma treatment to a glass slide. The top view inlay depicts the scaffold support edges that allow the seeded scaffold to be placed in direct contact with the flow field. (b) Side profile schematic of the assembled device depicting the scaffold location, luminal flow and interstitial media reservoir (not to scale). The scanning electron micr oscopy (SEM) inlay depicts the porosity of the bottom surface of the lyophilized silk scaffold (Scale bar – 20 µm).

Figure 3.3 Pressure driven peristaltic flow fluidic setup

a) Schematic of the pressure-dependent, peristaltic flow setup. COMSOL models of the (b) laminar flow within the device and (c) shear stress at the scaffold surface.

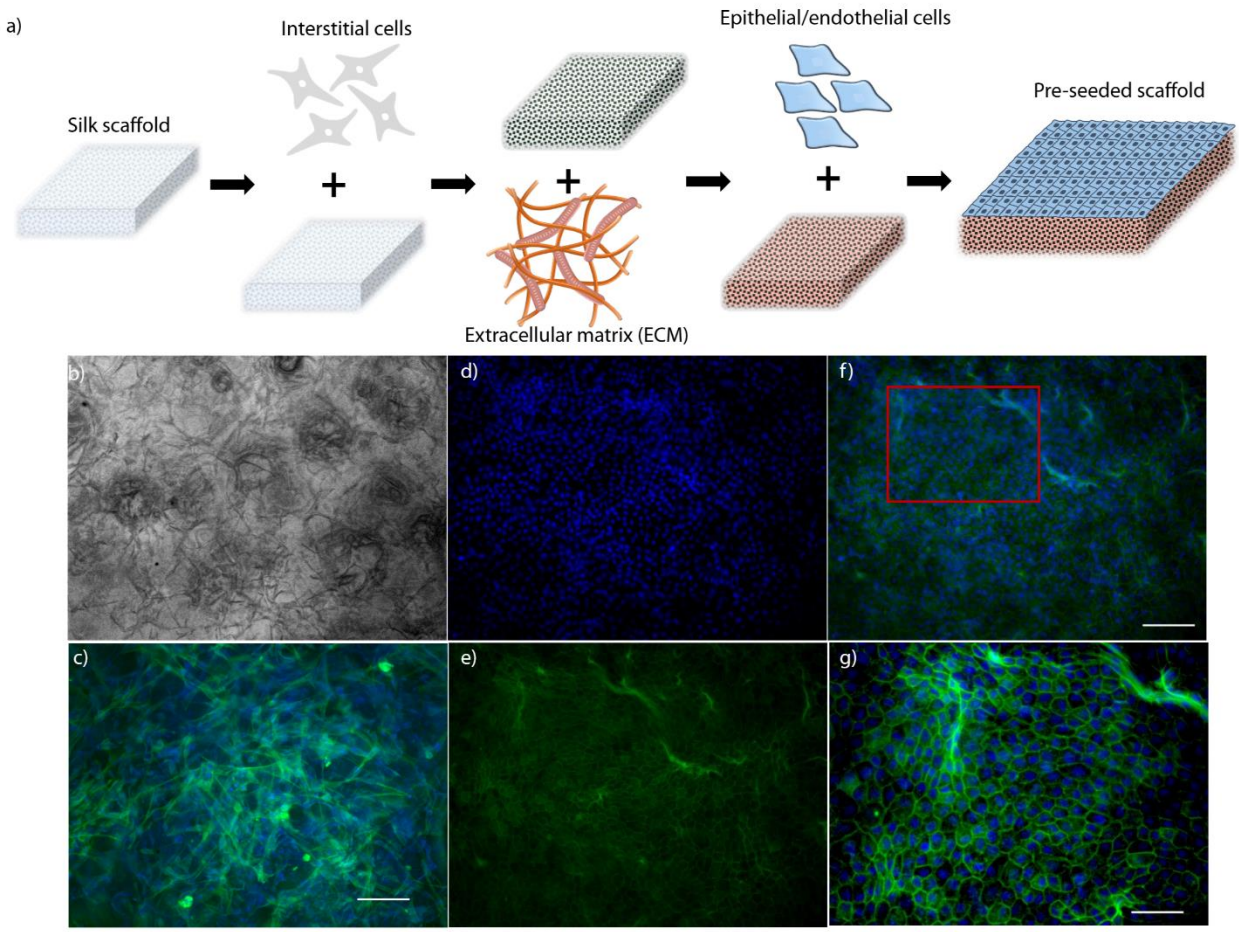

Figure 3.4 Off-device seeding of the silk scaffold with multiple cell types.

(a) Schematic overview of the seeding protocol for incorporating cell and extracellular matrix (ECM) within the bulk space and cells on the surface. (b,c) Brightfield image of the scaffold bulk with human foreskin fibroblasts seeded within. (d-g) Confluent coverage on the scaffold surface by renal proximal tubule epithelial cells (Full focus z-stacks, Scale bars – (b-f) 100 µm, (g) 50 µm, green – phalloidin, blue -DAPI) .

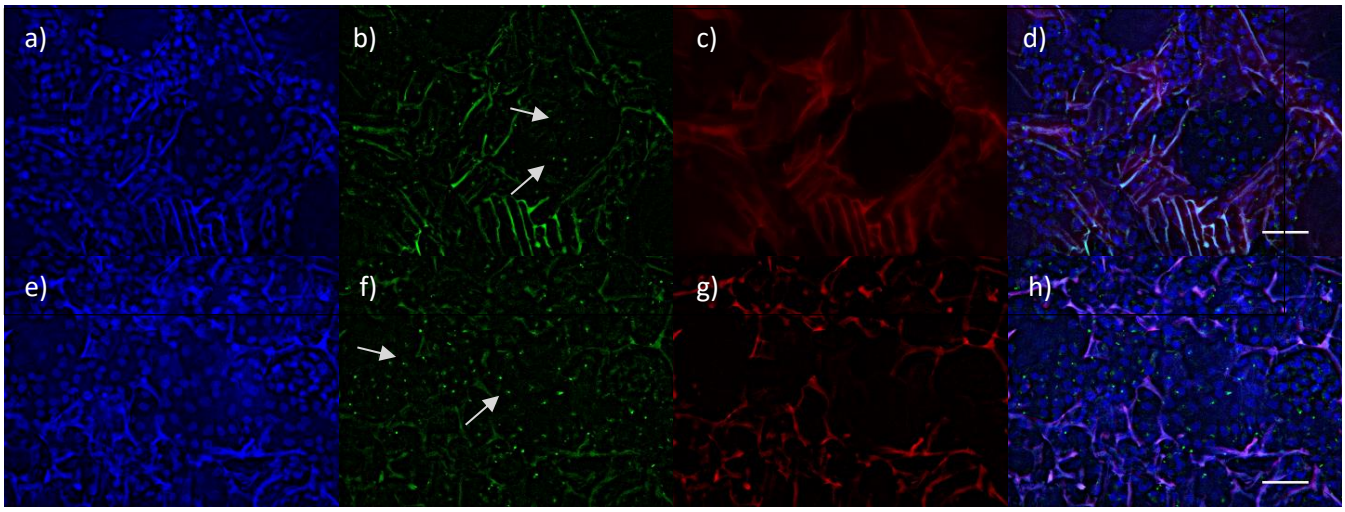

Figure 3.5 Cilia formation under static and perfusion conditions

Cilia formation by renal proximal tubule epithelial cells under static (a-d) and perfused (0.2 dyn/cm^2 for 4 days) conditions (e-h). (a,e) Adipored stain of the silk scaffold surface (b, f) DAPI (c,g) acetylated alpha tubulin (d, h) image overlay (scale bar - 50 µm)

Chapter 4. SELF-ORGANIZING RENAL EPITHELIAL TUBULES WITH POLARIZED LUMENS

ABSTRACT

Proximal tubular epithelial cells mediate a significant subset of the regulatory and endocrine functions in the kidney. Due to this functionality, these cells are also a major site of injury and pathogenesis. Accordingly, *in vitro* model systems are important tools for understanding disease pathogenesis and nephrotoxicity. We present a simple assay system for the *in vitro* formation of renal epithelial tubules using the telomerase immortalized human proximal tubule cell line (RPTEC/tert1). This methodology for *in vitro* kidney tubule formation is an adaptation of the methodology used for *in vitro* angiogenesis on the surface of gelled basement membrane extract. Early cell migration and branching can be tracked using time-lapse microscopy. Confocal microscopy conducted on these structures after 1 week of culture verified the formation of three-dimensional luminal tubules with polarized epithelial cells expressing proximal tubule specific transporters. In the tubules, the RPTEC/tert1 cells assumed a cuboidal phenotype with an actin-rich apical surface suggestive of a brush border. The method was also adaptable to co-culture, where self-organization of renal epithelial cells occurred within mixed culture with kidney stromal cells. Direct mixing of stromal and epithelial cells yielded luminal structures whereas embedding stromal cells within the gelled matrix hindered lumen formation. Additionally, treatment with transforming growth factor beta (TGFβ1) resulted in a loss of tubule polarization and luminal morphology. Combined, these results support the utility of this approach for studies of tubule developmental and diseases associated with these structures.

4.1. INTRODUCTION

In vitro tissue models which recapitulate the phenotype and function of human renal tissue are valuable tools for studying kidney development, disease pathophysiology and nephrotoxicity. Fundamentally, three dimensional tissue engineering approaches provide systems for mimicking cell to cell and extracellular matrix interactions as found in native tissue (108). Of particular relevance to kidney tissue models is luminal morphology of epithelial tubules that comprise the nephron. Region specific epithelial polarity is necessary for the transport of solutes and fluids against concentration gradients that maintains homeostasis and regulate excretion (109). This polarization is comprised of an apical surface facing the lumen and a basolateral surface in contact with the basement membrane and interstitial fluid. In addition to the functional role of polarity, loss of this phenotype has been implicated in the development of certain diseases such as polycystic kidney disease and renal fibrosis (110-112). Accordingly, three dimensional (3D) tissue engineering approaches which yield luminal morphologies have gained significant interest as a tool for understanding kidney biology and disease pathology.

The formation of luminal structures *in vitro* has traditionally been achieved by embedding epithelial cells in hydrogels such as collagen or Matrigel. These established protocols use well-characterized kidney epithelial cell types such as Madin-Darby canine kidney (MDCK) or LLC-PK1 (derived from pig kidney) cells to form luminal cysts. These systems have been applied to studies of kidney development and disease (36, 113, 114). These approaches have also been used to study cyst formation by primary human cells

derived from patients with autosomal domain polycystic kidney disease (35, 40, 41). Despite the success of this technique for elucidating disease mechanisms, the formation of tubules with polarized lumens has not been fully realized using this methodology. For instance, MDCK undergo branching morphogenesis in the presence of hepatocyte growth factor, but these structures do not represent a fully differentiated epithelial phenotype (115).

Recently, alternative three dimensional tissue engineering approaches have been developed which achieve tubule structure formation. Advancements in bioprinting have enabled human telomerase immortalized human proximal tubule cells (RPTEC/tert1) to be grown in a perfusable channel surrounded by an extracellular matrix (ECM) (47). This approach achieved a polarized epithelium in convoluted channels (ranging from 400-550 µm in diameter) after 3 weeks of culture. At the same time, developments in the stepwise differentiation of human pluripotent stem cells has led to the formation of segmented nephrons in organoid cultures (51). The recapitulation of kidney organogenesis using human cell sources to achieve a diverse subset of renal cell types constitutes a significant advancement within the field. However, at the current stage of development, these organoids have more transcriptional similarity to first-trimester kidneys compared to an adult (53). This approach to organoid culture has also been combined with a "sandwich" 3D culture where cavitated spheroids formed tubule organoids after 23 days in culture (54). Although these novel approaches to kidney tissue engineering achieve a higher level of tissue architecture, they require significant culture time and complexity to achieve luminal phenotypes.

There remains a need for an assay system for kidney epithelial tubulogenesis that leads to the formation of polarized tubules at a physiologically relevant scale using human cell sources. Endothelial tube formation assays, whereby endothelial cells form capillary-like tubes on the surface of a gelled basement membrane extract, have been around since 1988 (116). This technique is commonly used to study angiogenesis signaling factors, angiogenic compounds and the role of paracrine signaling on angiogenesis (117-119). While not as developed, epithelial cells cultured on the surface of ECM has also been used for morphogenesis of human kidney cell sources in order to better the differentiated phenotypes of stem cells. This technique has yielded networks of cords or multicellular tubule-like structures, but consistent luminal tubule formation was not fully realized (120, 121).

The goal of the present study was to develop a methodology whereby RPTEC/tert1 cells form 3D tubules with polarized lumens when cultured on a Matrigel surface. The proximal tubule segment of the nephron is of particular interest as an *in vitro* model considering approximately two-thirds of filtered solutes and water are reabsorbed in this segment in addition to functions with respect to metabolic clearance, hormone regulation and drug secretion (122). RPTEC/tert1 cells are a well-characterized cell line which in 2D have transepithelial electrical resistance (TEER) confirmed barrier formation, parathyroid hormone stimulated cyclic adenosine monophosphate (cAMP) induction and sodium dependent uptake (13). Furthermore, this cell line has been validated to express the appropriate transporters for xenobiotic transport and pharmacokinetic studies in addition to sensitivity to repeat dose toxicity (72, 73). This approach to RPTEC/tert1 culture enables real time tracking of early tubule formation similar to the endothelial tube formation assays. Physiologically relevant structure formation after 1 week in culture was

characterized with respect to morphology, polarization and transporter expression. These structures are stable for at least 1 month of culture. Co-culture experiments and physiologically consistent tubule response to treatment with TGFβ1, a mediator of renal fibrosis, support the utility of this approach to future screening and disease studies.

4.2. METHODS

4.2.1. Cell Culture

All cells were maintained in a humidified 5% CO_2 incubator at 37°C. Immortalized renal cortical epithelial cells (RPTEC/TERT1, ATCC, Masasses, VA, USA) were cultured in DMEM:F12 (ATCC), 5pM triiodo-L-tyronine (Sigma-Aldrich, St. Louis, MO, USA), 10 ng/ml recombinant human epidermal growth factor (Life Technologies, Grand Island, NY), 1 % ITS (Life Technologies), 25 ng/ml prostaglandin E_1 (Millipore, Billerica, Ma). 25 ng/ml hydrocortisone (Sigma-Aldrich), 0.1 mg/ml G418 (Life Technologies), and penicillin-streptomycin (Life Technologies) (62).

FOXD1$^+$ stromal cells (from Foxd1^{LacZ+} mice), generously provided by our collaborator Thomas Carroll, were maintained in DMEM (Life Technologies) at 5% fetal bovine serum (FBS, Omega Scientific Inc., Tarzana, California) and penicillin-streptomycin (Life Technologies).

4.2.2. Tubule formation assay

For epithelial tube formation cells were cultured on the surface of phenol red free growth factor reduced Matrigel (Corning, Corning NY). Briefly, 200µl of Matrigel was evenly coated on the bottom of 24 well glass bottom plates (Cellvis, Mountain View, California) and incubated for at least 20 minutes at 37°C until gelation occurred. To maintain assay integrity, repeat freeze thaws of Matrigel were avoided. Unless otherwise

specified, 100,000 RPTEC/tert1 cells per well were seeded at a 1ml volume on the surface of the gel. Media was changed 3 times a week by replacing half of the volume with fresh media. Aspiration of media via pipette was used instead of a vacuum aspirator to limit disruption of structures forming on the surface.

Co-culture studies with $FOXD1^+$ stromal cells were conducted utilizing two different methodologies. $FOXD1^+$ cells were either re-suspended in Matrigel prior to gelation or mixed with RPTEC/tert1 cells at the time of seeding. For both approaches a concentration of 100,000 cells per well was used.

4.2.3. Time lapse microscopy

All time lapse imaging was conducted using a Keyence BZ-X700 inverted microscope (Osaka, Japan) with a small, desktop incubator attachment to maintain humidity, CO_2 concentration and temperature. Cells were observed using phase contrast microscopy and images were captured every 20 minutes.

4.2.4. Immunocytochemistry

Unless otherwise specified, all immunohistochemistry was conducted after 1 week of culture. Samples were washed with PBS and fixed in 4% paraformaldehyde for 12 minutes. For actin staining, samples were washed with PBS and probed with AlexaFluor488- or 568 phalloidin (1:40, Molecular Probes, Eugene, OR, USA) and DAPI (1:1000, Molecular Probes) for 1 hr at room temperature in 0.1% Triton and 1% bovine serum albumin (BSA). For other antibody staining, cells were permeabilized for 10 minutes in 0.1% Triton, blocked with 2% FBS and probed with primary antibody overnight at 4°C. Samples were then incubated with either AlexaFluor488 or 568 anti-mouse secondary antibody (molecular probes) for 1 hr at room temperature. For co-staining with

phalloidin, conjugated phalloidin was incubated alongside the secondary antibody. Primary antibodies utilized for these studies include aPKCζ (atypical protein kinase c, Santa Cruz Biotechnology, Dallas, Texas), SGLT2 (sodium-glucose transporter 2, Abcam, Cambridge, United Kindgdom), OAT1 (organic anion transporter 1, Abcam), and Ki67.

4.2.5. TGFβ1 Treatment

After 1 week of culture tubules were dosed with 10ng/ml of TGFβ for an additional week. Culture media containing TGFβ was replaced every other day. All experiments were conducted in triplicate.

4.3. RESULTS

4.3.1. Human renal proximal tubular epithelial cells self-organized to form 3D luminal structures

The formation of capillary-like structures that occurs after seeding endothelial cells on the surface of gelled basement membrane proteins is well established (116). A similar protocol whereby RPTEC/tert1 cells were cultured on the surface of growth factor reduced Matrigel also yielded luminal tubule structures. To characterize early structure formation, time-lapse phase contrast microscopy was used to observe cell migration and organization. Within 5 hours after the initial seeding, cells migrated into clusters (Figure 4.1a.b). Higher density cell clusters were observed in areas where there was a higher initial cell density. By hour 5, early branching occurred between the cell clusters that formed in areas with a lower initial cell density. At 15 hours post seeding RPTEC/tert1 cells continued to condense resulting in elongated branches and fewer cell islands (Figure 4.1c). Time-lapse video of this process revealed a shift from individual cell migration to tension between branches as the primary source of cellular reorganization on the culture

surface. This process continued until the formation of enclosed 3D structures which were characterized as early as day 6 post-seeding.

To optimize the formation of tubule structures, the relationship between initial seeding density and resulting structure formation was explored. Moreover, cell density has been shown to be a critical factor in the reproducibility of tube formation in endothelial cell tube formation assays (123). RPTEC/tert1 cells were seeded at densities of 50,000, 100,000 and 200,000 cells and tracked from day 1 to day 6. Cell density significantly altered structure morphology (Figure 4.2). Within 24 hours at a density of 50,000 cells per well, cells had condensed into isolated, truncated structures (Figure 4.2a) and by day 6 any elongated regions had further compressed (Figure 4.2b). At the highest density of 200,000 cells, the cells condensed into a combination of thick branches and cell islands, monolayer patches of cells (Figure 4.2e). After 6 days of culture, the continued remodeling and condensing was visualized via the decrease in the number of branches and gaps within the cell islands (Figure 4.2f). At this higher density, 3D structures formed, as indicated by the darker structure (black arrows), on the outer edges and where tubule branches have pulled away from adjacent cell islands.

At a density of 100,000 cells per well similar tubule condensing occurred. However, there were fewer initial cell islands and a greater number of independent tubule structures formed (Figure 4.2d-e). When stained for f-actin and nuclei the cellular organization within these structures was visualized (Figure 4.2, inlays). Fluorescence microscopy revealed a condensing of f-actin toward the center and a lining of nuclei along the edges of a presumptive lumen which is indicative of polarized structure formation.

Based on the higher frequency of condensed tubule formation at 100,000 cells per well this density was used for structure characterization and perturbation experiments. While this seeding density is optimal for short term experiments of 1 to 2 weeks, it has been visually observed that continued coiling can cause some structures to detach and float due to a loss of anchor points. At the same time, in some of the higher density cultures the continued coiling enabled the formation of larger structures that were be maintained for at least 1 month in culture (Figure 4.3). Although these aggregates also float, they were be monitored by eye during pipetting to prevent aspiration. Similar to the smaller tubules that form after 1 week at lower densities, these large tubule aggregates show nuclei lining the edge of the structure and f-actin condensed in the center when visualized as a z-stack from a standard fluorescent microscope (Figure 4.3). A cross-section of F-actin staining taken from a confocal z-stack depicts a tall, cuboidal epithelium surrounding the lumen (white arrows) similar to the morphology of proximal tubule epithelial cells *in vivo* (Figure 4.3d).

4.3.2. Human renal proximal tubular epithelial cells within 3D luminal structures displayed polarized phenotypes

Confocal sectioning and 3D reconstruction was used to assess 3D tubule polarization and morphology. After 1 week of culture, tubule structures consisting of a tall cuboidal epithelium and well-defined lumens were visualized via optical sectioning (Figure 4.4). The localization pattern of f-actin and aPKC in the *in vitro* tubule structures suggests physiologically relevant polarization (Figure 4.4). Upon 3D reconstruction, convoluted structure at the ends of the tubule were evident (Figure 4.4e).

In vitro tubule structures were stained for organic anion transporter 1 (OAT1) and sodium glucose transporter 2 (SGLT2) expression in order examine function. OAT1

staining was present on both the apical and basolateral surfaces of the luminal tubules whereas *in vivo* OAT1 is primarily localized to the basolateral membrane of the proximal tubule (Figure 4.5a) (124). SGLT2 expression was primarily localized to the luminal surface of fully formed tubules (white arrows, Figure 4.5b) (125). However, at points where a complete lumen was not present, SGLT2 expression localized to the outer edge of the plasma membrane.

4.3.3. Human renal proximal tubular epithelial cells retained 3D luminal structure formation in co-culture with stromal cells

A key goal in designing *in vitro* systems is to recapitulate the complexity and function observed *in vivo.* As a first step towards addressing this RPTEC/tert1 tubule formation was investigated in response to co-culture with stromal cells. Two strategies were employed; co-culture with kidney derived $FOXD1^{+}$ mouse stromal cells either by a 1:1 mixed culture on the Matrigel surface or by embedding the stromal cells within the ECM hydrogel prior to gelation followed by seeding of RPTEC/tert1. After 1 week of mixed epithelial-stromal culture, self-organization of epithelial cells into luminal tubules consisting of a cuboidal epithelium was visualized via optical sectioning after staining for f-actin (Figure 4.6a-b). A surrounding layer of elongated stromal cells (as indicated by the white arrows) was distinguished from the tubules by the change in cell morphology. When observed using phase contrast microscopy, the branching tubule structures, seen in the RPTEC/tert1 only culture, were not easily distinguished due to a dense halo of cells surrounding the structures (data not shown). Moreover, these structures were anchored to the Matrigel surface and could not be disturbed by aspiration in the same manner as the RPTEC/tert1 only culture.

When FOXD1^{+} stromal cells were embedded in the Matrigel layer prior to RPTEC/tert1 seeding, self-organization of epithelial cells was also visible (Figure 4.6c). A column of organized epithelial cells can be distinguished from the elongated morphologies of the stromal cells. However, when analyzed using optical sectioning a consistent lumen formation and structure polarization was not evident (Figure 4.6d).

4.3.4. TGFβ1 treatment of human renal proximal tubular epithelial cell forming tubules resulted in loss of polarity

To validate the utility of this methodology for use as a disease model, 1 week old RPTEC/tert1 tubules were treated with TGFβ1 for a week. TGFβ has been extensively studied *in vitro* and *in vivo* as a mediator of renal fibrosis (126). Untreated and treated structures were analyzed using confocal microscopy to determine changes in structure morphology, proliferation and polarization. After 2 weeks of culture of total culture time, untreated tubules maintain the cuboidal morphology and f-actin localization to the luminal surface and cell junctions as previously characterized at earlier time points (Figure 4.7a-b). In contrast, TGFβ treated structures showed a loss of centralized f-actin and a clear luminal structure (Figure 4.7c-d). Similarly, these structures lacked a consistent layer of cuboidal epithelium. Optical sectioning and aPKC staining were used to further confirm the loss of polarization. Compared to the untreated tubules, treated structures showed diminished luminal aPKC and f-actin staining (Figure 4.8). Moreover, in the original luminal space there was positive nuclei staining without any corresponding cytoskeletal staining. At 1 week, these structures also had Ki-67 nuclear staining at the convoluted ends of the structures, indicative of increased proliferation in response to treatment with TGFβ1 (Figure 4.8b).

4.4. DISCUSSION

In kidney tissue engineering, cystic morphologies can be achieved using standard 3D culture techniques where epithelial cells are embedded in an ECM hydrogel. On the other hand, current approaches to tubule formation typically require complex and time consuming techniques such as organoid differentiation and bioprinting. An easily deployed method for achieving physiologically relevant proximal tubule morphologies using a readily available human cell line can have applicability for a range of studies including disease development and nephrotoxicity.

We present a culture approach for the self-organization of renal epithelial cells *in vitro* to yield 3D tubules with polarized lumens on the surface of Matrigel. While the use of basement membrane extracts for tube formation assays in endothelial cell culture is well established, an equivalent approach for renal epithelial tubule formation had not been fully realized. Matrigel, which has a mesh structure of predominantly laminin and collagen type IV, mimics the basement membrane of proximal tubules *in vivo* (127-129). This approach which forms 3D structure on a 2D surface enables time lapse imaging using light microscopy to monitor cell migration and differentiation, along with tubule formation. Accordingly, this feature allows for the possibility of standardizing this assay within high-throughput well formats for computational analysis that can be used for functional screening of compounds (130, 131).

Another key distinction of this method from other approaches to generate lumens is the self-organization of differentiated structures in less than a week without complex differentiation protocols. The use of a readily available, well-characterized human proximal tubule cell line standardizes the approach for future assay applications and

reduces patient-to-patient variability associated with primary cell culture (13, 72, 73). Luminal structures are formed when culturing primary RPTEC cells using this approach, however, further optimization is necessary to achieve similarly polarized phenotypes (data not shown).

The formation of complex nephron structures from human pluripotent stem cells during organoid culture has the benefit of patient specific cell sourcing and the ability to study kidney functionality in the context of multiple cell types (14, 51, 54). However, structural immaturity and heterogeneity, in addition to longer culture times for organoid approaches (over 3 weeks before differentiated phenotypes are established), supports the need for supplementary methodologies using alternative cell sources. Moreover, the method presented here can potentially be used to provide insights into epithelial tubule formation and polarization that can ultimately be applied to enhance differentiation during organoid culture.

Morphological and phenotypical characterization of the luminal tubules confirmed the formation of polarized, luminal tubules. *In vivo* proximal tubules have a total diameter of about 40 microns and visual assessment of the *in vitro* tubules verifies the formation of structures within range of the physiological scale (132). *In vivo,* f-actin is concentrated in the microvilli of the brush border of proximal tubules, in addition to localization to the basolateral surfaces (133). Moreover, this localization is a necessary component of apical polarization and subsequent lumen initiation (134). Additionally, aPKC has been shown to maintain epithelial polarity and localize to tight junctions and the apical surface of kidney tubules (135, 136). Accordingly, mislocation of aPKC is known to disrupt tight junction formation and apical localization reflects luminal polarization (136, 137). The co-

staining of f-actin and aPKC at the apical surface of these structures suggests that epithelial polarization within these tubules occurs through established mechanisms of 3D morphogenesis (138).

The functionality of proximal tubules is directly dependent on transporter mediated reabsorption and secretion. SGLT2 is the primary transporter responsible for renal glucose reabsorption within the proximal tubules and OATs are responsible for the clearance of low molecular weight substrates, including drugs and toxins, from the kidney (139, 140). Specifically, SGLT2 at the luminal surface is responsible for glucose reabsorption in early segments of the proximal tubule and expression of this transporter is indicative of a differentiated phenotype (140). The expression of this phenotype within the *in vitro* tubules is not only important for normal function but for potential disease studies. The most prevalent cause of end-stage renal disease is diabetic nephropathy and SGLT2 inhibition has been recently targeted as an approach for reducing glucose with additional potential nephroprotectant properties (141). On the other hand, OAT1 expression on the basolateral surface is affiliated with proximal tubule secretion and the transportation of waste products and pharmaceutical compounds (142). The expression of OAT1 on all tubule surfaces is potentially indicative of incomplete polarization and more closely reflects the localization to the plasma membrane of human kidney cells that occurs in 2D culture (143). This outcome could be reflective of the fact that after tubule formation, these structures rest on top of the basement membrane and not all surfaces are in direct contact with the matrix as would be found under physiological conditions (109). Accordingly, further exploration of OAT transporter functionality is required before using this assay for assessing compound secretion into the luminal compartment.

To understand the potential for using this methodology for higher-order tissue culture studies we co-cultured RPTEC/tert1 cells with FOXD1^{+} stromal cells. Co-culture has been successfully used with endothelial tube formation assays to understand the role of paracrine signaling and direct content on angiogenesis (118, 144). Luminal tubule formation in mixed culture further validates epithelial self-organization using this culture approach. Moreover, these results suggests this methodology can be used to understand epithelial-stromal interactions during epithelial differentiation and disease development (145). The loss of luminal polarization in cultures where FOXD1^{+} cells were embedded within the ECM suggests a role of matrix mechanics in tubular morphogenesis. In 3D culture, stromal cells alter the biomechanical microenvironment by remodeling and condensing matrix density in a manner that can increase matrix stiffness (146, 147). Accordingly, MDCK cell morphology on the surface of Matrigel was dependent on the degree of cross-linking. On untreated Matrigel, MDCK cells assumed a 3D tulip hat-like morphology versus a flattened sheet morphology on cross-linked Matrigel (148). These results follow a similar pattern to the observations in the present study.

Finally, to evaluate the responsiveness of these structures to perturbation, we stimulated *in vitro* formed tubules with TGFβ1. TGFβ1 is known to facilitate the epithelial-to-mesenchymal transition, a pathophysiology of chronic kidney disease (EMT). Although EMT is implicated in the induction and development of renal fibrosis the mechanism is not fully understood (112, 149, 150). Upon treatment with TGFβ1, tubular structures responded with a significant change in morphology and a loss of epithelial polarization. This response was reflected in the loss of distinct luminal expression of f-actin and aPKC and positive Ki67 staining of cell proliferation. These phenotypic changes are in

agreement with the current understanding of EMT in the kidney and support the use of this assay as a tool for investigating the mechanisms of disease development (151, 152).

4.5. CONCLUSIONS

A method for forming 3D tubules using a human cell line, RPTEC/tert1 cultured on a Matrigel surface at an optimized cell density was established. Physiologically consistent lumen formation was confirmed with respect to structural morphology, polarization and glucose transporter expression. Co-culture experiments and TGFβ1 treatment response support the potential versatility of this approach for disease and development studies. Future characterization of the governing mechanisms of luminal polarization and relevant transporter expression will provide a deeper understanding of the applications of this approach. Additionally, this method can potentially be scaled for high-throughput drug screening and nephrotoxicity studies.

4.6. TABLES AND FIGURES

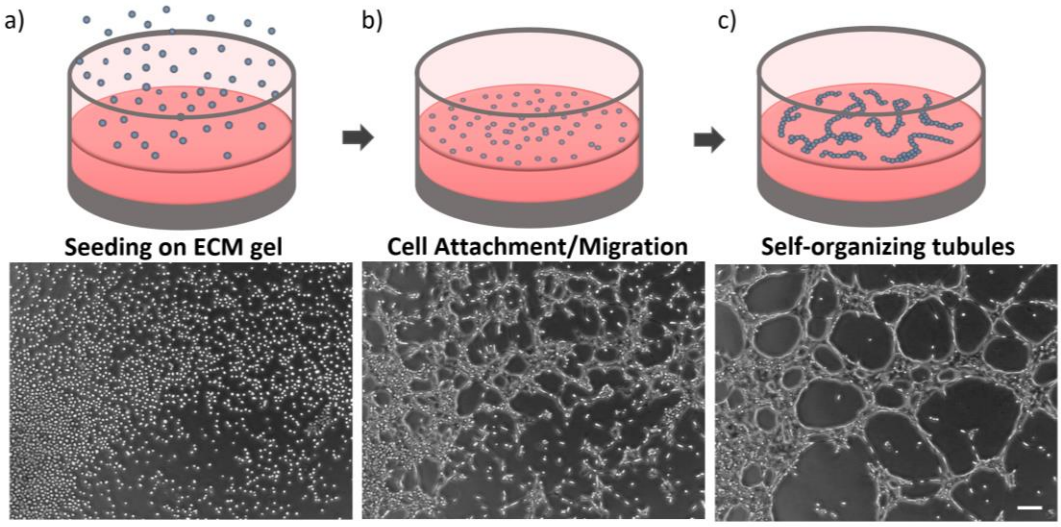

Figure 4.1. Schematic overview and time lapse imaging of the self-organization of RPTEC/tert1 cells

Representative images of a) 100,000 RPTEC/tert1 cells seeded on the surface of a thick layer of growth factor reduced Matrigel (hour 1). b) By hour 5 post-seeding cells attach and migrate into clusters and early branching begins to occur. c) Continued branching and condensing occurs within the culture until luminal tubules form (hour 15, scale bar – 100 µM)

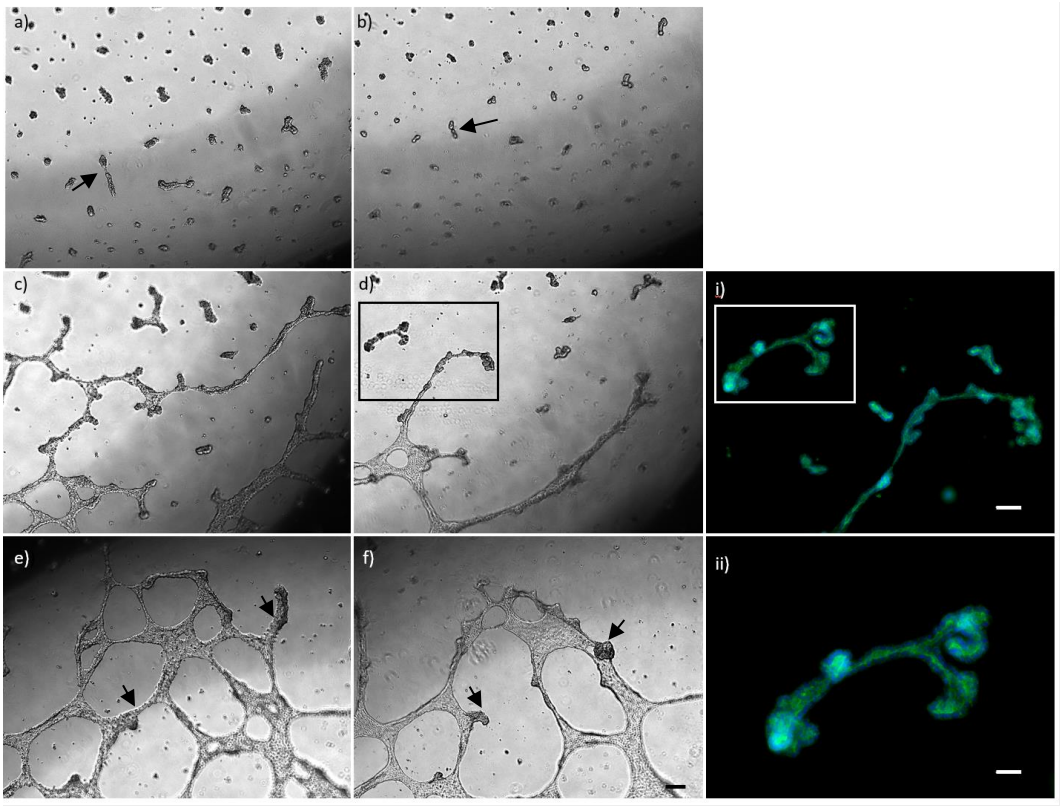

Figure 4.2 Seeding density and tubulogenesis

Representative images of cell density based differences in structure formation. Cells were seeded at 50,000 (a& b), 100,00 (c&d) and 200,000 (d&e) per well. Images were taken at 24 hours (a, c, & e) and 6 days (b, d, f) (Scale bar - 200µm). Inlays show full focus z-stack images of luminal structure formation (green – phalloidin, blue – DAPI, Scale bars are 100 and 50 µm respectively).

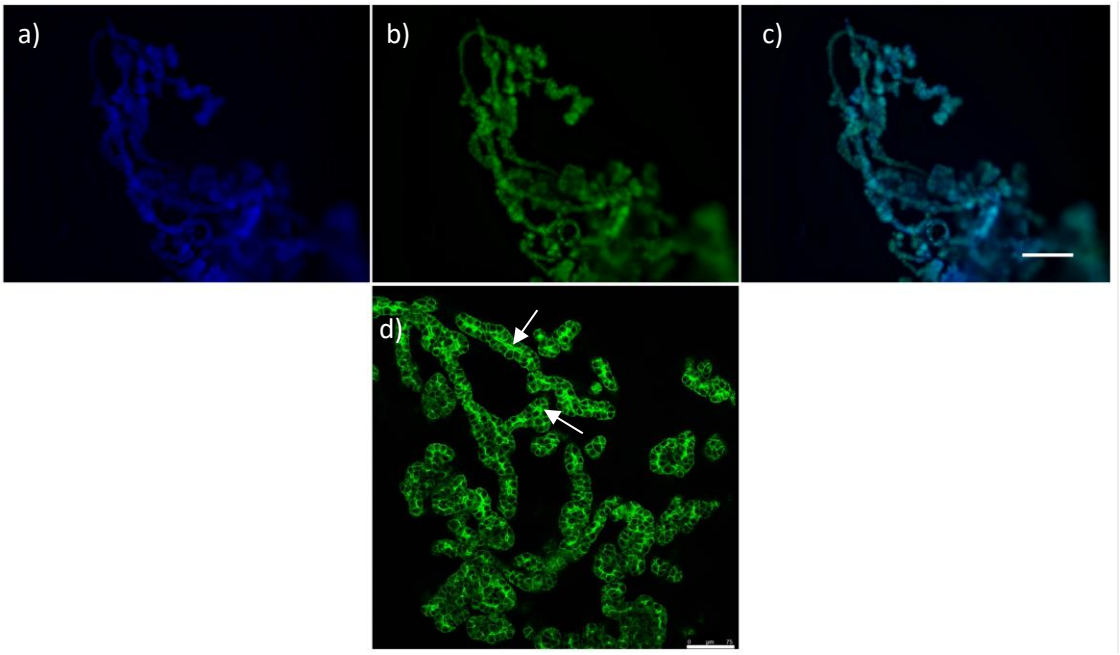

Figure 4.3 Tubule clusters from high density cultures at 1 month

Culturing higher density (200,000 cells) for long culture durations can result in tubule clusters that detach from the Matrigel surface. Full focus z-stack of a representative cluster (a-c, Scale bar - 200µm) and a confocal cross-section (Scale bar- 75µm) (green – phalloidin, blue – DAPI).

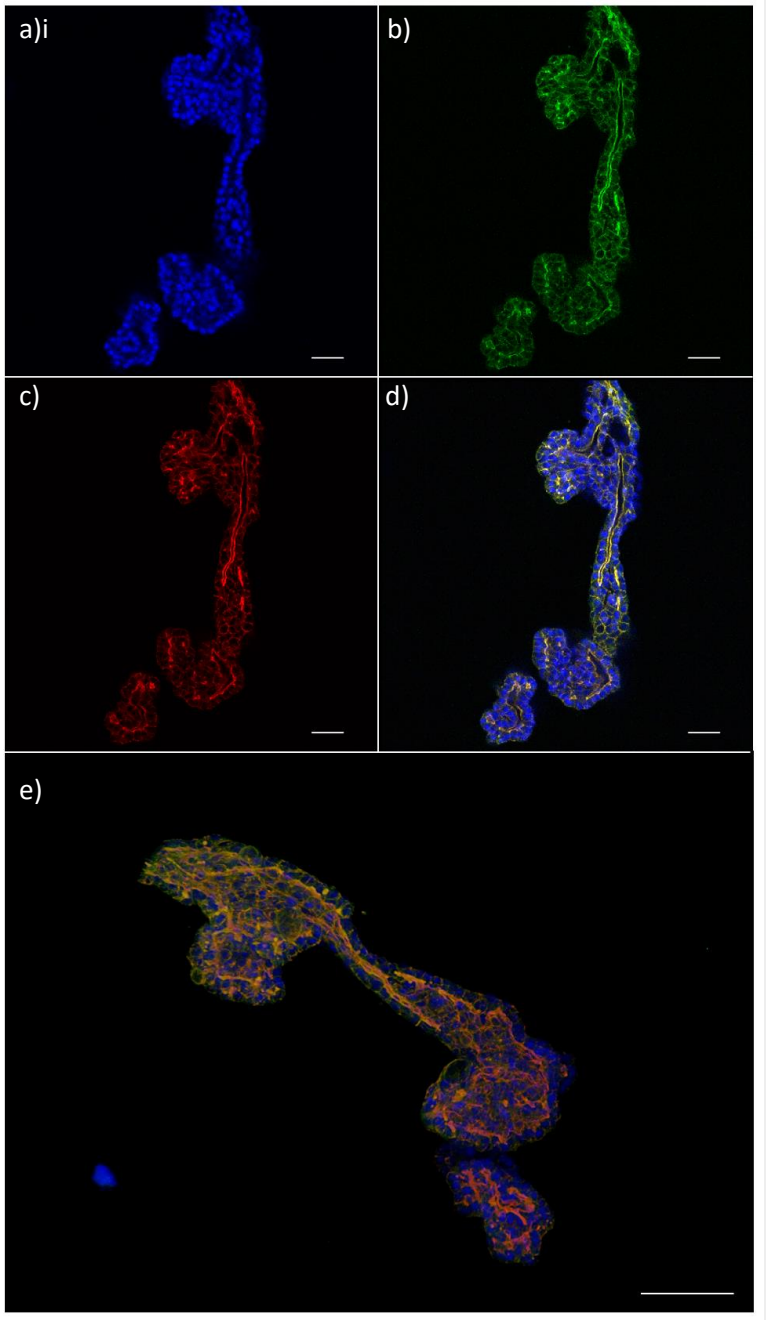

Figure 4.4 Luminal polarization of RPTEC/tert1 tubules after 1 week

Representative confocal images of tubule formation of RPTEC/tert1 cells after 1 week of culture. Cross-section of nuclei (a) aPKC (b) f-actin (c) and overlay (d) and a 3D reconstruction (DAPI-blue, aPKC-green, phalloidin-red, Scale bars - 50µm)

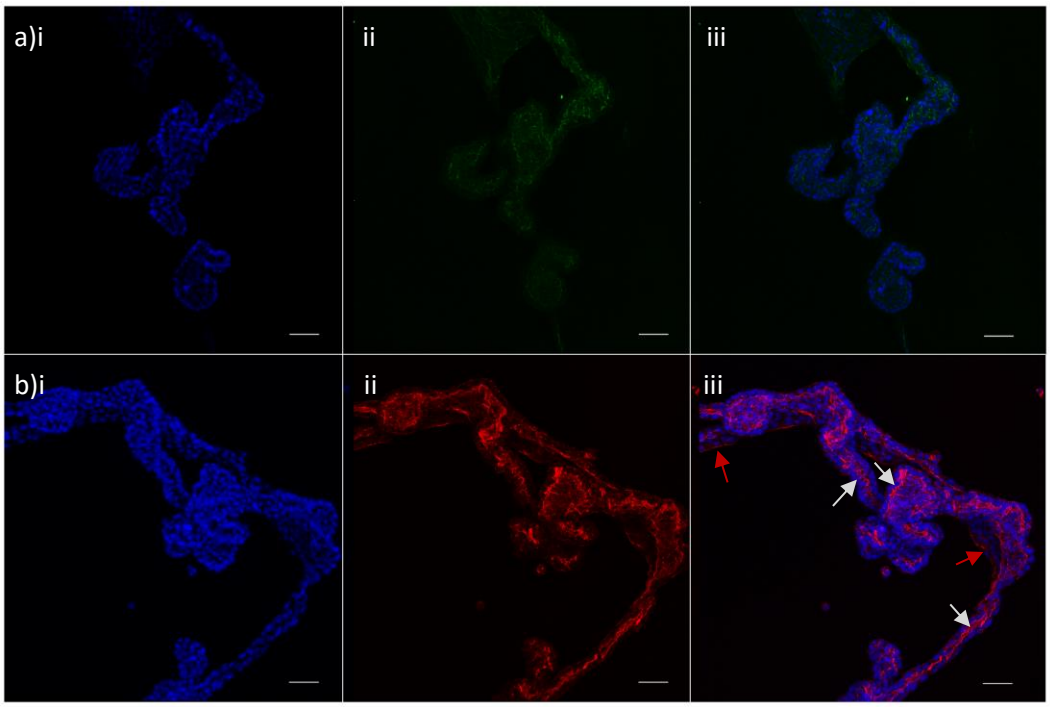

Figure 4.5 OAT1 and SGLT2 transporter expression in RPTEC/tert1 tubules

Representative confocal images of RPTEC/tert1 cells after 1 week of culture. Max projections of OAT1 (a) and SGLT2 (b) staining (DAPI-blue, OAT1 -green, SGLT2-red, Luminal tubule-white arrows, incomplete structures-red arrows, Scale bars - 50µm).

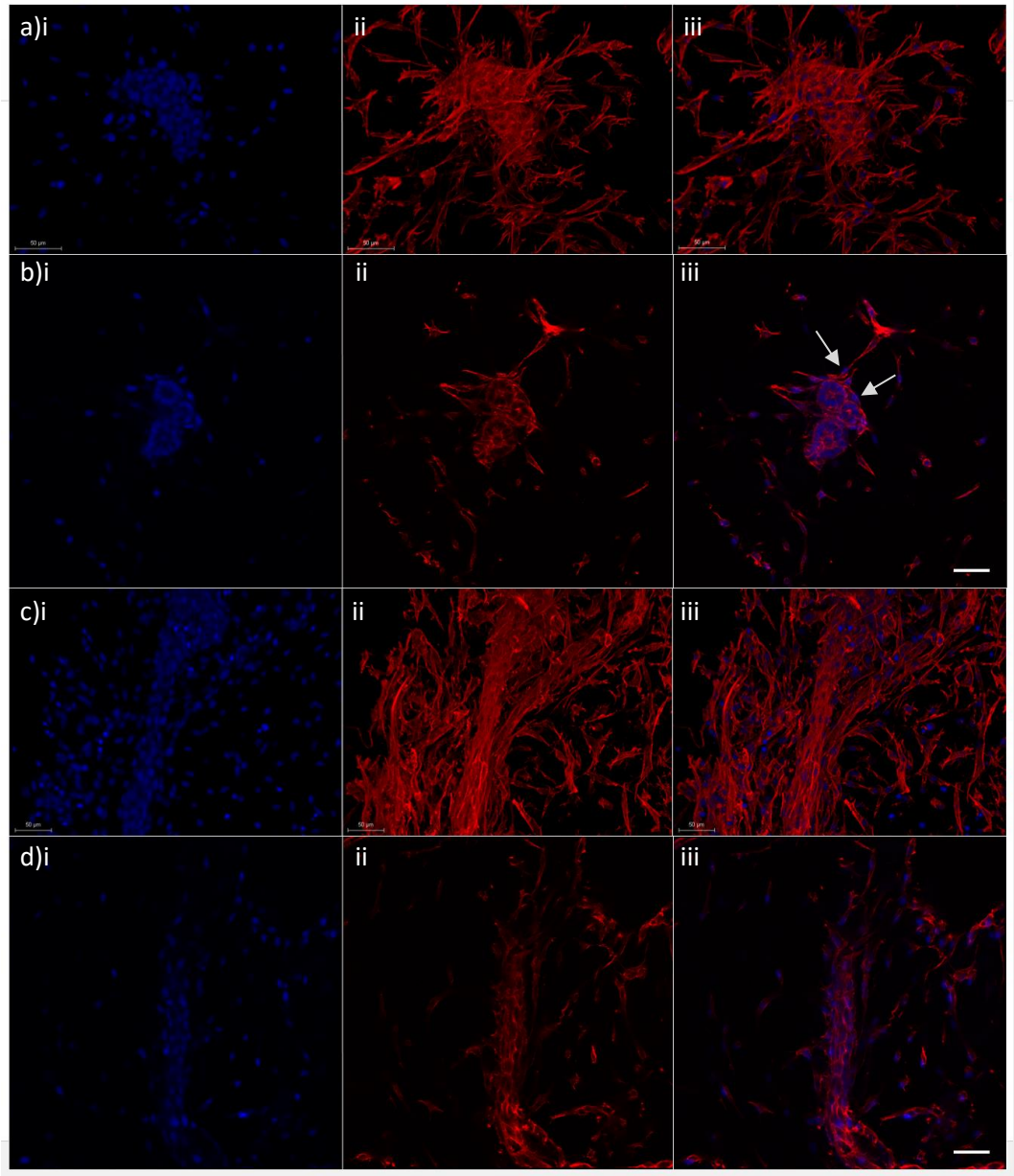

Figure 4.6 Co-culture of RPTEC/tert1 tubules with FOXD1+ stromal cells

Representative confocal images of tubule formation during RPTEC/tert1 co-culture with FOXD1^{+} stromal cells using two different seeding methods: mixed seeding of the two cell types on the Matrigel surface (a&b) and embedding of FOXD1^{+} cells in the Matrigel prior to RPTEC/tert1 seeding (c&d). 3D projections of z-stacks (a&c) and cross-sections (b&d) show resulting structure formation (blue – DAPI, red – phalloidin, Scale Bars - 50µm).

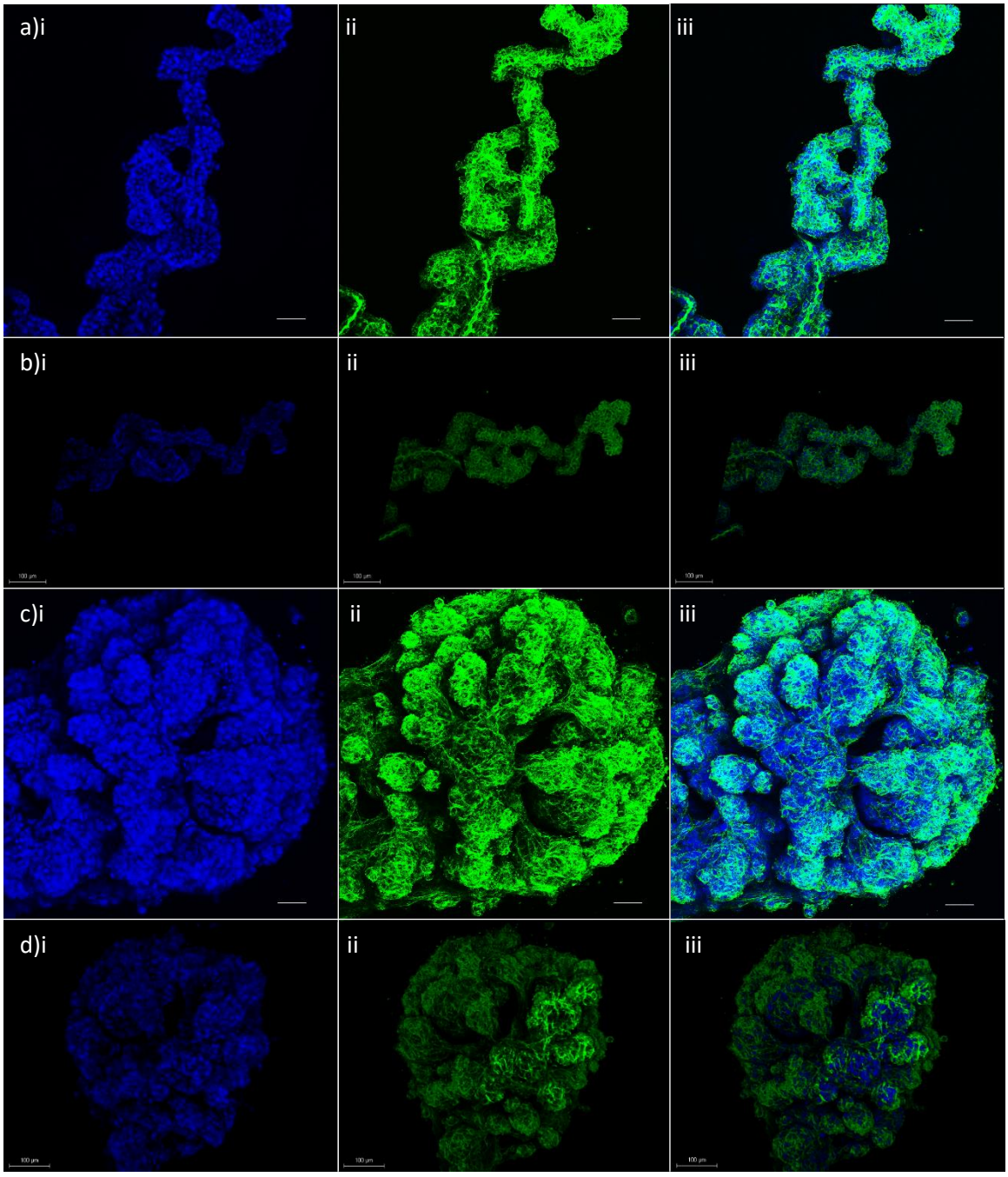

Figure 4.7 Morphological response to treatment with TGFβ1

Representative confocal images of changes in tubule morphology in response to treatment with TGFβ1 for 1 week after initial tubule formation for 1 week. Untreated cultures (a & b) and treated cultures (c&d). Max projection images (a&c) and 3D reconstruction (b&d). (blue – DAPI, green – phalloidin, Scale Bars - 50µm).

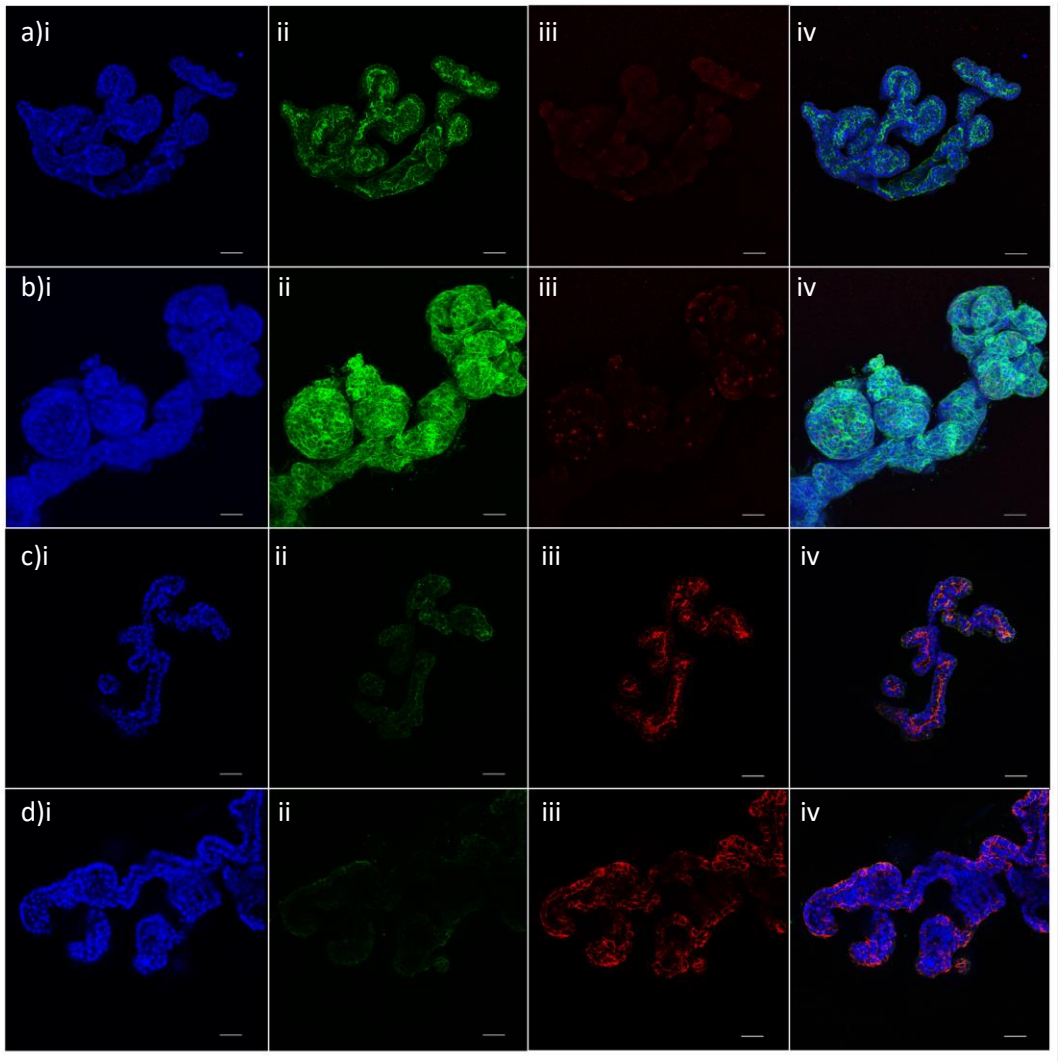

Figure 4.8 Proliferation and loss of polarization in response to treatment with TGFβ

Representative confocal images of changes in tubule polarization and proliferation in response to treatment with TGFβ for 1 week after initial tubule formation for 1 week. Untreated cultures (a & c) and treated cultures (b&d). Comparative max projection images of phalloidin staining (green) and Ki67 (red) (a&b). Comparative optical sections of aPKC (green) and phallodin (red) (c&d). (Scale Bars - 50µm).

Chapter 5. FUTURE DIRECTIONS

ABSTRACT

The anatomical and physiological complexity of the human kidney presents a significant challenge to tissue engineering. However, microfluidic and 3D tissue culture approaches enable key functional or phenotypic characteristics to be replicated *in vitro*. As such, instead of seeking to recapitulate total functionality, targeting a specific subset of these functions and phenotypes enables robust tissue engineered models to be established while minimalizing system complexity. The toolset presented here embodies this approach with respect to long term changes in morphology in static cyst cultures, maintenance of mechanosensory phenotypes in a 3D planar bioreactor or morphogenesis of tubules with polarized lumens on the surface of gelled basement membrane. These methodologies can be applied to future disease and development studies which require similar phenotypes and functionalities. Despite their utility, alternative strategies will also need to be developed in order for kidney tissue engineering to ultimately replace *in vivo* animal models or for tissue regeneration. As such, we propose further development of the perfusion bioreactor and tubulogenesis assay in order to meet these challenges. Accordingly, we suggest developing the scaffold and bioreactor to support the perfusion of a channel array for epithelial, endothelial and interstitial co-culture. Furthermore, we outline approaches for further characterizing and optimizing the tubule formation assay which are relevant to nephrotoxicity and tissue regeneration. In addition, we propose a silk film support for patterned structure formation and translation *in vivo.*

5.1. NEXT GENERATION 3D BIOREACTORS

While the bioreactor outlined in Chapter 3 provides a simple modular approach to 3D perfusion studies, this approach can be modified to support more complex cultures. Of particular interest in kidney tissue engineering are tubule bundles and parallel culture of epithelial and endothelial cell types. Sustained culture of all kidney cell types in a perfusion system has yet to be achieved and this level of complexity is required to further understand kidney development and disease. For instance, stromal-epithelial crosstalk has been shown to regulate progenitor cell differentiation during development (145). Similarly, tubulovascular communication has been shown to be necessary for the maintenance of peritubular capillaries and homeostasis (153). While increasing the complexity will ultimately decrease the throughput of the system, these further developments in *in vitro* kidney model systems are essential to mimicking *in vivo* physiology. To achieve this goal we propose a modified bioreactor system that translates the current bioreactor into a luminal device.

5.1.1. Scaffold and bioreactor design

PDMS bioreactors which support perfusion through a silk tube have been previously established in our lab (154). This approach has been successfully used to model the bone marrow niche for *ex vivo* platelet collection (155). However, the silk tube used for these studies does not provide the necessary cell-to-cell interaction required for modeling the kidney. To circumvent this issue, the bioreactor design used in the perfusion device in chapter 3 can be translated to accommodate a lyophilized silk sponge which has been shown to support both fibroblasts and a confluent kidney epithelial cell layer. Moreover, previous work has demonstrated the ability to form channels in these silk scaffolds using arrays of PTFE coated wires inserted into aqueous silk solution prior to lyophilization (64,

156, 157). Using this methodology channel diameter can be varied by changing the diameter of the wire and the spacing in between the channels can also be appropriately controlled.

To increase the versatility and allow for increasing complexity of a luminal device, a two-part mold consisting of the PDMS negative for base of the device and wire-guide adaptor (Figure 5.1). The wire guide adaptor will be a laser cut plug that can be swapped to accommodate alternative channel configurations as necessary (Figure 5.1c). This approach was successfully used to fabricate a dual channel bioreactor (Figure 5.1c). A silk scaffold can be fabricated within the device by inserting a PTFE wire through the port thereby mimicking the previous established protocols (Figure 5.1b). As necessary, the porosity of the scaffold can be varied by altering the freezing rate and alternative silk volume percentages. Prototype devices were fabricated using a 6% w/v silk solution. Moreover, to minimize media consumption in this device, the perfusion setup established in Chapter 3 can be directly translated to support the multichannel luminal devices.

5.1.2. Cell culture in a luminal device

Culture of kidney cell types in this system can first be optimized under static conditions using a systematic seeding protocol (Figure 5.2). Interstitial cells can be incorporated into the bulk followed by an ECM infusion and injection of luminal cell types into the channels. This approach was verified using the same collagen type1:Matrigel ECM composition as Chapter 3 for the culture of RPTEC/tert1 cells. At day 5 post-seeding, a confluent layer of RPTEC/tert1 has been achieved in a porous, 500 micron silk channel. These results support the utility of this methodology for luminal cell culture. To adapt this system for the culture of kidney endothelial, epithelial, and interstitial cell types the

culture environment should be optimized for each of these cell types individually, under static conditions. If the current Matrigel-collagen ECM does not support the culture of any of all the cell types an alternative approach whereby the optimal ECM for the interstitial compartment (which *in vivo* is predominately collagen 1) can be infused into the scaffold and the channels coated with the ECM proteins which enable confluent epithelial and endothelial coatings. Unlike approaches which rely solely on hydrogels for channel formation, the silk scaffold will limit contraction and can provide additional control of the mechanical microenvironment without cross-linking.

For application of the luminal device for differentiation of stem cells and nephron development a better understanding of the ECM composition in the developing kidney is required. Mass spectroscopy analysis of kidney ECM at different stages of develop will provide insight into how the ECM composition changes over time and the appropriate culture conditions for stem cells depending on the their developmental stage. Moreover, in addition to commercially available sources of ECM proteins, silk scaffolds can be infused with ECM hydrogels formed from decellularized kidney extract (158). Replacement of commercial sources with decellularized kidney ECM will also be necessary for future tissue regeneration applications where scaffolds would ultimately be implanted *in vitro*.

5.1.3. Outcomes and Applications

To determine the utility for potential applications, culture needs to be assessed with respect to cell phenotype and function. While ultimately this approach could be used to support the culture of differentiated stem cells and a variety kidney epithelial cell types, the current state-of-the-art differentiation protocols have not been sufficiently

developed to yield a broad range of mature kidney epithelial and endothelial cells. For scaffold and bioreactor evaluation and optimization model cell lines, such as RPTEC/tert1 and human umbilical vein endothelial cells, should be used.

Epithelial and endothelial cell types cultured within the channeled scaffolds should achieve complete coverage of the scaffold surface with positive staining for tight junction formation which can be quantitatively assessed using TEER measurements. Using RPTEC/tert1 as a model cell line enables phenotype and function to be assessed using well-established metrics for proximal tubule function (Table 5.1) (47, 50, 93). As previously discussed, the functionality specific to an intended application should be thoroughly assessed such as transporter mediated secretion for nephrotoxicity studies. For a complete understanding of the effects of perfusion and channeled culture, characterization experiments should be conducted using a range of control including standard 2D TCP, culture on an equivalent planar scaffold, static channel culture (off-device to ensure sufficient media saturation within the channels) and perfusion channel culture.

The proposed next generation bioreactor design has strengths and limitations compared to current 3D kidney perfusion culture systems. The use of a channeled silk scaffold provides additional structural support with the potential for translation *in vivo*. This characteristic is particularly important considering the shift within the field towards tissue development and regeneration. This structural integrity comes at the loss of geometrical complexity that bioprinting provides. Bioprinting can yield convoluted channel geometries compared to the parallel arrays limited within silk scaffolds. However, the scale-ability of bioprinting approaches is not fully known meanwhile channel arrays

have already been established in silk channels. Alternatively, this integrity and scale-ability does limit the use of standard live imaging approaches. Silk scaffolds are not optically transparent and require additional post-processing such as sectioning or optical clearing. This limitation means functional assessments of transport will either need to be end-point studies or based on the collection of the effluent perfusate.

5.2. DEVELOPMENT AND SCALING OF SELF-ORGANIZING RENAL EPITHELIAL TUBULES

In chapter 4 we presented a robust culture approach for the self-organization of renal epithelial cells *in vitro* to yield 3D tubules with polarized lumens on the surface of Matrigel. This method offers significant advantages such as live imaging, use of an established cell line, and luminal tubule formation without additional perturbation. Additionally, this simplicity lends itself to potential high-throughput translation for quantitative assessment of epithelial tubule formation and treatment response. In the following section we will discuss further characterization and development necessary for translating this methodology to studies of pharmacokinetics, nephrotoxicity and tubulogenesis.

5.2.1. Development for pharmacokinetic and nephrotoxicity studies

Transporter mediated secretion is relevant for the assessment of pharmacokinetics and nephrotoxic response. This methodology is well suited for secretion studies considering there is direct access to the media surrounding the basolateral surface and fully formed tubule structures have an enclosed luminal space. In order to translate this approach for these applications the following is required a) further analysis of transporter expression and functionality b) increased throughput and c) testing of the system with

known nephrotoxins. These steps will provide a complete understanding of the utility of these renal proximal tubules.

Assessment of transporter expression within the tubule cultures should initially be conducted using similar methods to Chapter 4. However, to gain the most complete understanding of transporter expression stability and initial polarization these studies should include shorter and longer term time points. Previously conducted time lapse experiment suggest there are still significant culture dynamics at 72 hours. Accordingly, suggested end points include day 4, week 1, week 2, 1 month and 2 months of culture. The inclusion of long term culture is particularly important considering repeat dose toxicity experiments have been used to identify novel renal injury biomarkers (72). Compared to *in vitro* nephrotoxicity experiments which perform proof of principle studies at toxic concentrations this approach repeatedly exposes cultures to sub-cytotoxic concentrations over longer culture periods. In order to improve polarized transporter expression it may necessary to further optimize the culture conditions. Specifically, Matrigel containing media (at concentrations of 2%-5%) has been shown to preserve tubular-like morphology and polarization in isolated proximal tubules (159). This approach could potentially provide additional basolateral signaling without significantly altering the system complexity.

In addition to the transporters and barrier studies outlined in Table 5.1 a more comprehensive list was compiled by Aschauer et al (73). Immunostaining provides the greatest depth of insight with respect to expression and localization, transcriptomic analysis should be performed to gain a better understanding of the expression compared to 2D membrane culture. Functionality of these transporters can be further confirmed

though fluorescent uptake experiment. Accordingly, OAT function can be validated using basolateral uptake of 6-carboxyfluorecein (6-CF) and treatment with OAT inhibitor probenecid (159). In this experiment it is expected for the fluorescence in untreated tubules to be significantly higher than tubules treated with probenecid. Similarly, OCT uptake can be studied using DAPI considering DAPI uptake is mediated by OCT1 in live kidney epithelial cells (159). This functionality should be inhibited by metformin treatment.

To translate this approach to high-throughput screening applications this assay will need to transition from a 24 well format to at least a 96 well culture system (if not 384 well). To accomplish this transition an array of cell densities and Matrigel coating thicknesses will need to be assessed. The data from Chapter 4 supports the need for an optimal cell density considering high density culture leads to cell sheet formation and low densities yielded isolated spheroids. Therefore, for the Matrigel coating it will be necessary to minimize meniscus formation which can cluster cells towards the center. Within the 24-well format it was also observed that too thin a coating led to matrix separation from the glass bottom plate and thicker cultures limited structure formation (data not shown). If reliable tubule formation cannot be achieved using this array of conditions it may be necessary to dilute the Matrigel, to decrease the viscosity, or to cross-link with genipin to increase the culture stiffness.

Treatment of the luminal tubules with known nephrotoxins such as cisplatin or cyclosporine A will complete the validation of this approach for nephrotoxicity testing. Proof of principle experiments of *in vitro* models typically confirm toxicity through structural degradation and upregulated kidney injury molecule-1 (KIM-1) expression(52).

Additionally, supernatant lactate concentration has also been used to gain insight into the timing and extent of cell death (160).

5.2.2. Tubulogenesis and kidney regeneration applications

The self-organization of renal epithelial cells using the tubule assay detailed in Chapter 4 suggests the potential of a stepwise approach for tissue regeneration. A systematic approach will ultimately be necessary for forming large organized bundles of tubules and elucidating the governing mechanisms behind tubulogenesis that can be translated to the culture of renal progenitor cells. To realize this potential we propose a) patterned structure formation b) incorporating silk films as an alternative to Matrigel only culture or c) a combination of these two strategies. The increase in culture complexity and the use of alternative biomaterials will enable precise control of environmental parameters that have the potential to influence tubule organization. Moreover, this understanding will enable the translation of this culture method from assay to regenerative tissue engineering.

Although RPTEC/tert1 epithelial cells are able to self-organize into luminal tubules at a physiologically relevant scale, we are unable to control the location of this process. To transition from a well-plate format to a patterned format we propose bioprinting Matrigel on low adhesion tissue culture plates. As a proof of concept we demonstrated localized cellular attachment and tubule formation (without a confirmed lumen) on 10 µl Matrigel streaks (Figure 5.3). For this approach to be reproducible, a 3D bio-inks printer contained within a temperature controlled enclosure for should be used (161). Patterned tubules should be characterized with respect to the same criteria used in Chapter 4. Patterned structures also have the potential to become an alternative high-throughput format for

drug screening. This technique is specifically amenable to this application based on the reduced reagent use and increased reproducibility. Moreover, the combination of patterning and self-organization optimized for RPTEC/tert1 culture could eventually be used for organized renal progenitor cell differentiation outside of organoid culture.

Despite the success and potential of this approach, the use of Matrigel to achieve differentiated phenotypes ultimately limits the ability to translate into *in vivo* studies considering its origin from mouse sarcoma cells and the inherent batch-to-batch variability. To circumvent this limitation we suggest optimization of a silk film substitute. Silk films enable significant control of culture environment with respect to surface porosity, degradation mechanics, mechanical properties and functionality. Initial assessment of the potential of silk films to form epithelial structures can be accomplished by doping Matrigel into the silk biomaterial to provide the known necessary signaling from the basement membrane proteins. If Matrigel doped films do not yield polarized tubules the mechanical properties can be optimized to match the original surface culture. The molecular weight of the silk, beta-sheeting, glycerol content and porosity of the film can be altered as necessary in conjunction with mechanical testing to further understand the role of surface mechanics on structure formation (162, 163). Once the silk properties are optimized, human sourced laminin, collagen IV, and collagen I can be doped into the material as a replacement for Matrigel. This transition to a silk biomaterial platform allows for the systematic study of parameters that influence tubule formation which can used to inform the formation of tubules from alternative cell sources. Moreover, the surface of the film can be regionally functionalized for the localized, controlled release of growth factors which are found to dictate kidney cell fate (164).

Lastly, we propose a blueprint for scaling this approach to match the demands of kidney tissue regeneration. In this approach, silk films are utilized to provide the necessary structural support and regional stimuli while patterning provides organized structure formation (Figure 5.3). We envision a completely modular approach that can be modified to meet the specific culture conditions necessary for differentiating human stem cells to mature kidney cell fates. Furthermore, silk films have the potential to be rolled and/or stacked to achieve additional tissue hierarchy. The tunable properties offered by the silk film culture approach will allow for the necessary culture optimization and stimulation required for stem cell differentiation towards an array of renal epithelial lineages.

5.3. TABLES AND FIGURES

Table 5.1 Proximal tubule assessment

Phenotype-Function	Assay	Expected Outcome (47, 49, 50)
Receptor mediated endocytosis	Megalin, Cubilin expression	Apical localization
	Fluorescent albumin uptake	Quantitative increase compared to controls (flow cytometry), co-staining with transporters
Transporter mediated reabsorption	Glucose transporter (SGLT2, GLUT2) expression	Apical localization
	Fluourescent glucose uptake/inhibition	Cellular accumulation (loss from luminal fluid), decreased uptake in the presence of inhibitor (apigenin or dapagliflozin)
Transporter mediated secretion	Transporter expression (organic cation transporter 2, OAT1, OAT3)	Basolateral localization
	Para-aminohippurate (PAH) transport and inhibition with probenecid	Transport from basal side to luminal tubule which is reduced in response to inhibitor treatment
Additional Polarization	Tight Junction (ZO-1 expression, TEER)	Cell junction ZO-1 expression, TEER around (75 Ω cm^{-1})
	Brush Border (f-actin, aPKC)	Apical surface
Ammonia secretion	Ammonia secretion in response to a drop in PH	Lower pH yields an increase in ammonia secretion
Cellular morphology	Electron microscopy	Single primary cilium per cell, brush border, cuboidal morphology

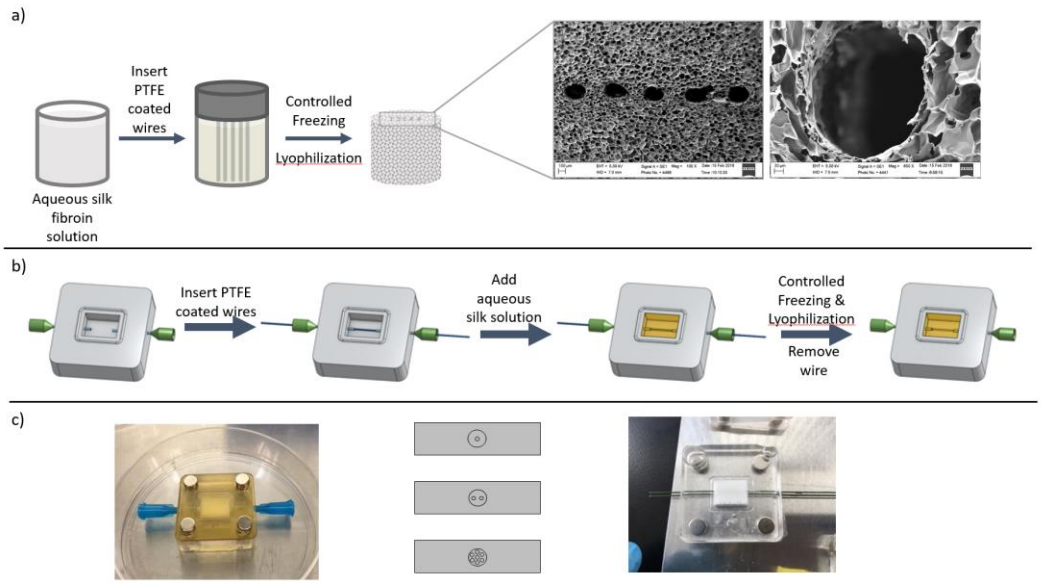

Figure 5.1 Schematics for next generation bioreactor system

Schematics and images of scaffold fabrication and next generation bioreactor design. (a) Fabrication process for lyophilized silk scaffolds with parallel channel arrays and scanning electron microscopy of scaffold and channel porosity. (b) Fabrication of silk scaffolds within PDMS bioreactors for improved port-to-channel connection. (c) Images of next generation PDMS bioreactor with magnetic lid for channeled scaffold culture, modular port configurations and dual-channel scaffold fabricated within the bioreactor.

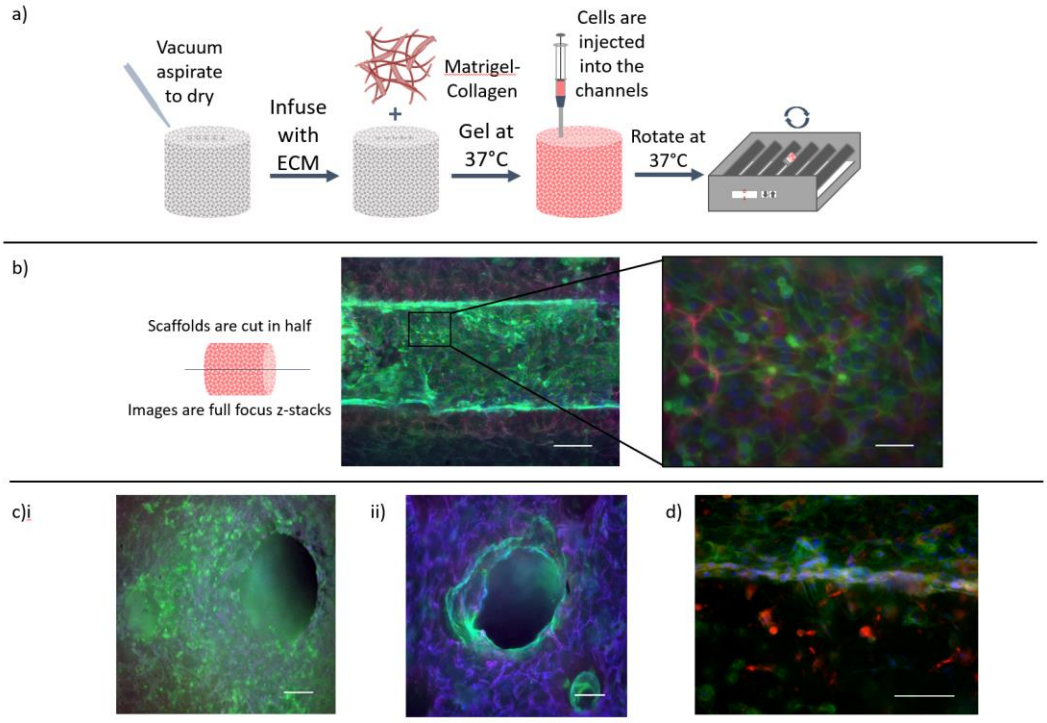

Figure 5.2 Seeding of RPTEC/tert1 cells within channeled scaffolds

a) Schematic of stepwise protocol used to seed a confluent layer of epithelial cells within the channel. b) Immunostaining of RPTEC/ter1 cells after 5 days in static culture within the channel (blue-DAPI, green-phalloidin, red-silk(adipoRed), Scale bars – 200/50µm). c) Scaffolds seeded without ECM infusion (i) and with Matrigel-collagen infusion (ii) (blue-DAPI, green-phalloidin, red-silk(adipoRed), Scale bars – 200 µm). d) Fibroblasts after 5 days of cultures in the porous bulk space with RPTEC/tert1 in the channels (blue-DAPI, green-phalloidin, red-DiD labeled fibroblasts, Scale bars – 100 µm).

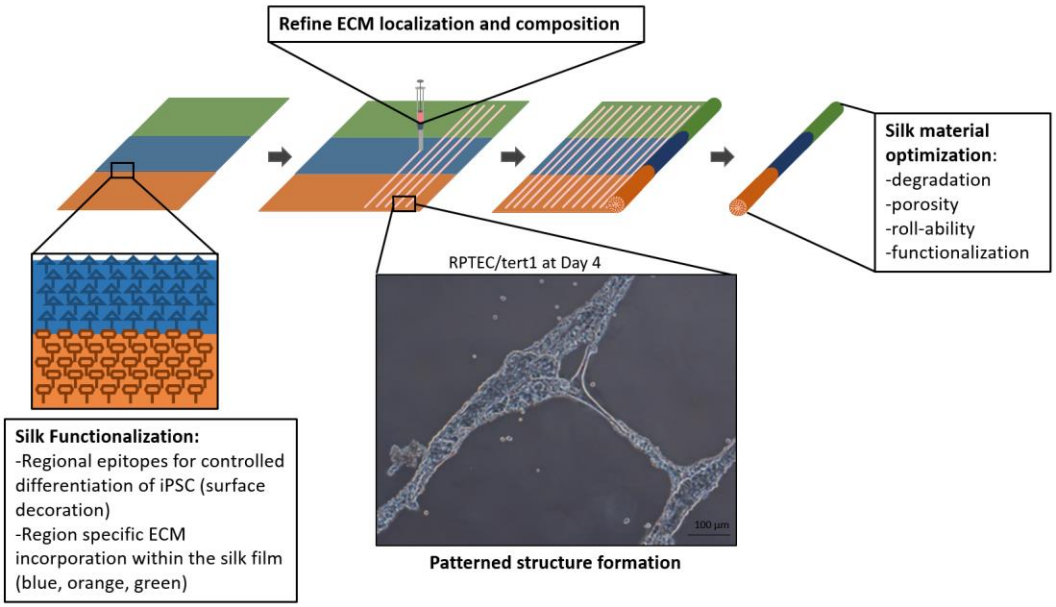

Figure 5.3 Blueprint for patterned tissue regeneration on the surface of silk films

Chapter 6. REFERENCES

1. Kriz W. Structural organization of the renal medulla: comparative and functional aspects. Am J Physiol. 1981;241(1):R3-16. PubMed PMID: 7018270.

2. Remuzzi G, Perico N, Macia M, Ruggenenti P. The role of renin-angiotensin-aldosterone system in the progression of chronic kidney disease. Kidney Int Suppl. 2005(99):S57-65. doi: 10.1111/j.1523-1755.2005.09911.x. PubMed PMID: 16336578.

3. System USRD. *2014 USRDS Annual Data Report: An Overview of the Epidemiology of Kidney*

*Disease in the United States. National Institutes of Health*2014 USRDS Annual Data Report: An Overview of the Epidemiology of Kidney

Disease in the United States. National Institutes of Health. National Institute of Diabetes and Digestive and Kidney Diseases, 2014.

4. Dieterle F, Sistare F, Goodsaid F, Papaluca M, Ozer JS, Webb CP, Baer W, Senagore A, Schipper MJ, Vonderscher J, Sultana S, Gerhold DL, Phillips JA, Maurer G, Carl K, Laurie D, Harpur E, Sonee M, Ennulat D, Holder D, Andrews-Cleavenger D, Gu YZ, Thompson KL, Goering PL, Vidal JM, Abadie E, Maciulaitis R, Jacobson-Kram D, Defelice AF, Hausner EA, Blank M, Thompson A, Harlow P, Throckmorton D, Xiao S, Xu N, Taylor W, Vamvakas S, Flamion B, Lima BS, Kasper P, Pasanen M, Prasad K, Troth S, Bounous D, Robinson-Gravatt D, Betton G, Davis MA, Akunda J, McDuffie JE, Suter L, Obert L, Guffroy M, Pinches M, Jayadev S, Blomme EA, Beushausen SA, Barlow VG, Collins N, Waring J, Honor D, Snook S, Lee J, Rossi P, Walker E, Mattes W. Renal biomarker qualification submission: a dialog between the FDA-EMEA and Predictive Safety Testing Consortium. Nat Biotechnol. 2010;28(5):455-62. doi: 10.1038/nbt.1625. PubMed PMID: 20458315.

5. Mason RM, Wahab NA. Extracellular matrix metabolism in diabetic nephropathy. J Am Soc Nephrol. 2003;14(5):1358-73. PubMed PMID: 12707406.

6. Schlöndorff D, Banas B. The mesangial cell revisited: no cell is an island. J Am Soc Nephrol. 2009;20(6):1179-87. doi: 10.1681/ASN.2008050549. PubMed PMID: 19470685.

7. Satchell SC, Braet F. Glomerular endothelial cell fenestrations: an integral component of the glomerular filtration barrier. Am J Physiol Renal Physiol. 2009;296(5):F947-56. doi: 10.1152/ajprenal.90601.2008. PubMed PMID: 19129259; PMCID: PMC2681366.

8. Miner JH. The glomerular basement membrane. Exp Cell Res. 2012;318(9):973-8. doi: 10.1016/j.yexcr.2012.02.031. PubMed PMID: 22410250; PMCID: PMC3334451.

9. Greka A, Mundel P. Cell biology and pathology of podocytes. Annu Rev Physiol. 2012;74:299-323. doi: 10.1146/annurev-physiol-020911-153238. PubMed PMID: 22054238; PMCID: PMC3600372.

10. Hull RN, Cherry WR, Weaver GW. The origin and characteristics of a pig kidney cell strain, LLC-PK. In Vitro. 1976;12(10):670-7. PubMed PMID: 828141.

11. Lang F, Paulmichl M. Properties and regulation of ion channels in MDCK cells. Kidney Int. 1995;48(4):1200-5. PubMed PMID: 8569081.

12. Ryan MJ, Johnson G, Kirk J, Fuerstenberg SM, Zager RA, Torok-Storb B. HK-2: an immortalized proximal tubule epithelial cell line from normal adult human kidney. Kidney Int. 1994;45(1):48-57. PubMed PMID: 8127021.

13. Wieser M, Stadler G, Jennings P, Streubel B, Pfaller W, Ambros P, Riedl C, Katinger H, Grillari J, Grillari-Voglauer R. hTERT alone immortalizes epithelial cells of renal proximal tubules without changing their functional characteristics. Am J Physiol Renal Physiol. 2008;295(5):F1365-75. doi: 10.1152/ajprenal.90405.2008. PubMed PMID: 18715936.

14. Takasato M, Er PX, Becroft M, Vanslambrouck JM, Stanley EG, Elefanty AG, Little MH. Directing human embryonic stem cell differentiation towards a renal lineage generates a self-organizing kidney. Nat Cell Biol. 2014;16(1):118-26. doi: 10.1038/ncb2894. PubMed PMID: 24335651.

15. Xia Y, Nivet E, Sancho-Martinez I, Gallegos T, Suzuki K, Okamura D, Wu MZ, Dubova I, Esteban CR, Montserrat N, Campistol JM, Izpisua Belmonte JC. Directed differentiation of human pluripotent cells to ureteric bud kidney progenitor-like cells. Nat Cell Biol. 2013;15(12):1507-15. doi: 10.1038/ncb2872. PubMed PMID: 24240476.

16. Taguchi A, Kaku Y, Ohmori T, Sharmin S, Ogawa M, Sasaki H, Nishinakamura R. Redefining the in vivo origin of metanephric nephron progenitors enables generation of complex kidney structures from pluripotent stem cells. Cell Stem Cell. 2014;14(1):53-67. doi: 10.1016/j.stem.2013.11.010. PubMed PMID: 24332837.

17. Levey AS, Stevens LA, Schmid CH, Zhang YL, Castro AF, Feldman HI, Kusek JW, Eggers P, Van Lente F, Greene T, Coresh J, Collaboration) C-ECKDE. A new equation to estimate glomerular filtration rate. Ann Intern Med. 2009;150(9):604-12. PubMed PMID: 19414839; PMCID: PMC2763564.

18. Rodriguez-Barbero A, L'Azou B, Cambar J, López-Novoa JM. Potential use of isolated glomeruli and cultured mesangial cells as in vitro models to assess nephrotoxicity. Cell Biol Toxicol. 2000;16(3):145-53. PubMed PMID: 11032358.

19. Jat PS, Noble MD, Ataliotis P, Tanaka Y, Yannoutsos N, Larsen L, Kioussis D. Direct derivation of conditionally immortal cell lines from an H-2Kb-tsA58 transgenic mouse. Proc Natl Acad Sci U S A. 1991;88(12):5096-100. PubMed PMID: 1711218; PMCID: PMC51818.

20. Satchell SC, Tasman CH, Singh A, Ni L, Geelen J, von Ruhland CJ, O'Hare MJ, Saleem MA, van den Heuvel LP, Mathieson PW. Conditionally immortalized human glomerular endothelial cells expressing fenestrations in response to VEGF. Kidney Int. 2006;69(9):1633-40. doi: 10.1038/sj.ki.5000277. PubMed PMID: 16557232.

21. Saleem MA, O'Hare MJ, Reiser J, Coward RJ, Inward CD, Farren T, Xing CY, Ni L, Mathieson PW, Mundel P. A conditionally immortalized human podocyte cell line demonstrating nephrin and podocin expression. J Am Soc Nephrol. 2002;13(3):630-8. PubMed PMID: 11856766.

22. Slater SC, Beachley V, Hayes T, Zhang D, Welsh GI, Saleem MA, Mathieson PW, Wen X, Su B, Satchell SC. An in vitro model of the glomerular capillary wall using electrospun collagen nanofibres in a bioartificial composite basement membrane. PLoS One. 2011;6(6):e20802. doi: 10.1371/journal.pone.0020802. PubMed PMID: 21731625; PMCID: PMC3123297.

23. Baudoin R, Griscom L, Monge M, Legallais C, Leclerc E. Development of a renal microchip for in vitro distal tubule models. Biotechnol Prog. 2007;23(5):1245-53. doi: 10.1021/bp0603513. PubMed PMID: 17725364.

24. Snouber LC, Letourneur F, Chafey P, Broussard C, Monge M, Legallais C, Leclerc E. Analysis of transcriptomic and proteomic profiles demonstrates improved Madin-Darby canine kidney cell function in a renal microfluidic biochip. Biotechnol Prog. 2012;28(2):474-84. doi: 10.1002/btpr.743. PubMed PMID: 22095740.

25. Choucha Snouber L, Jacques S, Monge M, Legallais C, Leclerc E. Transcriptomic analysis of the effect of ifosfamide on MDCK cells cultivated in microfluidic biochips. Genomics. 2012;100(1):27-34. doi: 10.1016/j.ygeno.2012.05.001. PubMed PMID: 22580237.

26. Choucha-Snouber L, Aninat C, Grsicom L, Madalinski G, Brochot C, Poleni PE, Razan F, Guillouzo CG, Legallais C, Corlu A, Leclerc E. Investigation of ifosfamide

nephrotoxicity induced in a liver-kidney co-culture biochip. Biotechnol Bioeng. 2013;110(2):597-608. doi: 10.1002/bit.24707. PubMed PMID: 22887128.

27. Jang KJ, Suh KY. A multi-layer microfluidic device for efficient culture and analysis of renal tubular cells. Lab Chip. 2010;10(1):36-42. doi: 10.1039/b907515a. PubMed PMID: 20024048.

28. Jang KJ, Cho HS, Kang DH, Bae WG, Kwon TH, Suh KY. Fluid-shear-stress-induced translocation of aquaporin-2 and reorganization of actin cytoskeleton in renal tubular epithelial cells. Integr Biol (Camb). 2011;3(2):134-41. doi: 10.1039/c0ib00018c. PubMed PMID: 21079870.

29. Gao X, Tanaka Y, Sugii Y, Mawatari K, Kitamori T. Basic structure and cell culture condition of a bioartificial renal tubule on chip towards a cell-based separation microdevice. Anal Sci. 2011;27(9):907-12. PubMed PMID: 21908919.

30. Frohlich EM, Zhang X, Charest JL. The use of controlled surface topography and flow-induced shear stress to influence renal epithelial cell function. Integr Biol (Camb). 2012;4(1):75-83. doi: 10.1039/c1ib00096a. PubMed PMID: 22139064.

31. Ferrell N, Desai RR, Fleischman AJ, Roy S, Humes HD, Fissell WH. A microfluidic bioreactor with integrated transepithelial electrical resistance (TEER) measurement electrodes for evaluation of renal epithelial cells. Biotechnol Bioeng. 2010;107(4):707-16. doi: 10.1002/bit.22835. PubMed PMID: 20552673; PMCID: PMC3903011.

32. Jang KJ, Mehr AP, Hamilton GA, McPartlin LA, Chung S, Suh KY, Ingber DE. Human kidney proximal tubule-on-a-chip for drug transport and nephrotoxicity assessment. Integr Biol (Camb). 2013;5(9):1119-29. doi: 10.1039/c3ib40049b. PubMed PMID: 23644926.

33. Desrochers TM, Palma E, Kaplan DL. Tissue-engineered kidney disease models. Adv Drug Deliv Rev. 2014;69-70:67-80. doi: 10.1016/j.addr.2013.12.002. PubMed PMID: 24361391; PMCID: PMC4019700.

34. O Bukanov N, Husson H, Dackowski WR, Lawrence BD, Clow PA, Roberts BL, Klinger KW, Ibraghimov-Beskrovnaya O. Functional polycystin-1 expression is developmentally regulated during epithelial morphogenesis in vitro: downregulation and loss of membrane localization during cystogenesis. Hum Mol Genet. 2002;11(8):923-36. PubMed PMID: 11971874.

35. Grantham JJ, Uchic M, Cragoe EJ, Kornhaus J, Grantham JA, Donoso V, Mangoo-Karim R, Evan A, McAteer J. Chemical modification of cell proliferation and fluid secretion in renal cysts. Kidney Int. 1989;35(6):1379-89. PubMed PMID: 2770116.

36. Kuo IY, DesRochers TM, Kimmerling EP, Nguyen L, Ehrlich BE, Kaplan DL. Cyst formation following disruption of intracellular calcium signaling. Proc Natl Acad Sci U S A. 2014;111(39):14283-8. doi: 10.1073/pnas.1412323111. PubMed PMID: 25228769; PMCID: PMC4191767.

37. Montesano R, Ghzili H, Carrozzino F, Rossier BC, Féraille E. cAMP-dependent chloride secretion mediates tubule enlargement and cyst formation by cultured mammalian collecting duct cells. Am J Physiol Renal Physiol. 2009;296(2):F446-57. doi: 10.1152/ajprenal.90415.2008. PubMed PMID: 19052103.

38. Subramanian B, Rudym D, Cannizzaro C, Perrone R, Zhou J, Kaplan DL. Tissue-engineered three-dimensional in vitro models for normal and diseased kidney. Tissue Eng Part A. 2010;16(9):2821-31. doi: 10.1089/ten.TEA.2009.0595. PubMed PMID: 20486787; PMCID: PMC2928330.

39. Subramanian B, Ko WC, Yadav V, DesRochers TM, Perrone RD, Zhou J, Kaplan DL. The regulation of cystogenesis in a tissue engineered kidney disease system by abnormal matrix interactions. Biomaterials. 2012;33(33):8383-94. doi: 10.1016/j.biomaterials.2012.08.020. PubMed PMID: 22940218; PMCID: PMC3449278.

40. Carone FA, Nakamura S, Bacallao R, Nelson WJ, Khokha M, Kanwar YS. Impaired tubulogenesis of cyst-derived cells from autosomal dominant polycystic kidneys. Kidney Int. 1995;47(3):861-8. PubMed PMID: 7752585.

41. Wallace DP, Grantham JJ, Sullivan LP. Chloride and fluid secretion by cultured human polycystic kidney cells. Kidney Int. 1996;50(4):1327-36. PubMed PMID: 8887295.

42. Yamaguchi T, Reif GA, Calvet JP, Wallace DP. Sorafenib inhibits cAMP-dependent ERK activation, cell proliferation, and in vitro cyst growth of human ADPKD cyst epithelial cells. Am J Physiol Renal Physiol. 2010;299(5):F944-51. doi: 10.1152/ajprenal.00387.2010. PubMed PMID: 20810616; PMCID: PMC2980397.

43. Astashkina AI, Mann BK, Prestwich GD, Grainger DW. A 3-D organoid kidney culture model engineered for high-throughput nephrotoxicity assays. Biomaterials. 2012;33(18):4700-11. doi: 10.1016/j.biomaterials.2012.02.063. PubMed PMID: 22444643.

44. DesRochers TM, Suter L, Roth A, Kaplan DL. Bioengineered 3D human kidney tissue, a platform for the determination of nephrotoxicity. PLoS One. 2013;8(3):e59219. doi: 10.1371/journal.pone.0059219. PubMed PMID: 23516613; PMCID: PMC3597621.

45. Jansen J, De Napoli IE, Fedecostante M, Schophuizen CM, Chevtchik NV, Wilmer MJ, van Asbeck AH, Croes HJ, Pertijs JC, Wetzels JF, Hilbrands LB, van den Heuvel LP, Hoenderop JG, Stamatialis D, Masereeuw R. Human proximal tubule epithelial cells cultured on hollow fibers: living membranes that actively transport organic cations. Sci Rep. 2015;5:16702. doi: 10.1038/srep16702. PubMed PMID: 26567716; PMCID: PMC4644946.

46. Mu X, Zheng W, Xiao L, Zhang W, Jiang X. Engineering a 3D vascular network in hydrogel for mimicking a nephron. Lab Chip. 2013;13(8):1612-8. doi: 10.1039/c3lc41342j. PubMed PMID: 23455642.

47. Homan KA, Kolesky DB, Skylar-Scott MA, Herrmann J, Obuobi H, Moisan A, Lewis JA. Bioprinting of 3D Convoluted Renal Proximal Tubules on Perfusable Chips. Sci Rep. 2016;6:34845. doi: 10.1038/srep34845. PubMed PMID: 27725720; PMCID: PMC5057112.

48. Tourovskaia A, Fauver M, Kramer G, Simonson S, Neumann T. Tissue-engineered microenvironment systems for modeling human vasculature. Exp Biol Med (Maywood). 2014;239(9):1264-71. doi: 10.1177/1535370214539228. PubMed PMID: 25030480; PMCID: PMC4469377.

49. Weber EJ, Chapron A, Chapron BD, Voellinger JL, Lidberg KA, Yeung CK, Wang Z, Yamaura Y, Hailey DW, Neumann T, Shen DD, Thummel KE, Muczynski KA, Himmelfarb J, Kelly EJ. Development of a microphysiological model of human kidney proximal tubule function. Kidney Int. 2016;90(3):627-37. doi: 10.1016/j.kint.2016.06.011. PubMed PMID: 27521113; PMCID: PMC4987715.

50. Nieskens TT, Wilmer MJ. Kidney-on-a-chip technology for renal proximal tubule tissue reconstruction. Eur J Pharmacol. 2016;790:46-56. doi: 10.1016/j.ejphar.2016.07.018. PubMed PMID: 27401035.

51. Takasato M, Er PX, Chiu HS, Little MH. Generation of kidney organoids from human pluripotent stem cells. Nat Protoc. 2016;11(9):1681-92. doi: 10.1038/nprot.2016.098. PubMed PMID: 27560173.

52. Morizane R, Lam AQ, Freedman BS, Kishi S, Valerius MT, Bonventre JV. Nephron organoids derived from human pluripotent stem cells model kidney development and

injury. Nat Biotechnol. 2015;33(11):1193-200. doi: 10.1038/nbt.3392. PubMed PMID: 26458176; PMCID: PMC4747858.

53. Takasato M, Er PX, Chiu HS, Maier B, Baillie GJ, Ferguson C, Parton RG, Wolvetang EJ, Roost MS, Chuva de Sousa Lopes SM, Little MH. Kidney organoids from human iPS cells contain multiple lineages and model human nephrogenesis. Nature. 2015;526(7574):564-8. doi: 10.1038/nature15695. PubMed PMID: 26444236.

54. Freedman BS, Brooks CR, Lam AQ, Fu H, Morizane R, Agrawal V, Saad AF, Li MK, Hughes MR, Werff RV, Peters DT, Lu J, Baccei A, Siedlecki AM, Valerius MT, Musunuru K, McNagny KM, Steinman TI, Zhou J, Lerou PH, Bonventre JV. Modelling kidney disease with CRISPR-mutant kidney organoids derived from human pluripotent epiblast spheroids. Nat Commun. 2015;6:8715. doi: 10.1038/ncomms9715. PubMed PMID: 26493500; PMCID: PMC4620584.

55. Moll S, Ebeling M, Weibel F, Farina A, Araujo Del Rosario A, Hoflack JC, Pomposiello S, Prunotto M. Epithelial cells as active player in fibrosis: findings from an in vitro model. PLoS One. 2013;8(2):e56575. doi: 10.1371/journal.pone.0056575. PubMed PMID: 23457584; PMCID: PMC3572957.

56. Swenson-Fields KI, Vivian CJ, Salah SM, Peda JD, Davis BM, van Rooijen N, Wallace DP, Fields TA. Macrophages promote polycystic kidney disease progression. Kidney Int. 2013;83(5):855-64. doi: 10.1038/ki.2012.446. PubMed PMID: 23423256; PMCID: PMC4028685.

57. Harris PC, Torres VE. Polycystic kidney disease. Annu Rev Med. 2009;60:321-37. doi: 10.1146/annurev.med.60.101707.125712. PubMed PMID: 18947299; PMCID: PMC2834200.

58. Gallagher AR, Germino GG, Somlo S. Molecular advances in autosomal dominant polycystic kidney disease. Adv Chronic Kidney Dis. 2010;17(2):118-30. doi: 10.1053/j.ackd.2010.01.002. PubMed PMID: 20219615; PMCID: PMC2837604.

59. Torres VE, Harris PC. Autosomal dominant polycystic kidney disease: the last 3 years. Kidney Int. 2009;76(2):149-68. doi: 10.1038/ki.2009.128. PubMed PMID: 19455193; PMCID: PMC2812475.

60. Torres VE, Harris PC. Polycystic kidney disease: genes, proteins, animal models, disease mechanisms and therapeutic opportunities. J Intern Med. 2007;261(1):17-31. doi: 10.1111/j.1365-2796.2006.01743.x. PubMed PMID: 17222165.

61. Torres VE, Harris PC. Polycystic kidney disease in 2011: Connecting the dots toward a polycystic kidney disease therapy. Nat Rev Nephrol. 2011;8(2):66-8. doi: 10.1038/nrneph.2011.196. PubMed PMID: 22158473; PMCID: PMC4096714.

62. Macosko EZ, Basu A, Satija R, Nemesh J, Shekhar K, Goldman M, Tirosh I, Bialas AR, Kamitaki N, Martersteck EM, Trombetta JJ, Weitz DA, Sanes JR, Shalek AK, Regev A, McCarroll SA. Highly Parallel Genome-wide Expression Profiling of Individual Cells Using Nanoliter Droplets. Cell. 2015;161(5):1202-14. doi: 10.1016/j.cell.2015.05.002. PubMed PMID: WOS:000355152600025.

63. Rockwood DN, Preda RC, Yücel T, Wang X, Lovett ML, Kaplan DL. Materials fabrication from Bombyx mori silk fibroin. Nat Protoc. 2011;6(10):1612-31. doi: 10.1038/nprot.2011.379. PubMed PMID: 21959241; PMCID: PMC3808976.

64. Rnjak-Kovacina J, Wray LS, Burke KA, Torregrosa T, Golinski JM, Huang W, Kaplan DL. Lyophilized Silk Sponges: A Versatile Biomaterial Platform for Soft Tissue Engineering. ACS Biomater Sci Eng. 2015;1(4):260-70. doi: 10.1021/ab500149p. PubMed PMID: 25984573; PMCID: PMC4426347.

65. Chebib FT, Sussman CR, Wang X, Harris PC, Torres VE. Vasopressin and disruption of calcium signalling in polycystic kidney disease. Nat Rev Nephrol. 2015;11(8):451-64. doi: 10.1038/nrneph.2015.39. PubMed PMID: 25870007; PMCID: PMC4539141.

66. Kuo IY, Ehrlich BE. Ion channels in renal disease. Chem Rev. 2012;112(12):6353-72. doi: 10.1021/cr3001077. PubMed PMID: 22809040; PMCID: PMC3511917.

67. Anyatonwu GI, Estrada M, Tian X, Somlo S, Ehrlich BE. Regulation of ryanodine receptor-dependent calcium signaling by polycystin-2. Proc Natl Acad Sci U S A. 2007;104(15):6454-9. doi: 10.1073/pnas.0610324104. PubMed PMID: 17404231; PMCID: PMC1851053.

68. Wallace DP. Cyclic AMP-mediated cyst expansion. Biochim Biophys Acta. 2011;1812(10):1291-300. doi: 10.1016/j.bbadis.2010.11.005. PubMed PMID: 21118718; PMCID: PMC3081913.

69. Wilson PD. Polycystic kidney disease. N Engl J Med. 2004;350(2):151-64. doi: 10.1056/NEJMra022161. PubMed PMID: 14711914.

70. Fischer E, Legue E, Doyen A, Nato F, Nicolas JF, Torres V, Yaniv M, Pontoglio M. Defective planar cell polarity in polycystic kidney disease. Nat Genet. 2006;38(1):21-3. doi: 10.1038/ng1701. PubMed PMID: 16341222.

71. Grantham JJ. Mechanisms of progression in autosomal dominant polycystic kidney disease. Kidney Int Suppl. 1997;63:S93-7. PubMed PMID: 9407432.

72. Aschauer L, Limonciel A, Wilmes A, Stanzel S, Kopp-Schneider A, Hewitt P, Lukas A, Leonard MO, Pfaller W, Jennings P. Application of RPTEC/TERT1 cells for investigation of repeat dose nephrotoxicity: A transcriptomic study. Toxicol In Vitro. 2015;30(1 Pt A):106-16. doi: 10.1016/j.tiv.2014.10.005. PubMed PMID: 25450743.

73. Aschauer L, Carta G, Vogelsang N, Schlatter E, Jennings P. Expression of xenobiotic transporters in the human renal proximal tubule cell line RPTEC/TERT1. Toxicol In Vitro. 2015;30(1 Pt A):95-105. doi: 10.1016/j.tiv.2014.12.003. PubMed PMID: 25500123.

74. Bryant DM, Datta A, Rodríguez-Fraticelli AE, Peränen J, Martín-Belmonte F, Mostov KE. A molecular network for de novo generation of the apical surface and lumen. Nat Cell Biol. 2010;12(11):1035-45. doi: 10.1038/ncb2106. PubMed PMID: 20890297; PMCID: PMC2975675.

75. Nowak G, Schnellmann RG. L-ascorbic acid regulates growth and metabolism of renal cells: improvements in cell culture. Am J Physiol. 1996;271(6 Pt 1):C2072-80. PubMed PMID: 8997210.

76. Taub M, Chuman L, Saier MH, Sato G. Growth of Madin-Darby canine kidney epithelial cell (MDCK) line in hormone-supplemented, serum-free medium. Proc Natl Acad Sci U S A. 1979;76(7):3338-42. PubMed PMID: 291007; PMCID: PMC383820.

77. van der Valk J, Brunner D, De Smet K, Fex Svenningsen A, Honegger P, Knudsen LE, Lindl T, Noraberg J, Price A, Scarino ML, Gstraunthaler G. Optimization of chemically defined cell culture media--replacing fetal bovine serum in mammalian in vitro methods. Toxicol In Vitro. 2010;24(4):1053-63. doi: 10.1016/j.tiv.2010.03.016. PubMed PMID: 20362047.

78. Zheng X, Baker H, Hancock WS, Fawaz F, McCaman M, Pungor E. Proteomic analysis for the assessment of different lots of fetal bovine serum as a raw material for cell culture. Part IV. Application of proteomics to the manufacture of biological drugs. Biotechnol Prog. 2006;22(5):1294-300. doi: 10.1021/bp060121o. PubMed PMID: 17022666.

79. Weaver VM, Petersen OW, Wang F, Larabell CA, Briand P, Damsky C, Bissell MJ. Reversion of the malignant phenotype of human breast cells in three-dimensional culture and in vivo by integrin blocking antibodies. J Cell Biol. 1997;137(1):231-45. PubMed PMID: 9105051; PMCID: PMC2139858.

80. Zegers MM, O'Brien LE, Yu W, Datta A, Mostov KE. Epithelial polarity and tubulogenesis in vitro. Trends Cell Biol. 2003;13(4):169-76. PubMed PMID: 12667754.

81. Griffith LG, Swartz MA. Capturing complex 3D tissue physiology in vitro. Nat Rev Mol Cell Biol. 2006;7(3):211-24. doi: 10.1038/nrm1858. PubMed PMID: 16496023.

82. Kim HJ, Huh D, Hamilton G, Ingber DE. Human gut-on-a-chip inhabited by microbial flora that experiences intestinal peristalsis-like motions and flow. Lab Chip. 2012;12(12):2165-74. doi: 10.1039/c2lc40074j. PubMed PMID: 22434367.

83. Huh D, Kim HJ, Fraser JP, Shea DE, Khan M, Bahinski A, Hamilton GA, Ingber DE. Microfabrication of human organs-on-chips. Nat Protoc. 2013;8(11):2135-57. doi: 10.1038/nprot.2013.137. PubMed PMID: 24113786.

84. Zhao F, Chella R, Ma T. Effects of shear stress on 3-D human mesenchymal stem cell construct development in a perfusion bioreactor system: Experiments and hydrodynamic modeling. Biotechnol Bioeng. 2007;96(3):584-95. doi: 10.1002/bit.21184. PubMed PMID: 16948169.

85. Bhatia SN, Ingber DE. Microfluidic organs-on-chips. Nat Biotechnol. 2014;32(8):760-72. doi: 10.1038/nbt.2989. PubMed PMID: 25093883.

86. Booth R, Kim H. Characterization of a microfluidic in vitro model of the blood-brain barrier (μBBB). Lab Chip. 2012;12(10):1784-92. doi: 10.1039/c2lc40094d. PubMed PMID: 22422217.

87. Achyuta AK, Conway AJ, Crouse RB, Bannister EC, Lee RN, Katnik CP, Behensky AA, Cuevas J, Sundaram SS. A modular approach to create a neurovascular unit-on-a-chip. Lab Chip. 2013;13(4):542-53. doi: 10.1039/c2lc41033h. PubMed PMID: 23108480.

88. Huh D, Leslie DC, Matthews BD, Fraser JP, Jurek S, Hamilton GA, Thorneloe KS, McAlexander MA, Ingber DE. A human disease model of drug toxicity-induced pulmonary edema in a lung-on-a-chip microdevice. Sci Transl Med. 2012;4(159):159ra47. doi: 10.1126/scitranslmed.3004249. PubMed PMID: 23136042.

89. Krause S, Maffini MV, Soto AM, Sonnenschein C. A novel 3D in vitro culture model to study stromal-epithelial interactions in the mammary gland. Tissue Eng Part C Methods. 2008;14(3):261-71. doi: 10.1089/ten.tec.2008.0030. PubMed PMID: 18694322.

90. Cox TR, Erler JT. Remodeling and homeostasis of the extracellular matrix: implications for fibrotic diseases and cancer. Dis Model Mech. 2011;4(2):165-78. doi: 10.1242/dmm.004077. PubMed PMID: 21324931; PMCID: PMC3046088.

91. Tibbitt MW, Anseth KS. Hydrogels as extracellular matrix mimics for 3D cell culture. Biotechnol Bioeng. 2009;103(4):655-63. doi: 10.1002/bit.22361. PubMed PMID: 19472329; PMCID: PMC2997742.

92. Nguyen DH, Stapleton SC, Yang MT, Cha SS, Choi CK, Galie PA, Chen CS. Biomimetic model to reconstitute angiogenic sprouting morphogenesis in vitro. Proc Natl Acad Sci U S A. 2013;110(17):6712-7. doi: 10.1073/pnas.1221526110. PubMed PMID: 23569284; PMCID: PMC3637738.

93. Adler M, Ramm S, Hafner M, Muhlich JL, Gottwald EM, Weber E, Jaklic A, Ajay AK, Svoboda D, Auerbach S, Kelly EJ, Himmelfarb J, Vaidya VS. A Quantitative Approach to Screen for Nephrotoxic Compounds In Vitro. J Am Soc Nephrol. 2015. doi: 10.1681/ASN.2015010060. PubMed PMID: 26260164.

94. Zeisberg M, Bonner G, Maeshima Y, Colorado P, Müller GA, Strutz F, Kalluri R. Renal fibrosis: collagen composition and assembly regulates epithelial-mesenchymal transdifferentiation. Am J Pathol. 2001;159(4):1313-21. doi: 10.1016/S0002-9440(10)62518-7. PubMed PMID: 11583959; PMCID: PMC1850511.

95. Nakayama KH, Batchelder CA, Lee CI, Tarantal AF. Decellularized rhesus monkey kidney as a three-dimensional scaffold for renal tissue engineering. Tissue Eng Part A. 2010;16(7):2207-16. doi: 10.1089/ten.tea.2009.0602. PubMed PMID: 20156112; PMCID: PMC2947947.

96. Wen JH, Vincent LG, Fuhrmann A, Choi YS, Hribar KC, Taylor-Weiner H, Chen S, Engler AJ. Interplay of matrix stiffness and protein tethering in stem cell differentiation. Nat Mater. 2014;13(10):979-87. doi: 10.1038/nmat4051. PubMed PMID: 25108614; PMCID: PMC4172528.

97. Desai SP, Freeman DM, Voldman J. Plastic masters-rigid templates for soft lithography. Lab Chip. 2009;9(11):1631-7. doi: 10.1039/b822081f. PubMed PMID: 19458873.

98. Chwalek K, Tang-Schomer MD, Omenetto FG, Kaplan DL. In vitro bioengineered model of cortical brain tissue. Nat Protoc. 2015;10(9):1362-73. doi: 10.1038/nprot.2015.091. PubMed PMID: 26270395.

99. Chen Y, Lin Y, Davis KM, Wang Q, Rnjak-Kovacina J, Li C, Isberg RR, Kumamoto CA, Mecsas J, Kaplan DL. Robust bioengineered 3D functional human intestinal epithelium. Sci Rep. 2015;5:13708. doi: 10.1038/srep13708. PubMed PMID: 26374193; PMCID: PMC4571649.

100. Abbott RD, Raja WK, Wang RY, Stinson JA, Glettig DL, Burke KA, Kaplan DL. Long term perfusion system supporting adipogenesis. Methods. 2015;84:84-9. doi: 10.1016/j.ymeth.2015.03.022. PubMed PMID: 25843606; PMCID: PMC4526405.

101. Nazarov R, Jin HJ, Kaplan DL. Porous 3-D scaffolds from regenerated silk fibroin. Biomacromolecules. 2004;5(3):718-26. doi: 10.1021/bm034327e. PubMed PMID: 15132652.

102. An B, DesRochers TM, Qin G, Xia X, Thiagarajan G, Brodsky B, Kaplan DL. The influence of specific binding of collagen-silk chimeras to silk biomaterials on hMSC behavior. Biomaterials. 2013;34(2):402-12. doi: 10.1016/j.biomaterials.2012.09.085. PubMed PMID: 23088839; PMCID: PMC3490004.

103. Murab S, Chameettachal S, Bhattacharjee M, Das S, Kaplan DL, Ghosh S. Matrix-embedded cytokines to simulate osteoarthritis-like cartilage microenvironments. Tissue Eng Part A. 2013;19(15-16):1733-53. doi: 10.1089/ten.TEA.2012.0385. PubMed PMID: 23470228; PMCID: PMC3700141.

104. Qin D, Xia Y, Whitesides GM. Soft lithography for micro- and nanoscale patterning. Nat Protoc. 2010;5(3):491-502. doi: 10.1038/nprot.2009.234. PubMed PMID: 20203666.

105. Dewey CF, Bussolari SR, Gimbrone MA, Davies PF. The dynamic response of vascular endothelial cells to fluid shear stress. J Biomech Eng. 1981;103(3):177-85. PubMed PMID: 7278196.

106. Besschetnova TY, Kolpakova-Hart E, Guan Y, Zhou J, Olsen BR, Shah JV. Identification of signaling pathways regulating primary cilium length and flow-mediated adaptation. Curr Biol. 2010;20(2):182-7. doi: 10.1016/j.cub.2009.11.072. PubMed PMID: 20096584; PMCID: PMC2990526.

107. Verghese E, Weidenfeld R, Bertram JF, Ricardo SD, Deane JA. Renal cilia display length alterations following tubular injury and are present early in epithelial repair. Nephrol Dial Transplant. 2008;23(3):834-41. doi: 10.1093/ndt/gfm743. PubMed PMID: 17962379.

108. Pampaloni F, Reynaud EG, Stelzer EH. The third dimension bridges the gap between cell culture and live tissue. Nat Rev Mol Cell Biol. 2007;8(10):839-45. doi: 10.1038/nrm2236. PubMed PMID: 17684528.

109. Matlin KS, Caplan MJ. Epithelial cell structure and polarity 2013.

110. Li L, Zepeda-Orozco D, Patel V, Truong P, Karner CM, Carroll TJ, Lin F. Aberrant planar cell polarity induced by urinary tract obstruction. Am J Physiol Renal Physiol. 2009;297(6):F1526-33. doi: 10.1152/ajprenal.00318.2009. PubMed PMID: 19794107; PMCID: PMC2801343.

111. Luyten A, Su X, Gondela S, Chen Y, Rompani S, Takakura A, Zhou J. Aberrant regulation of planar cell polarity in polycystic kidney disease. J Am Soc Nephrol. 2010;21(9):1521-32. doi: 10.1681/ASN.2010010127. PubMed PMID: 20705705; PMCID: PMC3013531.

112. Kalluri R, Neilson EG. Epithelial-mesenchymal transition and its implications for fibrosis. J Clin Invest. 2003;112(12):1776-84. doi: 10.1172/JCI20530. PubMed PMID: 14679171; PMCID: PMC297008.

113. Martín-Belmonte F, Yu W, Rodríguez-Fraticelli AE, Ewald AJ, Ewald A, Werb Z, Alonso MA, Mostov K. Cell-polarity dynamics controls the mechanism of lumen formation in epithelial morphogenesis. Curr Biol. 2008;18(7):507-13. doi: 10.1016/j.cub.2008.02.076. PubMed PMID: 18394894; PMCID: PMC2405957.

114. Schlüter MA, Margolis B. Apical lumen formation in renal epithelia. J Am Soc Nephrol. 2009;20(7):1444-52. doi: 10.1681/ASN.2008090949. PubMed PMID: 19497970.

115. Santos OF, Nigam SK. HGF-induced tubulogenesis and branching of epithelial cells is modulated by extracellular matrix and TGF-beta. Dev Biol. 1993;160(2):293-302. doi: 10.1006/dbio.1993.1308. PubMed PMID: 8253265.

116. Kubota Y, Kleinman HK, Martin GR, Lawley TJ. Role of laminin and basement membrane in the morphological differentiation of human endothelial cells into capillary-like structures. J Cell Biol. 1988;107(4):1589-98. PubMed PMID: 3049626; PMCID: PMC2115245.

117. Staton CA, Reed MW, Brown NJ. A critical analysis of current in vitro and in vivo angiogenesis assays. Int J Exp Pathol. 2009;90(3):195-221. doi: 10.1111/j.1365-2613.2008.00633.x. PubMed PMID: 19563606; PMCID: PMC2697546.

118. Merfeld-Clauss S, Gollahalli N, March KL, Traktuev DO. Adipose tissue progenitor cells directly interact with endothelial cells to induce vascular network formation. Tissue Eng Part A. 2010;16(9):2953-66. doi: 10.1089/ten.tea.2009.0635. PubMed PMID: 20486792; PMCID: PMC2928048.

119. Montesano R, Pepper MS, Orci L. Paracrine induction of angiogenesis in vitro by Swiss 3T3 fibroblasts. J Cell Sci. 1993;105 (Pt 4):1013-24. PubMed PMID: 7693734.

120. Morizane R, Monkawa T, Fujii S, Yamaguchi S, Homma K, Matsuzaki Y, Okano H, Itoh H. Kidney specific protein-positive cells derived from embryonic stem cells reproduce tubular structures in vitro and differentiate into renal tubular cells. PLoS One. 2014;8(6):e64843. doi: 10.1371/journal.pone.0064843. PubMed PMID: 23755150; PMCID: PMC3670839.

121. Narayanan K, Schumacher KM, Tasnim F, Kandasamy K, Schumacher A, Ni M, Gao S, Gopalan B, Zink D, Ying JY. Human embryonic stem cells differentiate into functional renal proximal tubular-like cells. Kidney Int. 2013;83(4):593-603. doi: 10.1038/ki.2012.442. PubMed PMID: 23389418.

122. Eckardt KU, Coresh J, Devuyst O, Johnson RJ, Köttgen A, Levey AS, Levin A. Evolving importance of kidney disease: from subspecialty to global health burden. Lancet. 2013;382(9887):158-69. doi: 10.1016/S0140-6736(13)60439-0. PubMed PMID: 23727165.

123. Arnaoutova I, Kleinman HK. In vitro angiogenesis: endothelial cell tube formation on gelled basement membrane extract. Nat Protoc. 2010;5(4):628-35. doi: 10.1038/nprot.2010.6. PubMed PMID: 20224563.

124. Motohashi H, Sakurai Y, Saito H, Masuda S, Urakami Y, Goto M, Fukatsu A, Ogawa O, Inui K. Gene expression levels and immunolocalization of organic ion transporters in the human kidney. J Am Soc Nephrol. 2002;13(4):866-74. PubMed PMID: 11912245.

125. Vrhovac I, Balen Eror D, Klessen D, Burger C, Breljak D, Kraus O, Radović N, Jadrijević S, Aleksic I, Walles T, Sauvant C, Sabolić I, Koepsell H. Localizations of Na(+)-D-glucose cotransporters SGLT1 and SGLT2 in human kidney and of SGLT1 in human small intestine, liver, lung, and heart. Pflugers Arch. 2015;467(9):1881-98. doi: 10.1007/s00424-014-1619-7. PubMed PMID: 25304002.

126. Yao Q, Pawlaczyk K, Ayala ER, Styszynski A, Breborowicz A, Heimburger O, Qian JQ, Stenvinkel P, Lindholm B, Axelsson J. The role of the TGF/Smad signaling pathway in

peritoneal fibrosis induced by peritoneal dialysis solutions. Nephron Exp Nephrol. 2008;109(2):e71-8. doi: 10.1159/000142529. PubMed PMID: 18600031.

127. LeBleu VS, Macdonald B, Kalluri R. Structure and function of basement membranes. Exp Biol Med (Maywood). 2007;232(9):1121-9. doi: 10.3181/0703-MR-72. PubMed PMID: 17895520.

128. Chen WC, Lin HH, Tang MJ. Regulation of proximal tubular cell differentiation and proliferation in primary culture by matrix stiffness and ECM components. Am J Physiol Renal Physiol. 2014;307(6):F695-707. doi: 10.1152/ajprenal.00684.2013. PubMed PMID: 25056346.

129. Klein G, Langegger M, Timpl R, Ekblom P. Role of laminin A chain in the development of epithelial cell polarity. Cell. 1988;55(2):331-41. PubMed PMID: 3048705.

130. Guidolin D, Fede C, Albertin G, De Caro R. Investigating in vitro angiogenesis by computer-assisted image analysis and computational simulation. Methods Mol Biol. 2015;1214:197-214. doi: 10.1007/978-1-4939-1462-3_12. PubMed PMID: 25468606.

131. Sanz L, Pascual M, Muñoz A, González MA, Salvador CH, Alvarez-Vallina L. Development of a computer-assisted high-throughput screening platform for anti-angiogenic testing. Microvasc Res. 2002;63(3):335-9. doi: 10.1006/mvre.2001.2389. PubMed PMID: 11969310.

132. Tanner GA, Evan AP. Glomerular and proximal tubular morphology after single nephron obstruction. Kidney Int. 1989;36(6):1050-60. PubMed PMID: 2601255.

133. Brown D, Lee R, Bonventre JV. Redistribution of villin to proximal tubule basolateral membranes after ischemia and reperfusion. Am J Physiol. 1997;273(6 Pt 2):F1003-12. PubMed PMID: 9435690.

134. Yang Z, Zimmerman S, Brakeman PR, Beaudoin GM, Reichardt LF, Marciano DK. De novo lumen formation and elongation in the developing nephron: a central role for afadin in apical polarity. Development. 2013;140(8):1774-84. doi: 10.1242/dev.087957. PubMed PMID: 23487309; PMCID: PMC3621492.

135. Suzuki A, Hirata M, Kamimura K, Maniwa R, Yamanaka T, Mizuno K, Kishikawa M, Hirose H, Amano Y, Izumi N, Miwa Y, Ohno S. aPKC acts upstream of PAR-1b in both the establishment and maintenance of mammalian epithelial polarity. Curr Biol. 2004;14(16):1425-35. doi: 10.1016/j.cub.2004.08.021. PubMed PMID: 15324659.

136. Elias BC, Das A, Parekh DV, Mernaugh G, Adams R, Yang Z, Brakebusch C, Pozzi A, Marciano DK, Carroll TJ, Zent R. Cdc42 regulates epithelial cell polarity and cytoskeletal function during kidney tubule development. J Cell Sci. 2015;128(23):4293-305. doi: 10.1242/jcs.164509. PubMed PMID: 26490995; PMCID: PMC4712811.

137. Hurd TW, Gao L, Roh MH, Macara IG, Margolis B. Direct interaction of two polarity complexes implicated in epithelial tight junction assembly. Nat Cell Biol. 2003;5(2):137-42. doi: 10.1038/ncb923. PubMed PMID: 12545177.

138. Datta A, Bryant DM, Mostov KE. Molecular regulation of lumen morphogenesis. Curr Biol. 2011;21(3):R126-36. doi: 10.1016/j.cub.2010.12.003. PubMed PMID: 21300279; PMCID: PMC3771703.

139. Roth M, Obaidat A, Hagenbuch B. OATPs, OATs and OCTs: the organic anion and cation transporters of the SLCO and SLC22A gene superfamilies. Br J Pharmacol. 2012;165(5):1260-87. doi: 10.1111/j.1476-5381.2011.01724.x. PubMed PMID: 22013971; PMCID: PMC3372714.

140. Vallon V, Platt KA, Cunard R, Schroth J, Whaley J, Thomson SC, Koepsell H, Rieg T. SGLT2 mediates glucose reabsorption in the early proximal tubule. J Am Soc Nephrol. 2011;22(1):104-12. doi: 10.1681/ASN.2010030246. PubMed PMID: 20616166; PMCID: PMC3014039.

141. Fioretto P, Zambon A, Rossato M, Busetto L, Vettor R. SGLT2 Inhibitors and the Diabetic Kidney. Diabetes Care. 2016;39 Suppl 2:S165-71. doi: 10.2337/dcS15-3006. PubMed PMID: 27440829.

142. Varma MV, Feng B, Obach RS, Troutman MD, Chupka J, Miller HR, El-Kattan A. Physicochemical determinants of human renal clearance. J Med Chem. 2009;52(15):4844-52. doi: 10.1021/jm900403j. PubMed PMID: 19445515.

143. Breljak D, Ljubojević M, Hagos Y, Micek V, Balen Eror D, Vrhovac Madunić I, Brzica H, Karaica D, Radović N, Kraus O, Anzai N, Koepsell H, Burckhardt G, Burckhardt BC, Sabolić I. Distribution of organic anion transporters NaDC3 and OAT1-3 along the human nephron. Am J Physiol Renal Physiol. 2016;311(1):F227-38. doi: 10.1152/ajprenal.00113.2016. PubMed PMID: 27053689.

144. Li H, Chang J. Bioactive silicate materials stimulate angiogenesis in fibroblast and endothelial cell co-culture system through paracrine effect. Acta Biomater. 2013;9(6):6981-91. doi: 10.1016/j.actbio.2013.02.014. PubMed PMID: 23416471.

145. Das A, Tanigawa S, Karner CM, Xin M, Lum L, Chen C, Olson EN, Perantoni AO, Carroll TJ. Stromal-epithelial crosstalk regulates kidney progenitor cell differentiation. Nat Cell Biol. 2013;15(9):1035-44. doi: 10.1038/ncb2828. PubMed PMID: 23974041; PMCID: PMC3891676.

146. Shieh AC, Rozansky HA, Hinz B, Swartz MA. Tumor cell invasion is promoted by interstitial flow-induced matrix priming by stromal fibroblasts. Cancer Res. 2011;71(3):790-800. doi: 10.1158/0008-5472.CAN-10-1513. PubMed PMID: 21245098.

147. Grinnell F. Fibroblast mechanics in three-dimensional collagen matrices. J Bodyw Mov Ther. 2008;12(3):191-3. doi: 10.1016/j.jbmt.2008.03.005. PubMed PMID: 19083673; PMCID: PMC2605607.

148. Imai M, Furusawa K, Mizutani T, Kawabata K, Haga H. Three-dimensional morphogenesis of MDCK cells induced by cellular contractile forces on a viscous substrate. Sci Rep. 2015;5:14208. doi: 10.1038/srep14208. PubMed PMID: 26374384; PMCID: PMC4571640.

149. Zavadil J, Böttinger EP. TGF-beta and epithelial-to-mesenchymal transitions. Oncogene. 2005;24(37):5764-74. doi: 10.1038/sj.onc.1208927. PubMed PMID: 16123809.

150. Liu Y. Epithelial to mesenchymal transition in renal fibrogenesis: pathologic significance, molecular mechanism, and therapeutic intervention. J Am Soc Nephrol. 2004;15(1):1-12. PubMed PMID: 14694152.

151. Yang J, Liu Y. Dissection of key events in tubular epithelial to myofibroblast transition and its implications in renal interstitial fibrosis. Am J Pathol. 2001;159(4):1465-75. doi: 10.1016/S0002-9440(10)62533-3. PubMed PMID: 11583974; PMCID: PMC1850509.

152. Lu H, Chen B, Hong W, Liang Y, Bai Y. Transforming growth factor-β1 stimulates hedgehog signaling to promote epithelial-mesenchymal transition after kidney injury. FEBS J. 2016;283(20):3771-90. doi: 10.1111/febs.13842. PubMed PMID: 27579669.

153. Dimke H, Sparks MA, Thomson BR, Frische S, Coffman TM, Quaggin SE. Tubulovascular cross-talk by vascular endothelial growth factor a maintains peritubular microvasculature in kidney. J Am Soc Nephrol. 2015;26(5):1027-38. doi: 10.1681/ASN.2014010060. PubMed PMID: 25385849; PMCID: PMC4413754.

154. Lovett M, Rockwood D, Baryshyan A, Kaplan DL. Simple modular bioreactors for tissue engineering: a system for characterization of oxygen gradients, human mesenchymal stem cell differentiation, and prevascularization. Tissue Eng Part C Methods. 2010;16(6):1565-73. doi: 10.1089/ten.TEC.2010.0241. PubMed PMID: 20528664; PMCID: PMC2988631.

155. Pallotta I, Lovett M, Kaplan DL, Balduini A. Three-dimensional system for the in vitro study of megakaryocytes and functional platelet production using silk-based vascular tubes. Tissue Eng Part C Methods. 2011;17(12):1223-32. doi: 10.1089/ten.tec.2011.0134. PubMed PMID: 21895494; PMCID: PMC3226422.

156. Rnjak-Kovacina J, Wray LS, Golinski JM, Kaplan DL. Arrayed Hollow Channels in Silk-based Scaffolds Provide Functional Outcomes for Engineering Critically-sized Tissue Constructs. Adv Funct Mater. 2014;24(15):2188-96. doi: 10.1002/adfm.201302901. PubMed PMID: 25395920; PMCID: PMC4225637.

157. Wray LS, Rnjak-Kovacina J, Mandal BB, Schmidt DF, Gil ES, Kaplan DL. A silk-based scaffold platform with tunable architecture for engineering critically-sized tissue constructs. Biomaterials. 2012;33(36):9214-24. doi: 10.1016/j.biomaterials.2012.09.017. PubMed PMID: 23036961; PMCID: PMC3479404.

158. Caralt M, Uzarski JS, Iacob S, Obergfell KP, Berg N, Bijonowski BM, Kiefer KM, Ward HH, Wandinger-Ness A, Miller WM, Zhang ZJ, Abecassis MM, Wertheim JA. Optimization and critical evaluation of decellularization strategies to develop renal extracellular matrix scaffolds as biological templates for organ engineering and transplantation. Am J Transplant. 2015;15(1):64-75. doi: 10.1111/ajt.12999. PubMed PMID: 25403742; PMCID: PMC4276475.

159. Lawrence ML, Chang CH, Davies JA. Transport of organic anions and cations in murine embryonic kidney development and in serially-reaggregated engineered kidneys. Sci Rep. 2015;5:9092. doi: 10.1038/srep09092. PubMed PMID: 25766625; PMCID: PMC4357899.

160. Limonciel A, Aschauer L, Wilmes A, Prajczer S, Leonard MO, Pfaller W, Jennings P. Lactate is an ideal non-invasive marker for evaluating temporal alterations in cell stress and toxicity in repeat dose testing regimes. Toxicol In Vitro. 2011;25(8):1855-62. doi: 10.1016/j.tiv.2011.05.018. PubMed PMID: 21635945.

161. Snyder JE, Hamid Q, Wang C, Chang R, Emami K, Wu H, Sun W. Bioprinting cell-laden matrigel for radioprotection study of liver by pro-drug conversion in a dual-tissue microfluidic chip. Biofabrication. 2011;3(3):034112. doi: 10.1088/1758-5082/3/3/034112. PubMed PMID: 21881168.

162. Lu S, Wang X, Lu Q, Zhang X, Kluge JA, Uppal N, Omenetto F, Kaplan DL. Insoluble and flexible silk films containing glycerol. Biomacromolecules. 2010;11(1):143-50. doi: 10.1021/bm900993n. PubMed PMID: 19919091.

163. Vepari C, Kaplan DL. Silk as a Biomaterial. Prog Polym Sci. 2007;32(8-9):991-1007. doi: 10.1016/j.progpolymsci.2007.05.013. PubMed PMID: 19543442; PMCID: PMC2699289.

164. Pritchard EM, Kaplan DL. Silk fibroin biomaterials for controlled release drug delivery. Expert Opin Drug Deliv. 2011;8(6):797-811. doi: 10.1517/17425247.2011.568936. PubMed PMID: 21453189.